Neuronal Outgrowth on Patterned Surfaces: Effects of Geometry, Scale, and Superposition of Topographical and Chemical Cues

By

Steven R. Hart

A dissertation submitted in partial fulfillment of

the requirements for the degree of

Doctor of Philosophy

(Physics)

at the

University of Wisconsin-Madison

2013

Date of final oral examination: 7/23/13

The dissertation is approved by the following members of the Final Oral Committee:

Justin C. Williams, Associate Professor, Biomedical Engineering
Erik W. Dent, Associate Professor, Neuroscience
Pupa Gilbert, Professor, Physics
Franz Himpsel, Professor, Physics
Max Lagally, Professor, Materials Science and Engineering

Abstract:

The physical environment is fundamentally important in determining cellular behavior. I present research that is focused on changing the nano- and micro-environment of cultured primary cortical neurons. I developed a lithography-free methodology, notable for its simplicity, to create 2-D biochemical micropatterns and 3-D anisotropic grooved topographical features of various dimensions to guide and direct neuronal outgrowth. In particular, axonal outgrowth was found to orient parallel to lines of 8.3 μm periodicity, but perpendicular to lines of 1.7 μm periodicity. By superimposing topographical and chemical cues, it was found that topographical modification could enhance or inhibit outgrowth perpendicular to topography, depending on the combination scheme. By decreasing the topographical feature radius of curvature, axons could be induced to transition from a perpendicular to a parallel guidance relative to the topography. Also, neurons and glial cells could be made in co-culture to align parallel or perpendicular to each other. Work is continuing to determine the biophysical mechanisms which control the outgrowth process, which knowledge will form an integral part of our understanding of the nervous system.

Table of Contents

Note to Readers:

Chapter 1 of this work is a literature review covering the topics on which this dissertation is focused. Chapter 2 has been published under its given title (See S. R. Hart, Y. Huang, T. Fothergill, D. C. Lumbard, E. W. Dent and J. C. Williams, Adhesive micro-line periodicity determines guidance of axonal outgrowth, *Lab on a Chip*, 2013, **13**, 562-569.) Chapter 3 has been submitted for publication. Chapters 4 and 5 are ready to submit, or will be (Ch. 5) before the date of the oral defense, and are awaiting submission for publication, pending the editorial decision concerning the work of chapter 3. Chapter 6 outlines three projects which need continued work to be prepared for publication, but that show significant promise. Each chapter within this work is organized independently, with introduction, methods, results and references. Because each paper builds successively on the results of the previous, many items within the methodology will have a certain redundancy.

Acknowledgements:

I would like to thank my advisor, Justin Williams, for his continual support and assistance. Also, current and former members of his lab, including Yu Huang, Andrew Pierce, Josh Kolz, Sarah Brodnick, Amy Schendel, Tom Richner and everyone else who has ever let me talk through challenges with them. Josh was particularly instrumental in helping me put together chapter 5. I also wish to thank Erik Dent, whose collaboration made everything possible, and all of the current and former members of his lab.

Most importantly, I am forever grateful to my wife Mindy and our beautiful daughters Kylie and Shaelyn, who have put up with a dissertating husband and father all of these years.

Chapter 1: Review of Neuronal Outgrowth on Patterned Surfaces: Effects of Geometry, Scale, and Superposition of Topographical and Chemical Cues

Note to readers: This literature review is being prepared for submission as an invited review article. Modifications will include work done by the author not emphasized here, as in its current role this review is meant to introduce the research that preludes the author's work.

1.1 Abstract

Neuronal behavior, such as axon elongation or neuron migration, is subject to a variety of cues in the extracellular environment. In many studies, much attention is justifiably given to the identification of biochemical cues, the receptors for such on the neuron, and other relevant details of a biological nature. In concert with the inherent *biological* basis of neuronal behavior is the environmental *physical* basis of neuronal behavior. Surface texture, substrate rigidity, and the shape and size of regions permissive to growth are all physical effects which can dramatically influence neuronal behavior and axonal outgrowth. We examine foundational and recent efforts to study the behavior of neurons on surfaces which have been altered chemically, topographically, or by both means. This review will focus on axonal outgrowth on patterned surfaces, with a particular emphasis given to the effects that scale and geometry of anisotropic patterns have on neuronal outgrowth behavior.

1.2 Introduction

1.2.1 Overview

The nervous system is a fascinating machine of almost incalculable complexity, capable of controlling autonomous functions, gathering sensory information, producing motor output, storing and processing information, producing a myriad of emotions, applying logic and reason, and enabling consciousness. Within the physical, biological and medical sciences, there has been a growing interest in understanding many aspects of complex neural function that remain thus far entirely mysterious. In fact, within the United States, a recently announced research emphasis within the National Institutes of Health, titled the BRAIN Initiative[1], seeks to accelerate the pace of neuro-technological research and discovery. Success in this endeavor depends on a multi-faceted approach to researching the nervous system. The ability to explore the biophysical nature of individual neurons, and their behavior in micro- and nano-engineered environments, will contribute to the larger-scale effort of neuroscience discovery.

1.2.2 Neuronal Guidance *In Vivo*

Neuronal migration and outgrowth in the living organism is a complex process, crucial during development[2], required following peripheral nerve injury[3] in order to regain function, and inhibited following central nervous system (CNS) lesions[4]. Growth is generally understood to take place at the leading tip of an extending axon, at a structure known as the growth cone. Growth cones are responsible for integrating information from guidance cues, which may be either diffuse or contact-based, and either repulsive or attractive[5]. The environment in which

neurons migrate or elongate *in vivo* may be described as a mixture of biochemical cues and topographical structures. For example, recently differentiated neurons in the cerebral cortex migrate along radial glia to their final destinations[6], neuronal cells in subpial part of the medulla oblongata were observed to migrate and orient processes along pre-laid ECM fibers[7], and glial cells in the Drosophila CNS provide a physical scaffold for future pioneer axons[8]. Because in the developing organism it is impossible to isolate chemical and topographical cues and investigate each independently, it is necessary to construct *in vitro* model environments. Moreover, *in vitro* neuronal networks have been shown to behave differently than theoretically modeled networks[9], highlighting the need to complement the modeling of neural networks with experimental validation.

1.2.3 *In Vitro* Patterning Methods

While the purpose of this review is not to collect a comprehensive inventory of all patterning methods, some overview of common methods will be beneficial. For a full treatment of patterning techniques for cellular assays, Falconnet and colleagues recently wrote an excellent review[10]. Additional reviews, featuring the role of surface functionalization for neuronal adhesion and patterning[11], and the cytoskeletal effects of cells' interactions with micropatterns[12], are also very instructive.

Varying approaches to fabricate patterns for cellular assays feature some universal challenges. In order to culture cells on a surface, basic requirements of biocompatibility must be met: The materials must be non-toxic to the cell, and the substrate must be sterile to prevent the contamination of the cell culture by microorganisms. Many substrates are opaque, preventing many common biological imaging techniques. Many assays require a high data throughput,

necessitating parallelization of the fabrication method. Some applications require small features, increasing fabrication time and costs. For some studies, patterning flexibility is desired as

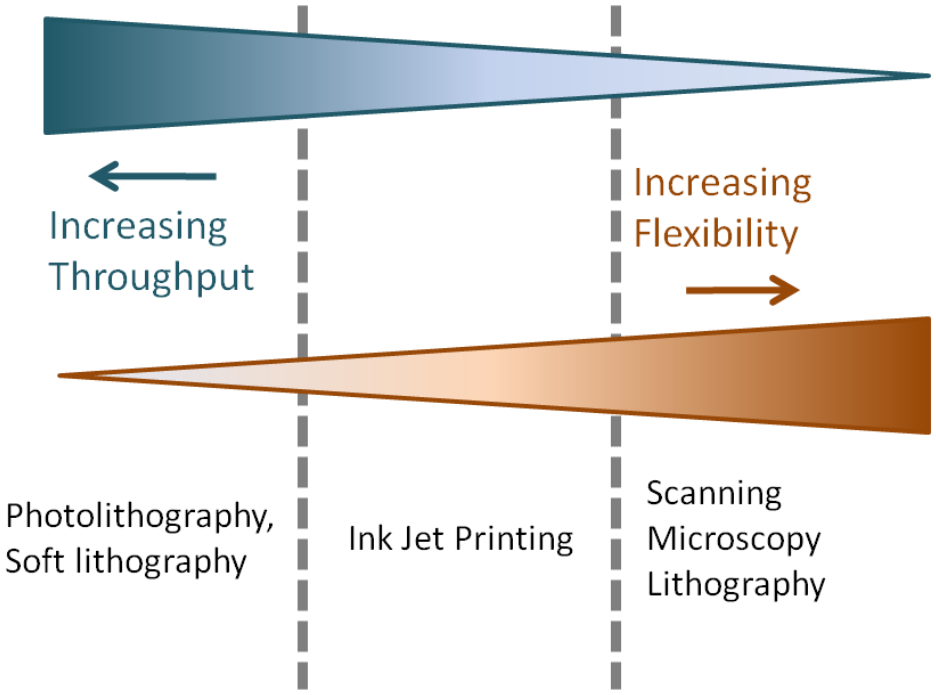

Figure 1 Throughput/Flexibility Spectrum for Cell Patterning Techniques Many techniques, such as photolithography or soft lithography can produce many patterns in parallel, increasing production throughput. However, new patterns require significant time and expense, hurting design flexibility. Other techniques achieve greater flexibility, including real-time design modification. However, typically patterns are produced serially, reducing throughput.

several design iterations may be required. Common patterning methods may be considered as part of a pattern throughput/flexibility spectrum (Figure 1.1). Some techniques, such as those employing photolithography or soft lithography[13] – so named because of the use of elastomeric polymers – achieve a high throughput by producing many patterns in parallel. However, new patterns require an entire repeat of the fabrication process, making successive design iterations

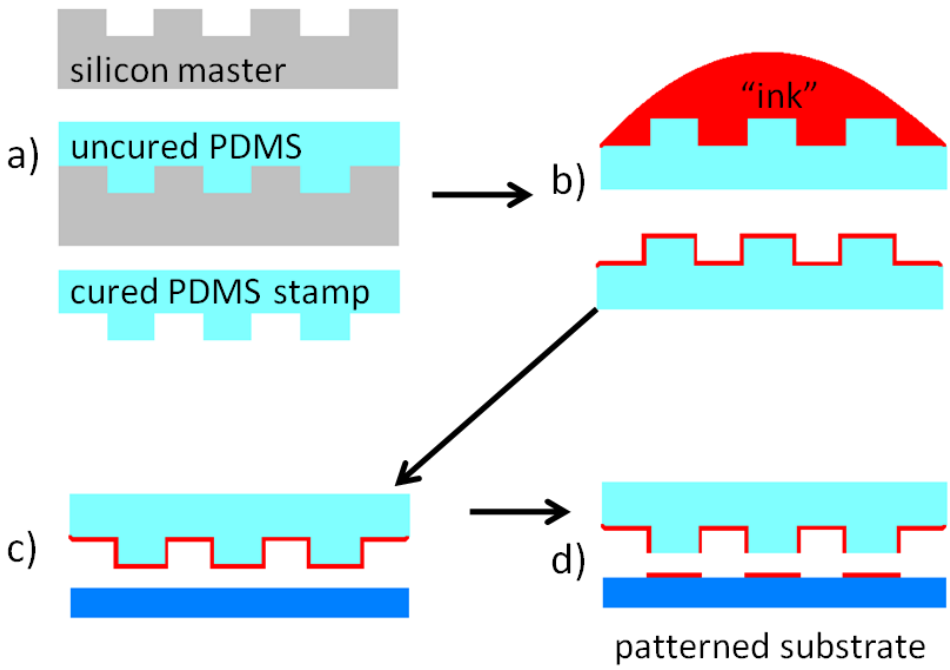

Figure 2 Micro-contact Printing
a) Typically a silicon master is made through common photolithography techniques. Polydimethylsiloxane (PDMS) is replicated off of this master, making a rubbery stamp. b) The PDMS stamp is inked with an alkanethiol, polypeptide, protein, or some other compound. c) The stamp is placed in contact with the substrate, with an applied force. d) The substrate is patterned with the desired 2-D pattern.

cost and time prohibitive. Methods with greater design flexibility are often able to accomplish design modification in real-time. However, this type of method usually produces patterns in series, severely limiting throughput potential. Some examples of this include atomic force microscope lithography, or nanoshaving[14], multi-photon excited fabrication[15] and dip-pen nano-lithography[16]. Besides design flexibility, these methods are able to achieve very high resolution, down to tens of nanometers. The effort to parallelize these fabrication techniques has significant potential and is an active area of technological development. Patterning by ink-jet printing[17] is an example of a technology which compromises throughput and flexibility. Such a method offers complete flexibility, a no-contact printing ability, and reasonable throughput. Resolution, however, is limited to ~10-20 μm.

Micro-contact printing[18] (μCP), a soft-lithographic patterning technique, is perhaps the most ubiquitous of all patterning methods. The widespread use of μCP for cell patterning is due to its simplicity, low cost, and capability of printing a variety of compounds or proteins. The process of μCP (Figure 1.2) begins with the creation of master, typically a silicon wafer. The desired 2-D pattern is printed on a mask, and through photolithographic processes, is transferred to the master. Polydimethylsiloxane (PDMS), an elastomer, is commonly used to replicate the features from the master. The PDMS replica, now a stamp, is inked with the desired compound, and then pressed on to the culture substrate to reproduce the pattern. Typically, this method is limited to a 1-2 μm resolution, and then only if using chrome mask. Masters can be created with nanoscale features using high-resolution patterning techniques, such as e-beam lithography. Beyond μCP, such masters may also be used in direct replica molding or imprint nanolithography[19].

1.3 2-D Chemical Patterning

1.3.1 Overview

Two-dimensional (2-D) patterning, for the sake of this review, is patterning that has some sort of controlled geometric variability in the two surface dimensions. As will be discussed later, it is not possible to create such patterns that do not alter the surface topography. But if the intent is to alter the 2-D landscape, it will form part of this section. The discussion will first focus on 'global' patterning, and then 'local' patterning. Commonly patterned materials include extracellular matrix (ECM) proteins such as laminin or fibronectin, or poly-lysine, an electrostatically adhesive polypeptide.

1.3.2 Spot Arrays

Many spot arrays have been formed by ink-jet printing. Typically formed in a rectangular array, spots are commonly made with diameters ranging from 100 μm to 400 μm[20, 21]. At this scale neuronal behavior is virtually unaffected by the spot size. Many neurons may be found on a single spot. It is, however, reported that the neurons and extending neurites are commonly at the edges of the pattern, which could be a manifestation of the 'coffee ring' effect[22], where differential evaporation rates along the radial profile of the deposited droplet lead to additional material being drawn to the periphery. Single cell isolation may be achieved[23] when the spot size is as small as 20 μm. Squares with a side length of 25, 10 and 5 μm and a pitch equal to twice of the pattern dimension, were patterned by means of a dry lift-off technique[24]. It was found that cortical cells spread randomly on the smallest squares, typically contacting multiple patterns. 10 and 25 μm squares could achieve single cell isolation and guide axons along the axes of the array. By using micro-contact printing, a compelling study of geometric effects was performed by Jang and Nam[25]. Besides spot arrays, micro-polygon arrays with 3, 4, 5 and 6-sided polygons were printed. Additionally, star shapes with varying degrees of concavity were printed. Two major findings include the prevalence of neuritogenesis at polygon vertices, and the preference for axons to form and elongate at the most acute vertex on micro-arrays of isosceles triangles.

1.3.3 Line Arrays

Line arrays consisting of parallel lines of patterned material are commonly used in the effort to orient neurite outgrowth. The arrays may be geometrically characterized by two measurements: line width and spacing, or alternatively, line width and pitch. Small (<3 μm) line

widths with a relatively large pitch (~40 μm) are good where cell isolation and guidance is desired. For example, laser ablation was used to pattern micron-wide lines of poly-lysine onto a polyethylene-glycol (PEG) background in order to study neurite growth dynamics on a 1-D substrate[26]. Oftentimes, likely because of ease of fabrication, relatively large line widths are combined with a relatively large pitch. Dorsal root ganglion neurons were found to experience the most rapid outgrowth on 40 μm wide lines in one study[27], but decreasing growth rates on increasing line width from 20 μm to 30 μm in another study[28]. There have only been a limited

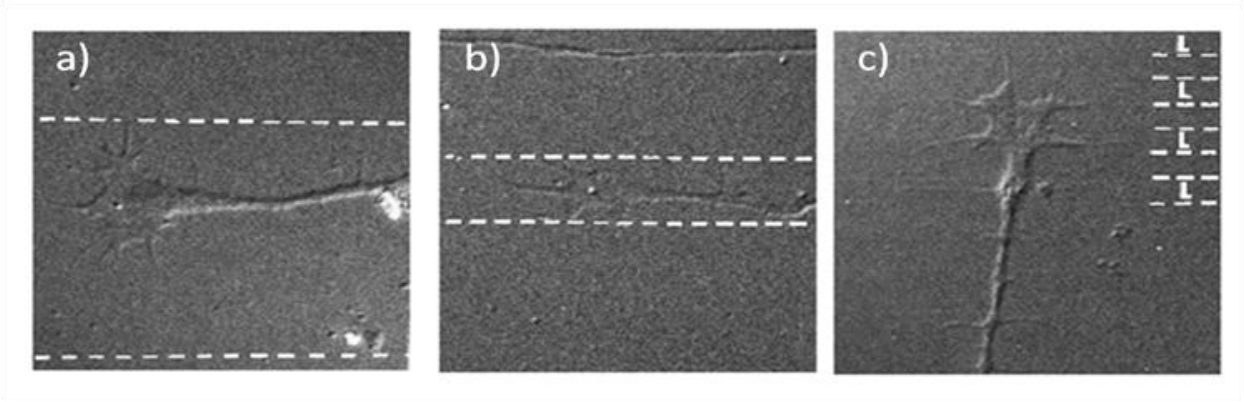

Figure 3 Neurite outgrowth on patterned lines of decreasing width and pitch
a, b) Neurites were guided parallel to tracks of 25 and 6 μm width, respectively. Area between dashed lines indicates regions of printed laminin. c) Neurites on 2 μm width lines, with 4 μm periodicity did not grow parallel to the lines. Figure adapted with permission[28].

number of studies examining the effect of changing the periodicity of lines down to a sub-cellular (≤10 μm) level. Most prominent among these was early work performed by Clark and colleagues in which chick embryonic cerebral neurons were cultured on laminin stripes of varying widths[29]. Consistently with reports given since, lines of relatively large width and periodicity guided the growing axons, with relatively narrow lines and large pitch having the most success. However, 2 μm lines with a 4 μm periodicity were reported to experience random

growth (Figure 3). On an even smaller scale, it has been reported that extending neurites are not able or do not prefer to follow patterned lines that are 800 nm in width[30]. Up to this point, the paradigm by which neuron growth has been considered is that narrow lines and narrow gaps produce random outgrowth. However, this has not been carefully examined, and there even seems to have been some initial indication that perhaps something like perpendicular guidance is occurring (Figure 3c).

1.3.4 Neuronal Networks

Much of the emphasis in patterning neurons revolves around creating networks. Most pattern templates for these 2-D networks consist of a rectangular grid, with nodes at each intersection. This has been accomplished numerous times, especially by μCP[31-34]. Additional methods that have recently been demonstrated include photopatterning polyfluorene[35], and a PEG-based patterning technique which was used to print a honeycomb grid[36].

By patterning nodes into the grids, the probability is increased that the soma will remain positioned at the intersection. Lacking additional cues, the axons may grow in any direction. Electrophysiological measurements, which are typically performed with patch-clamping or by use of micro-electrode arrays, reveal the cells form complex networks. Through triple-patch clamp measurements, Vogt and colleagues determined that linear pathways, feedback loops, and converging and diverging pathways were all circuit elements displayed by neurons growing on a grid template[37]. In later work they found that predicting synapse formation, even for neuronal networks constrained by geometry, was entirely non-trivial[38]. It is clear that in order to create more clearly defined neural networks, it will be necessary to improve the patterning specificity.

1.3.5 Asymmetric Patterns and Neuronal Polarity

Because of the importance of neuron placement and axonal outgrowth direction in creating defined neuronal networks, a primary task is to create micropatterns that achieve both goals. As discussed earlier, a shape like an isosceles triangle may, through its asymmetry, influence axonal outgrowth to occur at a certain point. Limited success in polarization of individual neurons has been accomplished with a variety of geometries. An early attempt used a central spot with 4 lines extending outward[39]. One long, continuous line was complemented with 3 discontinuous lines, achieving polarization via axon elongation on the continuous line for 76% of the cells. However, when this arrangement was replicated with many cells, such as is necessary for neuronal network creation, the pattern failed to produce a dominant directional polarization[40]. Some success has been seen using nano-shaving[14], creating a large square for the cell to initially adhere, with a single thin line extending outward. This process, however, is not ideal for large network formation, as patterns are produced serially by this technique. One-dimensional arrays of triangles of various widths and heights were found to produce polarization in a defined direction for about 2/3 of all neurons[41], though no attempt was made to form this into a network. An interesting study formed a pattern which consisted of a central spot, with 3 lines extending outward, two of which were spaced closer together[42]. It was found that polarization would occur predominantly on the more isolated track, a result that was attributed to the possibility of maximizing cytoskeletal tension. Additional attempts at controlling neuronal polarization have been made using topographical modification of surfaces, to be discussed throughout the next section.

1.4 Topographical Patterning

1.4.1 Isotropic Topography: Surface Roughening

Purely isotropic surface topography modification is typically achieved through some form of surface roughening. The effect of surface roughness, measured in terms of average feature size R_a, on neuronal adhesion, viability, and activity has been examined. For example, it has been found that on nanorough TiN films (R_a: 1.3-5.6 nm) neuronal adhesion was reduced relative to a control of PDL on glass[43]. In another study, it was found that neuronal adhesion on roughened silicon was optimized at R_a = 64 nm, but decreased at higher or lower values of roughness[44]. Similarly, a group found that roughened silicon in the range of R_a = 20 to 50nm was the best suited for neuronal adhesion[45]. Contrarily, in a more recent study, surface roughness of gold was systematically varied from R_a =36 to 100 nm, and it was found that neurons experienced a loss of adhesion and an increase in necrosis that both scaled with surface roughness, cells adhering best most viable on smooth controls[46]. Besides global roughening, it is also possible to pattern the roughened areas, as did one of the aforementioned groups[45].

1.4.2 Nanopillars and Nanopores

Although sometimes treated as isotropic, due to their relative isotropy compared to grooved features, micro/nano arrays of pillars can have a pronounced influence on the directional outgrowth of neurons. In one study, the effect of changing the pillar size and spacing was examined. For pillars of 10 μm diameters and 10 μm spacing, neurite outgrowth was predominantly in the direction of the array. As the size of the pillars and spacing grew, most neurites grew randomly, although frequently some were observed to wrap around posts of 50 to 100 μm diameter[47]. In an earlier study, the size of posts was either 2 μm or 0.5 μm in diameter,

with spacing of 4.5, 3, or 1.5 μm[48]. Especially with the larger posts, the outgrowth would become very straight, aligning with the axis of the pillar array, as the spacing grew smaller (Figure 4). These results are fascinating, in that it seems that a periodic topographic cue is able to induce guidance. Indeed, in a very recent study rectangular and hexagonal arrays of pillars of

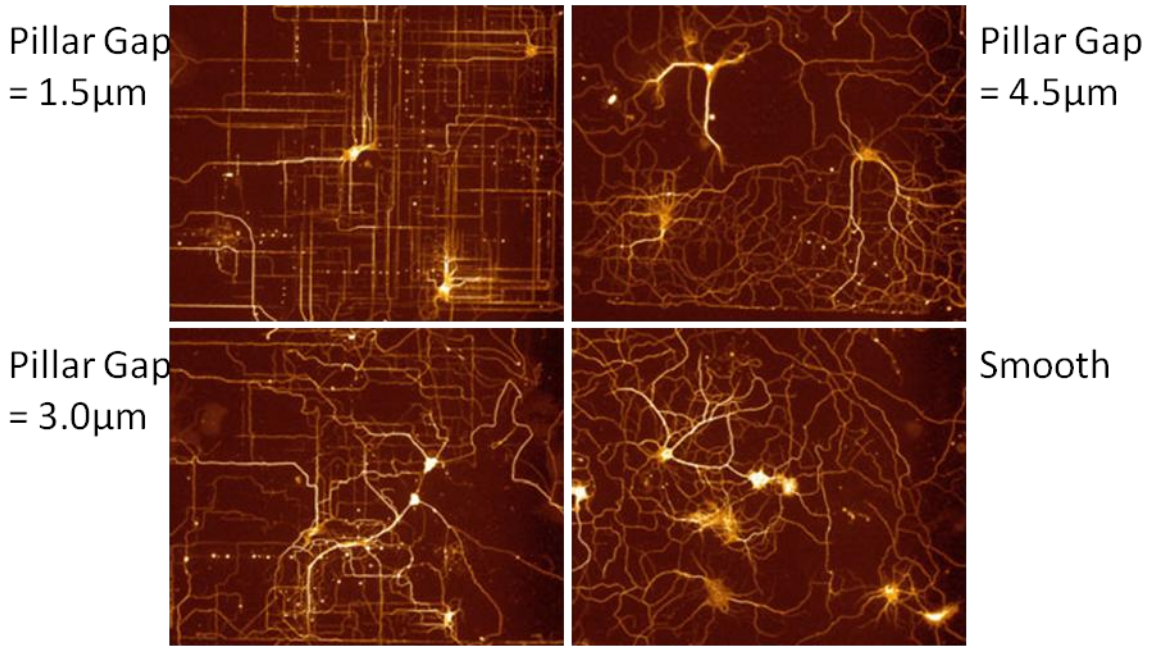

Figure 4 Neurite outgrowth on micro pillar arrays of variable spacing
Micro pillars of 2 μm diameter were patterned onto a silicon surface. Hippocampal neurons stained for tubulin are shown here, revealing a tendency to grow very straight when the array spacing is small. Adapted with permission[48].

constant size (1.6 μm diameter, 3 um height) were given variable spacing of 0.6, 1.4, 1.8 or 4.0 μm. It was found that the neurite outgrowth was maximized when the spacing was 1.4 μm[49].

A recent study examined neuritogenesis of hippocampal neurons located in proximity to a nanopillar array. It was found that independent of pillar dimension, neurites would bud in the direction of the topographic features[50]. Another interesting use of nanopillars was demonstrated

by one group who showed that arrays of nanopillars would anchor attached neurons, reducing cell mobility, a desirable result for neurons that are patterned for electrophysiological measurement[51]. The effect of nanopores is less pronounced, but they have been shown to strongly influence filopodial behavior[52], and also in another case, to decrease neurite development[53].

1.4.3 Anisotropic Topography

Aligned Fibers Electrospun fibers present a quick and convenient method for creating tissue scaffolding on the scale of ECM matter. Cellular response on electospun fibers has been reviewed relatively recently[54]. Neuronal response, especially orientation, on aligned fibers may be very pronounced. In one study with varying degrees of fiber alignment, it was found that the alignment did not influence the number of cells with an axon, or overall axon length, but aligned fibers did directionally guide the axons along the fibers. The electrospun scaffold did, however, increase polarization relative to a smooth control [55]. In another study, the effect of fiber diameter, varied from 300nm to 1500nm, on neural stem cells was examined. Neurite outgrowth was parallel to the fibers, independent of size, but more cell differentiation was seen on the small fibers[56]. In another study, dorsal root ganglia explants were cultured on fibers with diameters of 293, 759, and 1325 nm. Neurites extended up to 70% longer on the fibers of larger diameter[57].

Grooved Substrata The most commonly studied anisotropic topographical surface is the grooved substrate. A rectangular profile is most common, being characterized by a groove depth, groove width and ridge width. Large scale features (>10μm) evoke different behavioral responses than smaller features. Parallel alignment of neurite outgrowth on 100 μm wide grooves with depths from 21 to 69 μm[58], and 100-250 μm wide grooves with depths of 150 μm[59]

has been reported. While parallel alignment is seen on large features, it seems that the effect is due more to constraint or confinement, than to providing guidance to the growing neuron. In one study, it was reported that a step size of 21 μm would prevent growing neurites from crossing. Even at 11 μm many of the neurites would turn, depending on the angle of approach, and travel parallel rather than cross[58]. And in another study, it was reported that walls as small as 4.7 μm were sufficient to prevent neurite crossing[60]. Most likely the mechanisms of parallel alignment may vary, depending on feature size.

On grooves of sub-cellular dimensions, parallel alignment of neurites to grooves has frequently been reported. Dorsal root ganglia aligned parallel to grooves 2 μm wide and 1 μm deep, an effect which increased with depth[61]. Consistent results were also observed on grooves composed of biodegradable polymers[62]. Hippocampal neurons aligned parallel, and interestingly, sometimes perpendicular to grooves of 2 μm and 300 nm dimensions[63]. Perpendicular and parallel alignment to grooves by hippocampal neurons was reported earlier by Rajnicek and colleagues. Neurons grew parallel to grooves that were 4 μm wide, 1.1 μm deep grooves, but perpendicular to 1 μm wide and 130 nm deep grooves[60]. Another study found that axons grew strongly parallel 2 μm wide, 800 nm deep grooves, but more perpendicular to 1 μm wide, 400 nm deep grooves[64]. It is interesting that the perpendicular guidance effect has not been reported on other scaffolds, such as on electro-spun fibers.

The effect of grooves of nano-scale dimensions on neuron behavior has received direct attention. It was found 500 nm grooves resulted in better alignment, partly due constrained focal adhesion formation, than what was accomplished by wider grooves[65]. Similarly ridges of 300nm depth and variable width were found to have better aligned focal adhesions on narrower ridges[66]. Ridges of 350 nm height and width were found to have a strong impact on filopodia of growth

cones, resulting in alignment and stability relative to unaligned filopodia[67]. On ridges of 300 nm height, from 100-1600 nm width, it was found that growing neurons would align with the features. Particularly of interest is the observation that they would align only on the ridge tops, not within the grooves[68].

Another interesting aspect to consider is the profile of the grooves. Aligned fibers will exhibit a periodic concave down profile. Most grooves substrata have rectangular profiles. Sinusoidal profiles have given consistent results as rectangular profiles of similar dimensions[69]. An interesting study looked at the effect on fibroblasts of changing the radius of curvature of the edges of a rectangular groove profile, finding better alignment on grooves with 'sharper' corners[70]. This is an area still in need of continued exploration.

1.4.4 Special Cases of Topographical Guidance

Some special cases of unique neuronal behavior on varying topographies deserves mention. In one study, polymer nanofibers were aligned, not with the surface, but at angle relative to vertical, giving the substrate a nano-topographic asymmetry. This asymmetry led to a bias in axonal growth direction, consistent with the model of a biased self-avoiding walk[71]. It has also been demonstrated in one study that motor neurons could grow through a silicon micro-tube[72], and in another that rolled silicon/germanium tubes could be sized to permit growth of a single axon through a tube[73]. These experiments show promise in creating a model surface to simulate myelination. Another interesting study showed that DRG neurons were capable of forming bridges, without any intermediate contact support, across wide grooves. The neurons would start in the groove, grow onto both adjacent plateaus, and then tensile forces would lift the neuron out of the groove. This happened most frequently across grooves which were 30 μm

wide and 50 μm deep[74]. A final interesting study worth mentioning consisted of growing neurons on single filaments of various diameters. As the filament diameter decreased from a diameter of 500 μm down to 30 μm, neurons were constrained to extend axons only in the axial direction of the filament. Moreover, growth on larger diameter filaments was also constrained such that growing axons displayed a minimum acceptable radius of curvature, the critical curvature, which was measured to be 257 μm. Thus the growing axons could wrap helically around the larger filaments, but were constrained to grow straight on the smaller ones[75].

1.5 Combination of Topographical and Chemical Patterning

1.5.1 Chemistry or Topography?

There remains a question still somewhat ambiguous when considering the growth of cells on patterned chemical or topographical surfaces: What are the relative roles of chemistry and topography? This question has been asked since some of the earliest days of modern methods of surface modification for directed cell growth[76, 77]. Much of the controversy exists because of the difficulty in completely isolating one type of cue from the other. Chemical micropatterns, themselves, have an inherent topography, whether or not the researcher tried to pattern topographically. And surface topography will create distinct chemical landscapes, especially along edges of features, where adsorption of proteins within the growth medium may be altered. The actual effects of topography on protein adsorption, remains a dynamic field of study with little consensus, as discussed in a recent review[78]. An example that illustrates this difficulty is presented in a recent study which found that neurons preferred to grow along the edge of micro-printed laminin stripes, an effect which increased with laminin concentration. This was attributed to the authors by the growth cone responding to the steepness in gradient of the

laminin[79]. However, the stripes have an inherent topography, which also would have likely increased with laminin concentration, although this measurement was not reported. A researcher focused on topography might have insisted topography, not the gradient of laminin concentration, causes the neurons to grow on the edges. As cells in their natural environment never truly encounter only chemical or only topographical cues, it is necessary to develop platforms to study the combination of the two.

1.5.2 Combination of Cues: Cooperation and Competition

The examination of the combined effects of topography and chemistry on neuronal behavior has taken one of two forms. Most commonly, the modulatory effect of different biochemical coatings on a particular topographical surface are studied. For example, laminin added to a grooved substrate enhanced neurite outgrowth[62], as it also did when added to a nanofiber substrate[80]. An improvement of neural cell adhesion and outgrowth was reported for grooves modified with a laminin derivative[81], while neuritogenesis was strongly influenced by topographic scale at low concentrations of nerve growth factor (NGF), but independent of topography at higher NGF

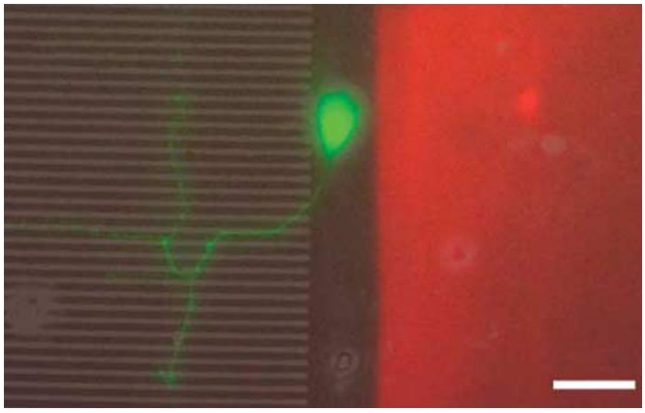

Figure 5 Competitive Cues
A hippocampal neuron, located in proximity to 2 μm grooves and immobilized NGF prefers to polarize into the topographically modified landscape. Scale bar: 25 μm. Figure adapted with permission[83].

concentrations[82].

While studying the modulatory effects of uniform chemical coatings is an important undertaking, it is perhaps even more fascinating to create competitive guidance platforms. One group selectively patterned one region with grooves, and another with NGF. Hippocampal neurons, fortuitously adhering between the regions, were seen to polarize most commonly into the topographical features (Figure 5), an effect which strengthened for narrower grooves[83]. In another study, grooves fabricated with PDMS were uniformly coated with PDL. Growing neurites, when encountering an edge, would either grow down into the groove, or remain on the ridge, depending on the angle of approach. But when the entire surface was also coated with matrigel, neurites would grow straight off of ridges into the matrigel, even though this meant losing contact with the PDL coated surface[58]. Very recent work combined arrays of micro-pillars with gradients of Netrin-1 (Net1), a chemoattractant, or with gradients of Semaphorin 3A (Sema3A), a chemorepellant. A Net1 gradient, superimposed on the pillar array, showed that the pillars and the attractive Net1 worked synergistically to guide neurite outgrowth. When a Sema3A gradient was superimposed over the topography mixed results were seen. For a spacing of 0.6 μm and 4 μm, the Sema3A was able to repel the neurites. But for a spacing of 1.4 μm and 1.8 μm, no significant repulsion was observed[49]. Thus the scale of the topography was influential in modulating the response of the extending neurites to the repulsive cue. Although studying the effect of competitive guidance cues has great potential, studies deliberately created for this purpose are relatively few. This should be an area of increased focus in coming years.

1.6 Summary

Neuronal behavior is strongly influenced by the physical micro/nano environment. The geometry and scale of patterned chemical cues is distinctly important in defining neuronal response, especially influencing polarization, outgrowth, and connectivity. Isotropic topographical features also have a pronounced effect on neuronal outgrowth and other behavior. Together, topographical and chemical cues compose much of the native environment of neurons *in vivo*. Understanding the relative roles of each type of cue, in isolation and especially in combination, is of immeasurably importance in our study of the nervous system.

1.7 References

1 T. R. Insel, S. C. Landis and F. C. Collins, The NIH BRAIN Initiative, *Science*, 2013, **340**, 687-688.

2 R. L. Sidman and P. Rakic, Neuronal migration, with special reference to developing human brain: a review, *Brain Research*, 1973, **62**, 1-35.

3 J. W. Faweet and R. J. Keynes, Peripheral nerve regeneration, *Annual Review of Neuroscience*, 1990, **13**, 43-60.

4 J. Silver and J. H. Miller, Regeneration beyond the glial scar, *Nature Reviews Neuroscience*, 2004, **5**, 146-156.

5 M. Tessier-Lavigne and C. S. Goodman, The molecular biology of axon guidance, *Science*, 1996, **274**, 1123-1133.

6 P. Malatesta, I. Appolloni and F. Calzolari, Radial glia and neural stem cells, *Cell and Tissue Research*, 2008, **331**, 165-178.

7 K. Ono and K. Kawamura, Migration of immature neurons along tangentially oriented fibers in the subpial part of the fetal mouse medulla oblongata, *Experimental Brain Research*, 1989, **78**, 290-300.

8 J. R. Jacobs and C. S. Goodman, Embryonic development of axon pathways in the Drosophila CNS. I. A glial scaffold appears before the first growth cones, *The Journal of Neuroscience*, 1989, **9**, 2402-2411.

9 R. Segev, M. Benveniste, E. Hulata, N. Cohen, A. Palevski, E. Kapon, Y. Shapira and E. Ben-Jacob, Long term behavior of lithographically prepared in vitro neuronal networks, *Physical Review Letters*, 2002, **88**, 118102.

10 D. Falconnet, G. Csucs, H. Michelle Grandin and M. Textor, Surface engineering approaches to micropattern surfaces for cell-based assays, *Biomaterials*, 2006, **27**, 3044-3063.

11 S. Khan and G. Newaz, A comprehensive review of surface modification for neural cell adhesion and patterning, *Journal of Biomedical Materials Research Part A*, 2010, **93**, 1209-1224.

12 M. Théry, Micropatterning as a tool to decipher cell morphogenesis and functions, *Journal of Cell Science*, 2010, **123**, 4201-4213.

13 R. S. Kane, S. Takayama, E. Ostuni, D. E. Ingber and G. M. Whitesides, Patterning proteins and cells using soft lithography, *Biomaterials*, 1999, **20**, 2363-2376.

14 C. Staii, C. Viesselmann, J. Ballweg, L. Shi, G.Y. Liu, J. C. Williams, E. W. Dent, S. N. Coppersmith and M. A. Eriksson, Positioning and guidance of neurons on gold surfaces by directed assembly of proteins using atomic force microscopy, *Biomaterials*, 2009, **30**, 3397.

15 B. Kaehr, R. Allen, D. J. Javier, J. Currie and J. B. Shear, Guiding neuronal development with in situ microfabrication, *Proceedings of the National Academy of Sciences of the United States of America*, 2004, **101**, 16104-16108.

16 R. D. Piner, J. Zhu, F. Xu, S. Hong and C. A. Mirkin, Dip-pen nanolithography, *Science*, 1999, **283**, 661-663.

17 E. A. Roth, T. Xu, M. Das, C. Gregory, J. J. Hickman and T. Boland, Inkjet printing for high-throughput cell patterning, *Biomaterials*, 2004, **25**, 3707-3715.

18 A. Kumar and G. M. Whitesides, Features of gold having micrometer to centimeter dimensions can be formed through a combination of stamping with an elastomeric stamp and an alkanethiol "ink" followed by chemical etching, *Applied Physics Letters*, 1993, **63**, 2002.

19 F. Johansson, P. Carlberg, N. Danielsen, L. Montelius and M. Kanje, Axonal outgrowth on nano-imprinted patterns, *Biomaterials*, 2006, **27**, 1251-1258.

20 F. Turcu, K. Tratsk-Nitz, S. Thano, W. Schuhmann and P. Heiduschka, Ink-jet printing for micropattern generation of laminin for neuronal adhesion, *Journal of Neuroscience Methods*, 2003, **131**, 141-148.

21 N. E. Sanjana and S. B. Fuller, A fast flexible ink-jet printing method for patterning dissociated neurons in culture, *Journal of Neuroscience Methods*, 2004, **136**, 151-163.

22 D. Soltman and V Subramanian, Inkjet-printed line morphologies and temperature control of the coffee ring effect, *Langmuir*, 2008, **24**, 2224-2231.

23 T. G. Allen, Preparation and maintenance of single-cell micro-island cultures of basal forebrain neurons, *Nature Protocols*, 2007, **1**, 2543-2550.

24 D. Martinez, C. Py, M. Denhoff, R. Monette, T. Comas, A. Krantis and G. Mealing, Polymer peel-off mask for high resolution surface derivatization, neuron placement and guidance, *Biotechnology and Bioengineering*, 2013.

25 M. J. Jang and Y. Nam, Geometric effect of cell adhesive polygonal micropatterns on neuritogenesis and axon guidance, *Journal of Neural Engineering*, 2012, **9**, 046019.

26 Z. D. Wissner-Gross, M. A. Scott, D. Ku, P. Ramaswamy and M. F. Yanik, Large-scale analysis of neurite growth dynamics on micropatterned substrates, *Integrative Biology*, 2011, **3**, 65-74.

27 M. Song and K. E. Uhrich, Optimal micropattern dimensions enhance neurite outgrowth rates, lengths, and orientations, *Annals of Biomedical Engineering*, 2007, **35**, 1812-1820.

28 H. C. Tai and H. M Buettner, Neurite outgrowth and growth cone morphology on micropatterned surfaces, *Biotechnology Progress*, 1998, **14**, 364-370.

29 P. Clark, S. Britland and P. Connolly, Growth cone guidance and neuron morphology on micropatterned laminin surfaces, *Journal of Cell Science*, 1993, **105**, 203-212.

30 D. Schwaab, Surface patterning by means of soft lithography for molecular and bio-electronics, Phd diss., 2007, Forschungszentrum, Zentralbibliotek.

31 A. Offenhäusser, S. Böker-Meffert, T. Decker, R. Helpenstein, P. Gasteier, J. Groll, M. Möller, A. Reska, S. Schäfer, P. Schulte and A. Vogt-Eisele, Microcontact printing of proteins for neuronal cell guidance, *Soft Matter*, 2007, **3**, 290-298.

32 A. A. Oliva Jr, C. D. James, C. E. Kingman, H. G. Craighead and G. A. Banker, Patterning axonal guidance molecules using a novel strategy for microcontact printing, *Neurochemical Research*, 2003, **28**, 1639-1648.

33 B. Liu, J. Ma, E. Gao, Y. He, F. Cui and Q. Xu, Development of an artificial neuronal network with post-mitotic rat fetal hippocampal cells by polyethylenimine, *Biosensors and Biolectronics*, 2008, **23**, 1221-1228.

34 K. Kang, G. Kang, B. S. Lee, I. S. Choi and Y. Nam, Generation of patterned neuronal networks on cell-repellant poly-ACHTUNGTRENNUNG (oligo (ethylene glycol) methacrylate) films, *Chemistry an Asian Journal*, 2010, **5**, 1804-1809.

35 N. S. Baek, Y. H. Kim, Y. H. Han, B. J. Lee, T. D. Kim, S. T. Kim, Y. S. Choi, G. H. Kim, M. A. Chung and S. D. Jung, Facile photopatterning of polyfluorene for patterned neuronal networks, *Soft Matter*, 2011, **7**, 10025-10031.

36 N. P. Huang, J. C. Shi, Y. Y. Wang and H. Yu, Simple fabrication of PEG-based chemical micropatterns for neural network formation, *Biomedical Engineering and Informatics (BMEI), 2011 4th International Conference*, **3**, 1256-1259.

37 A. K. Vogt, G. J. Brewer and A. Offenhäusser, Connectivity patterns in neuronal networks of experimentally defined geometry, *Tissue Engineering*, 2005, **11**, 1757-1767.

38 A. K. Vogt, G. J. Brewer, T. Decker, S. Böcker-Meffert, V. Jacobsen, M. Kreiter, W. Knoll and A. Offenhäusser, Independence of synaptic specificity from neuritic guidance, *Neuroscience*, 2004, **134**, 783-790.

39 D. A. Stenger, J. J. Hickman, K. E. Bateman, M. S. Ravenscroft, W. Ma, J. J. Pancrazio, K. Shaffer, A. E. Schaffner, D. H. Cribbs and C. W. Cotman, Microlithographic determination of axonal/dendritic polarity in cultured hippocampal neurons, *Journal of Neuroscience Methods*, 1998, **82**, 167-173.

40 A. K. Vogt, F. D. Stefani, A. Best, G. Nelles, A. Yasuda, W. Knoll and A. Offenhäusser, Impact of micropatterned surfaces on neuronal polarity, *Journal of Neuroscience Methods*, 2004, **134**, 191-198.

41 M. A. Scott, Z. D. Wissner-Gross and M. F. Yanik, Ultra-rapid laser protein Micropatterning: screening for directed polarization of single neurons, *Lab on a Chip*, 2012, **12**, 2265-2276.

42 S. Roth, M. Bisbal, J. Brocard, G. Bugnicourt, Y. Saoudi, A. Andrieux, S. Gory-Fauré and C. Villard, How morphological constraints affect axonal polarity in mouse neurons, *PloS one*, 2012, **7**, e33623.

43 L. A. Cyster, K. G. Parker, T. L. Parker and D. M. Grant, The effect of surface chemistry and nanotopography of titanium nitride (TiN) films on primary hippocampal neurons, *Biomaterials*, 2004, **25**, 97-107.

44 S. P. Khan, G. G. Auner and G. m Newaz, Influence of nanoscale surface roughness on neural cell attachment on silicon, *Nanomedicine: Nanotechnology, Biology and Medicine*, 2005, **1**, 125-129.

45 Y. W. Fan, F. Z. Cui, S. P. Hou, Q. Y. Xu, L. N. Chen, and I. S. Lee, Culture of neural cells on silicon wafers with nano-scale surface topograph, *Journal of Neuroscience Methods*, 2002, **120**, 17-23.

46 V. Brunetti, G. Maiorano, L. Rizzelo, B. Sorce, S. Sabella, R. Cingolani and P. P. Pompa, Neurons sense nanoscale roughness with nanometer sensitivity, *Proceedings of the National Academy of Science*, 2010, **107**, 6264-6269.

47 J. N. Hanson, M. J. Motala, M. L. Heien, M. Gillette, J. Sweedler and R. G. Nuzzo, Textural guidance cues for controlling process outgrowth of mammalian neurons, *Lab on a Chip*, 2009, **9**, 122-131.

48 N. M. Dowell-Mesfin, M. A. Abdul-Karim, A. M. P. Turner, S. Schanz, H. G. Craighead, B. Roysam, J. N. Turner and W. Shain, Topographically modified surfaces affect orientation and growth of hippocampal neurons, *Journal of Neural Engineering*, 2004, **1**, 78.

49 A. Kundu, L. Micholt, S. Friedrich, D. R. Rand, C. Bartic, D. Braeken and A. Levchenko, Superimposed topographic and chemical cues synergistically guide neurite outgrowth, *Lab on a Chip*, 2013.

50 L. Micholt, A. Gärtner, D. Prodanov, D. Braeken, C. G. Dotti and C. Bartic, Substrate topography determines neuronal polarization and growth in vitro, *PloS One*, 2013, **8**, e66170.

51 C. Xie, L. Hanson, W. Xie, Z. Lin, B. Cui and Y. Cui, Noninvasive neuron pinning with nanopillar arrays, *Nano Letter*, 2010, **10**, 4020-4024.

52 M. J. Dalby, N. Gadegaard, M. O. Riehle, C. D. Wilkinson and A. S. Curtis, Investigating filopodia sensing using arrays of defined nano-pits down to 35 nm diameter in size, *The International Journal of Biochemistry & Cell Biology*, 2004, **36**, 2005-2015.

53 F. Haq, V. Anandan, C. Keith and G. Zhang, Neurite development in PC12 cells cultured on nanopillars and nanopores with sizeds comparable with filopodia, *International Journal of Nanomedicine*, 2007, **2**, 107.

54 D. R. Nisbet, J. S. Forsythe, W. Shen, D. I. Finkelstein and M. K. Horne, Review paper: a review of the cellular response on electrospun nanofibers for tissue engineering, *Journal of Biomaterials Applications*, 2009, **24**, 7-29.

55 J. Y. Lee, C. A. Bashur, N. Gomez, A. S. Goldstein and C. E. Schmidt, Enhanced polarization of embryonic hippocampal neurons on micron scale electrospun fibers, *Journal of Biomedical Materials Research Part A*, 2010, **92**, 1398-1406.

56 F. Yang, R. Murugan, S. Wang and S. Ramakrishna, Electrospinning of nano/micro scale poly (L-lactic acid) aligned fibers and their potential in neural tissue engineering, *Biomaterials*, 2005, **26**, 2603-2610.

57 H. B. Wang, M. E. Mullins, J. M. Cregg, C. W. McCarthy and R. J. Gilbert, Varying the diameter of aligned electrospun fibers alters neurite outgrowth and Schwann cell migration, *Acta Biomaterialia*, 2010, **6**, 2970-2978.

58 N. Li and A. Folch, Integration of topographical and biochemical cues by axons during growth on microfabricated 3-D susbstrates, *Experimental Cell Research*, 2005, **311**, 307-316.

59 T. Houchin-Ray, L.A. Swift, J. H. Jang and L. D. Shea, Patterned PLG substrates for localized DNA delivery and directed neurite extension, *Biomaterials*, 2007, **28**, 2603-2611.

60 A. Rajnicek, S. Britland and C. McCaig, Contact guidance of CNS neurites on grooved quartz: influence of groove dimensions, neuronal age and cell type, *Journal of Cell Science*, 1997, **110**, 2905-2913.

61 T. Hirono, K. Torimitsu, A. Kawana and J. Fukuda, Recognition of artificial microstructures by sensory nerve fibers in culture, *Brain Research*, 1988, **446**, 189-194.

62 C. Miller, J. Srdija and S. Mallapragada, Synergistic effects of physical and chemical guidance cues on neurite alignment and outgrowth on biodegradable polymer substrates, *Tissue Engineering*, 2002, **8**, 367-378.

63 D. Y. Fozdar, J. Y. Lee, C. E. Schmidt and S. Chen, Hippocampal neurons respond uniquely to topographies of various sizes and shapes.

64 N. Gomez, Y. Lu, S. Chen and C. E. Schmidt, Immobilized nerve growth factor and microtopography have distinct effects on polarization versus axon elongation in hippocampal cells in culture, *Biomaterials*, 2007, **28**, 271-284.

65 A. Ferrari, M. Cecchini, A. Dhawan, S. Micera, I. Tonazzini, R. Stabile, D. Pisignano and F. Beltram, Nanotopographic control of neuronal polarity, *Nano Letters*, 2011, **11**, 505-511.

66 P. Wieringa, I. Tonazzini, S. Micera and M. Cecchini, Nanotopography induced contact guidance of the F11 cell line during neuronal differentiation: a neuronal model cell line for tissue scaffold development, *Nanotechnology*, 2012, **23**, 275102.

67 K. J. Jang, M. S. Kim, D. Feltrin, N. L. Jeon, K. Y. Suh and O. Pertz, Two distinct filopodia populations at the growth cone allow to sense nanotopographical extracellular matrix cues to guide neurite outgrowth, *PloS One*, 2010, **5**, e15966.

68 F. Johansson, P. Carlberg, N. Danielsen, L. Montelius and M. Kanje, Axonal outgrowth on nano-imprinted patterns, *Biomaterials*, 2006, **26**, 1251-1258.

69 J. K. Lee, H. Baac, S. H. Song, S. D. Lee, D. Park and S. J. Kim, The topographical guidance of neurons cultured on holographic photo-responsive polymer, *Engineering in Medicine and Biology Society, 2004, IEMBS'04, 26th Annual International Conference of the IEEE*, 2004, **2**, 4970-4973.

70 A. Mathur, S. W. Moore, M. P. Sheetz and J. Hone, The role of feature curvature in contact guidance, *Acta Biomaterialia*, 2012, **8**, 2595-2601.

71 R. Beighley, E. Spedden, K. Sekeroglu, T. Atherton, M C. Demirel and C. Staii, Neuronal alignment on asymmetric textured surfaces, *Applied Physics Letters*, 2012, **101**, 143701-143701.

72 S. Shulze, G. Huang, M. Krause, D. Aubyn, V. A. B. Quiñones, C. K. Schmidt, Y. Mei and O. G. Schmidt, Morphological differentiation of neurons on microtopographic substrates fabricated by rolled-up nanotechnology, *Advanced Engineering Materials*, 2010, **12**, B558-B564.

73 M. Yu, Y. Huang, J. Ballweg, H. Shin, M. Huang, D. Savage, M. G. Lagally, E. W. Dent, R. H. Blick and J. C. Williams, Semiconductor nanomembrane tubes: three-dimensional confinement for controlled neurite outgrowth, *ACS Nano*, 2011, **5**, 2447-2457.

74 J. S. Goldner, J. M. Bruder, G. Li, D. Gazzola and D. Hoffman-Kim, Neurite bridging across micropatterned grooves, *Biomaterials*, 2006, **27**, 460-472.

75 R. M. Smeal, R. Rabbitt, R. Biran and P. A. Tresco, Substrate curvature influences the direction of nerve outgrowth, *Annals of Biomedial Engineering*, 2005, **33**, 376-382.

76 A. S. Curtis and C. D. Wilkinson, Reaction of cells to topography, *Journal of Biomaterials Science, Polymer Edition*, 1998, **9**, 1313-1329.

77 A. Curtis and C. Wilkinson, Nantotechniques and approaches in biotechnology, *TRENDS in Biotechnology*, 2001, **19**, 97-101.

78 M. S. Lord, M. Foss and F. Besenbacher, Influence of nanoscale surface topography on protein adsorption and cellular response, *Nano Today*, 2010, **5**, 66-78.

79 S. Xing, W. Liu, Z. Huang, L. Chen, K. Sun, D. Han, W. Zhang and X. Jiang, Development of neurons on micropatterns reveals that growth cone responds to a sharp change of concentration of laminin, *Electrophoresis*, 2010, **31**, 3144-3151.

80 H. S. Koh, T. Yong, C. K. Chan and S. Ramakrishna, Enhancement of neurite outgrowth using nano-structured scaffolds coupled with laminin, *Biomaterials*, 2008, **29**, 3574-3582.

81 T. T. Yu and M. S. Shoichet, Guided cell adhesion and outgrowth in peptide-modified channels for neural tissue engineering, *Biomaterials*, 2005, **26**, 1507-1514.

82 J. D. Foley, E. W. Grunwald, P. F. Nealey and C. J. Murphy, Cooperative modulation of neuritogenesis by PC12 cells by topography and nerve growth factor, *Biomaterials*, 2005, **26**, 3639-3644.

83 N. Gomez, S. Chen, and C. E. Schmidt, Polarization of hippocampal neurons with competitive surface stimuli: contact guidance cues are preferred over chemical ligands, *Journal of The Royal Society Interface*, 2007, **4**, 223-233.

2.1 Title:

Adhesive Micro-Line Periodicity Determines Guidance of Axonal Outgrowth

2.2 Abstract

Adhesive micro-lines of various sub-cellular geometries were created using a non-traditional micro stamping technique. This technique employed the use of commercially available diffraction gratings as the molds for the micro stamps, a method which is quick and inexpensive, and which could easily be adopted as a patterning tool in a variety of research efforts. The atypical saw-tooth profile of the micro stamps enabled a unique degree of control and flexibility over patterned line and gap widths. Cortical neurons cultured on patterned poly-lysine micro-lines on PDMS exhibit a startling transition in axonal guidance: From the expected parallel guidance to an unexpected perpendicular guidance that becomes dominant as patterned lines and gaps become sufficiently narrow. This transition is most obvious when the lines are narrow relative to gaps, while the periodicity of the pattern is reduced. Axons growing perpendicular to micro-lines exhibited 'vinculated' growth, a unique morphological phenotype consisting of periodic orthogonal extensions along the axon. Additionally, as an example of design capability, micro-line stamps were used to study neurite behavior on an orthogonal poly-lysine grid of constant grid size, but variable line width. Grids formed with narrow lines were far less likely to induce turning in growing neurites.

2.3 Introduction

The ability to guide and direct the growth of axons with engineered precision is an on-going endeavor with broad implications for many diverse areas of research. These include implantable devices for nervous system injury recovery[1], the study of neurological disorders and diseases,[2] efforts to create well-defined neural networks,[3-4] as well as basic neuroscience investigations, such as signal transduction[5] and growth cone biomechanics.[6] While many efforts at the interface of engineering and neuroscience have yielded encouraging results, many avenues, including even the very accessible, have been left unexplored.

Surface patterning to direct cellular behavior is achieved through a variety of methods.[7] When patterning parallel lines to study neuron outgrowth, however, one of two motivations usually dictates the design parameters. For patterning ease, commonly both the patterned lines and gaps are relatively wide,[8-9] or for cell isolation, relatively narrow lines are separated by large gaps.[10] While axonal guidance response on typically patterned micro-lines is relatively well characterized, guidance on parallel patterned lines *and* gaps of small, sub-cellular dimensions is not. To understand the cause of this knowledge deficit, consideration of the following aspects of micropattern creation is useful: To create patterns over a 'large' area (> 1 mm^2), a useful size for studying statistically relevant sample sizes, relatively inexpensive methods such as micro-stamping (or micro-contact printing) are typically employed. But to create a microstamp with single-micron scale features requires an expensive mask. Moreover, if the desired features are parallel lines with equally small gaps, defects[11] may become too overwhelming to make this approach attractive. On the other hand, patterning at fairly high (~1 μm) resolution has been

accomplished by a variety of alternative techniques. However, these techniques are generally not well suited to pattern over a large area and require specialized and costly equipment and training. To create a large-scale pattern of parallel lines would be tedious. Moreover, the intuitive, widely-accepted paradigm of neuronal line guidance is that if patterned lines are spaced too closely, growth will simply become increasingly random. [12]

In this work, a non-traditional method of micro-stamping was employed. Commercially available diffraction gratings were used in lieu of a standard silicon master to create micro stamps. Although using stamps from diffraction gratings to create micropatterns has been previously accomplished,[13] such patterns have not been employed for cellular research generally, or for neural patterning specifically. These micro-line stamps have several advantages relative to traditional micro-stamps. They are very inexpensive and require only very simple fabrication techniques, and simultaneously grant access to single-micron resolution patterning. Although traditional micro-stamping is already viewed as reasonably accessible, the method presented here is exceedingly more so. Also, unlike many other high-resolution patterning schemes, this technique requires no expensive equipment and can be very easily adopted without specialized training. In spite of intrinsic pattern limitations due to commercial availability and design, this approach of micro-line stamping could easily be adopted by biology-based labs to perform a wide variety of experiments. Indeed, this study will show that neurons cultured on these micro-lines display extremely diverse modes of guidance, dependent primarily on the geometry of the underlying pattern. It is as of yet unclear whether there is a strong *in* vivo corollary for the results presented here. What is clear, though, is that the axon outgrowth behavior is non-intuitive and would be difficult or impossible to predict *in vivo* without the *in vitro* results made possible by this micro-line methodology.

Another interesting facet is that these stamps have an atypical surface profile (saw tooth vs. traditional rectangular). Thus, the stamped line width is easily tunable, a possibility previously conceived[14] and demonstrated,[15] yet heretofore unexploited in any biological experiment. Compared with the burdensome process of designing a line assay or other experiments with easily varied line widths using traditional micro stamps, this approach is quick and efficient. The scale of patterning is also of particular interest, given the large body of work devoted to neurite guidance on topographic features of similar scale in the lateral dimensions.[16-18]

2.4 Materials and Methods

2.4.1 *PDMS Micro-Stamp and Culture Substrate Creation*

Reflective ruled diffraction gratings were bought commercially (Optometrics). Diffraction gratings are characterized by two measurements: grooves per millimeter (g/mm) and

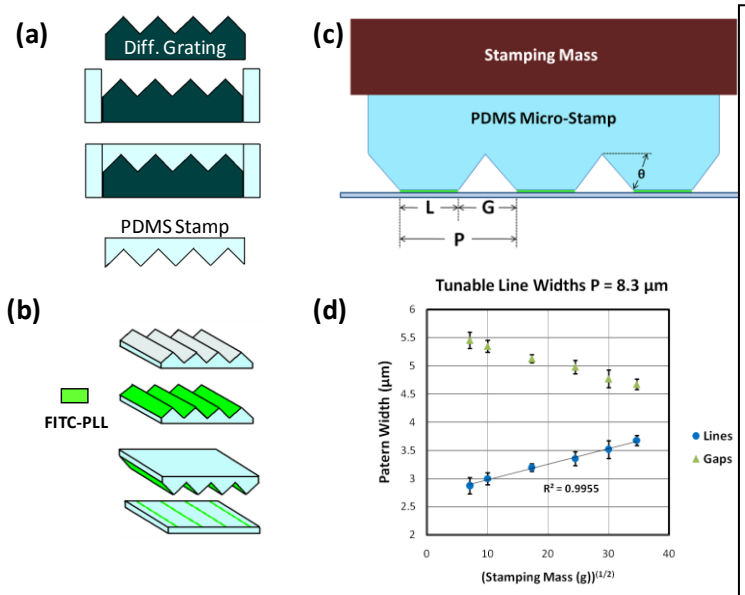

Figure 1. Stamp Fabrication and Characterization
(a) PDMS micro-stamps are molded off of a commercially-available diffraction grating. **(b)** PDMS stamps are inked with FITC-PLL, inverted and stamped onto surface (PDMS) with controlled force. **(c)** As stamping mass is increased, thus compressing the PDMS stamp, patterned line width (L) becomes larger and the gap width (G) becomes smaller in a codependent relationship with the periodicity (P) (L + G = P). θ is the blaze angle. **(d)** Increasing stamping force yields patterned lines (or gaps) of greater (lesser) width in a predictable manner. The line width scales with the mass (or equivalently, force) raised to the ½ power. Error bars: ± standard error (SE).

blaze angle (θ) (Fig. 1c). The blaze angle determines the degree of asymmetry of the surface profile, with a 45° angle being perfectly symmetric. In this study gratings with dimensions of 120 g/mm (θ=46° 3'), 150 g/mm (θ=35°), 300 g/mm (θ=36° 52'), and 600 g/mm (θ=28° 41') were used. These correspond to a line periodicity of 8.3µm, 6.7µm, 3.3µm, and 1.7µm, respectively. All gratings (and stamps) have surface areal dimensions of 12.75mmx12.75mm. Gratings were inserted into a custom made polydimethylsiloxane (PDMS) mold. PDMS (184 Sylgard – Dow Corning) was mixed in a 10:1 ratio (base: curing agent), poured into the mold, and baked on a covered hot plate for 30 min. at 85°C. The newly formed PDMS stamp was cut out and stored until inking, while the grating could be reused indefinitely. For the culture substrates, uncured PDMS (10:1) was poured into a 100mm petri dish, allowed to settle until flat, and baked for 30 min. at 85°C. 2cm x 2cm squares were cut out of the cured thick film (~0.5 mm) and autoclaved for 1 hr at 120°C.

2.4.2 *Inking and Stamping*

PDMS micro-stamps were covered in FITC labeled poly-L-lysine (30-70 kDa, P3069 Sigma-Aldrich) at a 1 mg/ml concentration for 1 hour, after which the surface was twice washed with sterile, distilled, deionized water. This process was repeated 3 times, after which the stamps were allowed 30 min to dry. Immediately prior to stamping and after autoclaving, the PDMS culture substrate was briefly (20 sec.) air-plasma treated using a plasma wand (ETP Model BD-20) to enhance FITC-PLL transfer. The pattern transfer was performed by inverting the stamp, setting it on the PDMS substrate, and applying force orthogonal to the surface. To achieve calibration of narrow lines, masses from 50g to 1200g were placed upon the stamp. Wider lines (uncharacterized) were achieved by larger forces, applied directly by hand. After the force was

applied for 60 sec. the stamp was lifted off, and the substrate kept in a darkened location until culturing.

2.4.3 *Line Width Characterization*

Micro-lines were imaged fluorescently using a 20x objective on an inverted microscope, with images captured in MetaMorph. Line profiles were taken using Image J software, averaged over at least 30 μm. The edge of the line was defined as a 20% increase in fluorescent intensity from the background level. Characterizations were performed by performing at least 4 independent stamping tests for each stamp dimension. Each test consisted of a minimum of 20 line width measurements from 4 different locations on the stamped surface. To measure the line width on substrates used for culture, at least 20 measurements were made from 4 different locations and averaged.

2.4.4 *Neuron Cell Culture and Immunostaining*

All mouse procedures were approved by the University of Wisconsin Committee on Animal Care and were in accordance with NIH guidelines. Neurons used in this study were E15.5 cortical neurons from Swiss Webster mice. Cells were isolated and cultured according to established methods.[19] Briefly, cells were dissociated by treating with trypsin (0.25%, 15 min, 37 C), triturated with a micropipette tip, and diluted in plating medium (neurobasal medium with 5% FBS, Hyclone, B27 supplement, 2mMglutamine, 37.5mMNaCl, and 0.3% glucose). Cells were plated onto PDMS substrates at a density of 6,000 cells/cm^2. One hour later, the sample is flooded with serum-free medium (plating medium without FBS) and incubated for 48 hours. Neurons were fixed in 4% PKS[20] (PFA/Krebs Solution) at 37 C for 15 min to retain cytoskeletal

integrity, before being washed three times with PBS. Cells that are to be immuno-stained were permeabilized for 10 min in 0.2% Triton X-100 then washed once with 1% BSA/PBS before blocking in 10% BSA/PBS for an hour. Anti-tyrosinated tubulin antibodies (Millipore) were used to label dynamic microtubules and actin filaments were revealed using Alexa-647 labeled Phalloidin (Invitrogen).

2.4.5 *Imaging and Data Analysis*

Non-stained cells were imaged with a 20x phase objective inverted microscope, captured with Metamorph software. For each sample 80-100 cells were imaged. For each given condition, 4-6 independent samples were analyzed. Although cells in close proximity to other cells displayed consistent outgrowth behavior, cells were chosen that were relatively isolated for clarity. The outgrowth direction was determined by the angle between the micropattern and a line from the tip of the axon to the soma. All angular measurements were made using Image J software. Statistical analysis as follows: Axons growing in a given direction were grouped in 10° bins, and the relative percentages in each bin and across micro-line geometries were compared by Single Factor ANOVA. Stained cells were imaged at 100x in DIC and widefield using a Nikon TE2000 inverted fluorescence microscope and manipulated using Metamorph software. TIRF microscopy was used for imaging FITC-labeled PDL lines to increase contrast. Overlaid images were created using Image J. In images that include the label for actin filaments (blue), a despeckling processing was used to enhance the image.

2.5 Results

2.5.1 *PDMS Stamp Characterization*

The periodicity of printed lines was varied by molding polydimethylsiloxane (PDMS) stamps off of diffraction gratings of different geometries (Fig. 1). PDMS stamps were molded off of these gratings, inked with poly-lysine and stamped onto a smooth PDMS surface. A greater range of periodicity is possible, but beyond the scope of the present study.

All experiments used a PDMS surface stamped with poly-lysine micro-lines. Along with traits of biocompatibility and optical transparence, PDMS is attractive for its potential biomechanical adaptability, including control over surface topography,[21] substrate elasticity,[22] and surface hydrophobicity.[23] Moreover, an uncoated PDMS substrate offers a relatively non-permissive background to growing neurons, a feature which is desirable in micro-pattern stamping for neuronal guidance.[24]

A very distinctive feature of micro line stamps cast from diffraction gratings is the ability to tune the patterned line widths by varying the stamping force, a feature which arises from the saw-tooth profile of the diffraction gratings. Line width was controlled by varying the force on the microstamp during the pattern transfer (Fig. 1c). Larger forces cause an increase of line width (L) and a decrease in gap width (G), as determined by the periodicity (P) (L+G = P). Characterizations were performed using the stamp with P = 8.3 μm. These stamps also benefited from being nearly perfectly symmetric (θ=46° 3’). On PDMS surfaces, line widths from 2.9 μm to 3.7 μm were obtained by using a stamping mass from 50 g to 1200 g (Fig. 1d.). Line widths from 3.7 μm up to 6.4 μm were also obtained, though by hand as the mass placement method became impractical beyond the characterized range. Line widths from 2.2 μm to 4.8 μm and 1.7 μm to 2.3 μm were obtained with the 6.7 μm and 3.3 μm periodicity stamps, respectively. All

successful stamping attempts with the 1.7 μm periodicity stamp yielded a line width of 0.9 ±1 μm.

2.5.2 *Axonal Guidance on Poly-lysine Micro-Lines*

Cortical neurons were cultured on the poly-lysine micro-lines and their outgrowth direction measured after 48 hours. Angle of outgrowth is defined as the angle between the micro-lines and a straight line drawn from the soma to the tip of the presumptive axon. The presumptive axon was morphologically identified as a neurite that was at least twice the length of the next longest neurite, and at least 50 μm in length. If the axon exhibited branching, only the most distal tip was considered. The neurons exhibited excellent outgrowth on the patterned PDMS surface, with the majority of the cells developing presumptive axons. Although outgrowth direction was generally well established by 48 hrs (2DIV), many of the cells were viable for longer periods – up to 7 DIV (data not shown).

Axonal guidance on micro-lines with constant L, varying G: In the first set of experiments L (line width) was held relatively constant, while G (gap width) was varied, by means of varying P (periodicity). L was maintained at 2.55 ± 0.25 μm while values of G = 5.5 μm, 4.4 μm, and 1.1 μm, were obtained by stamps of P = 8.3 μm, 6.7 μm, and 3.3 μm, respectively (Fig 2a). For relatively large G, guidance was dominantly parallel to the lines. Although the growing axons showed the ability to explore the uncoated PDMS surface, they were commonly found to extend along a single line for hundreds of microns. The axonal alignment to the lines is not entirely unexpected. Interesting, though, was the prominence of a sub-population of axons whose guidance is localized about a perpendicular orientation to the patterned lines. In decreasing G to 4.4 μm, the dominant guidance is still parallel, though less so

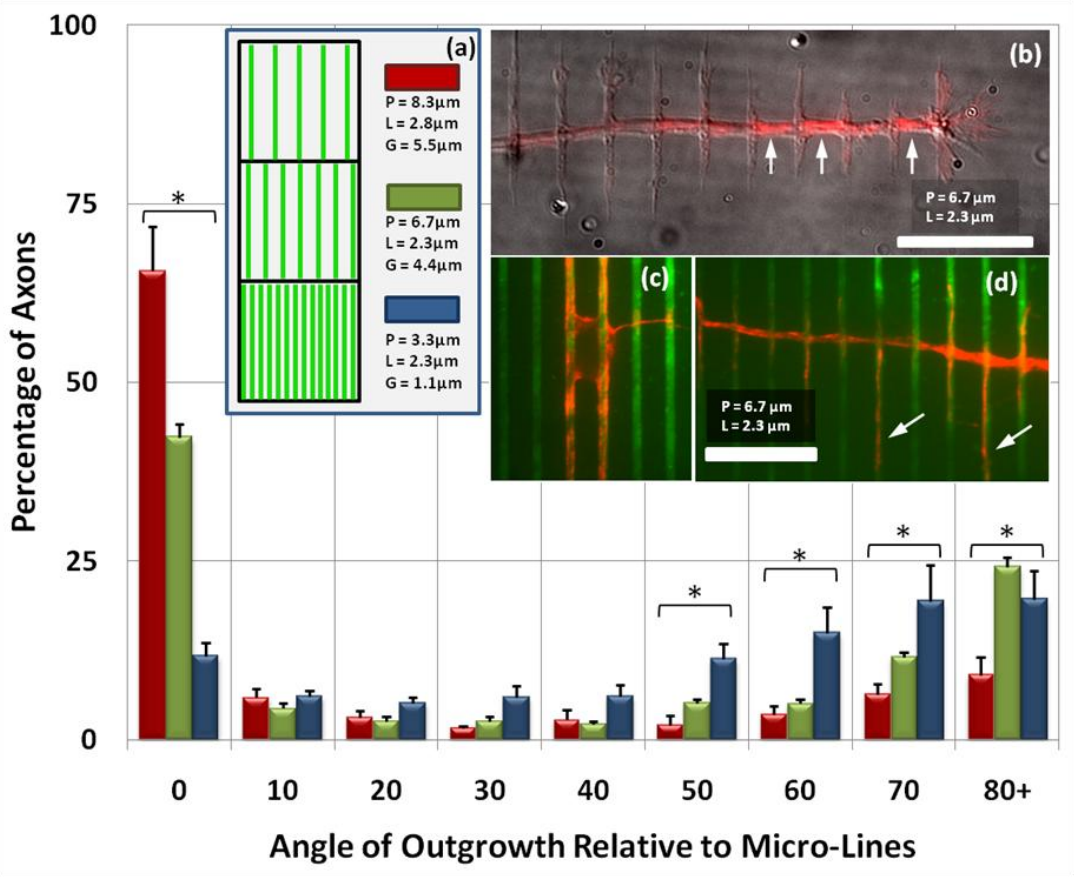

Figure 2. Axonal Orientation on Micro-Lines of Constant L, Varying G

(a). Micro-line patterns of constant line width (L = 2.55±0.25 µm) are created with a variety of periodicities (P), resulting in a varied gap width (G). These data show axonal outgrowth direction on PLL patterned micro-lines on PDMS. The outgrowth angle is defined as an angle between micropatterns and a straight line drawn from the soma to the axon tip. The axonal orientation is dominantly parallel for larger values of P. However, as P is decreased, perpendicular guidance is also observed. Error bars: ± SE. Outgrowth directions marked with * indicate $p<0.01$ for different values of P by single-factor ANOVA. **(b)** Perpendicular axonal outgrowth as seen on a P = 6.7 µm substrate. The image shows α-tubulin (red) overlaid on a DIC image (grey) (scale bar = 20 µm). Although a plurality of axons on this geometry grow parallel to the pattern with high fidelity, several axons turn in a perpendicular direction to the pattern. Along the perpendicular axonal shaft, several periodic extensions are growing on and parallel to the pattern, a hallmark of 'vinculated' growth. Interestingly, microtubules appear to be more concentrated in the gaps between lines (arrows). **(c)** The soma of a neuron with outgrowth oriented parallel to the micro-lines (green: FITC-PLL). **(d)** When perpendicular vinculated outgrowth is observed on the P = 6.7 µm micro-lines, frequently microtubules are seen invading orthogonal extensions (arrows). Scale bar (c) and (d): 20 µm.

than with larger G. The perpendicular guidance, however, is even more prevalent (Fig 2b, d) , with 36% of presumptive axons growing within 20° of the perpendicular orientation. (With

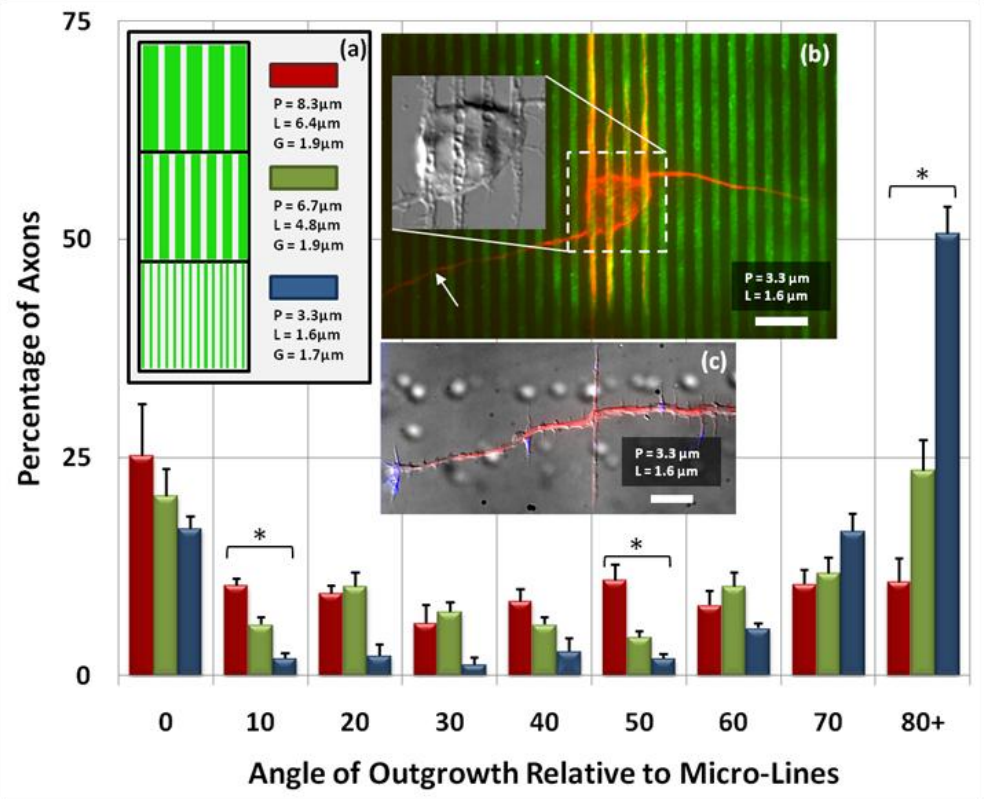

Figure 3. Axonal Orientation on Micro-Lines of Constant G, Varying L
In these data, L is varied by applying differential force across the range of P such that G is now held constant (G = 1.80 ±0.15 µm). For P = 3.3 µm, L is the minimum dimension achievable. For P = 8.3 µm, axonal growth is generally parallel to the lines, though outgrowth direction is becoming nearly randomized. And similar to Figure 2, as P is decreased, perpendicular outgrowth increases. When P = 3.3 µm, the axon outgrowth is strongly oriented perpendicular to the micro-lines. * indicates $p<0.01$ by ANOVA. Error bars: ± SE **(b)** Neuron on P = 3.3 µm pattern. Arrow indicates the axon. Other neurites (presumed dendrites) mostly prefer to grow along the micro-lines. Note also the increased microtubule presence along the micro-lines in the intra-somatic region. *Inset:* DIC image of soma reveals an alignment of cellular structure with the micro-lines. **(c)** An axon on a P = 3.3 µm pattern reveals vinculated growth along the axon labeled for actin filaments (blue: phalloidin, red: α-tubulin). Scale bar: 10 µm.

random outgrowth one would expect ~22 %.) When decreasing G to 1.1 µm, the growth becomes significantly more randomized, in line with intuitive expectations for $G \rightarrow 0$. However, far more axons grow within 20° of perpendicular (39%) than parallel (18%) to the lines. The decrease in parallel guidance can reasonably be understood, as single growth cones are able to contact more than one line simultaneously, allowing for dispersion in growth direction.

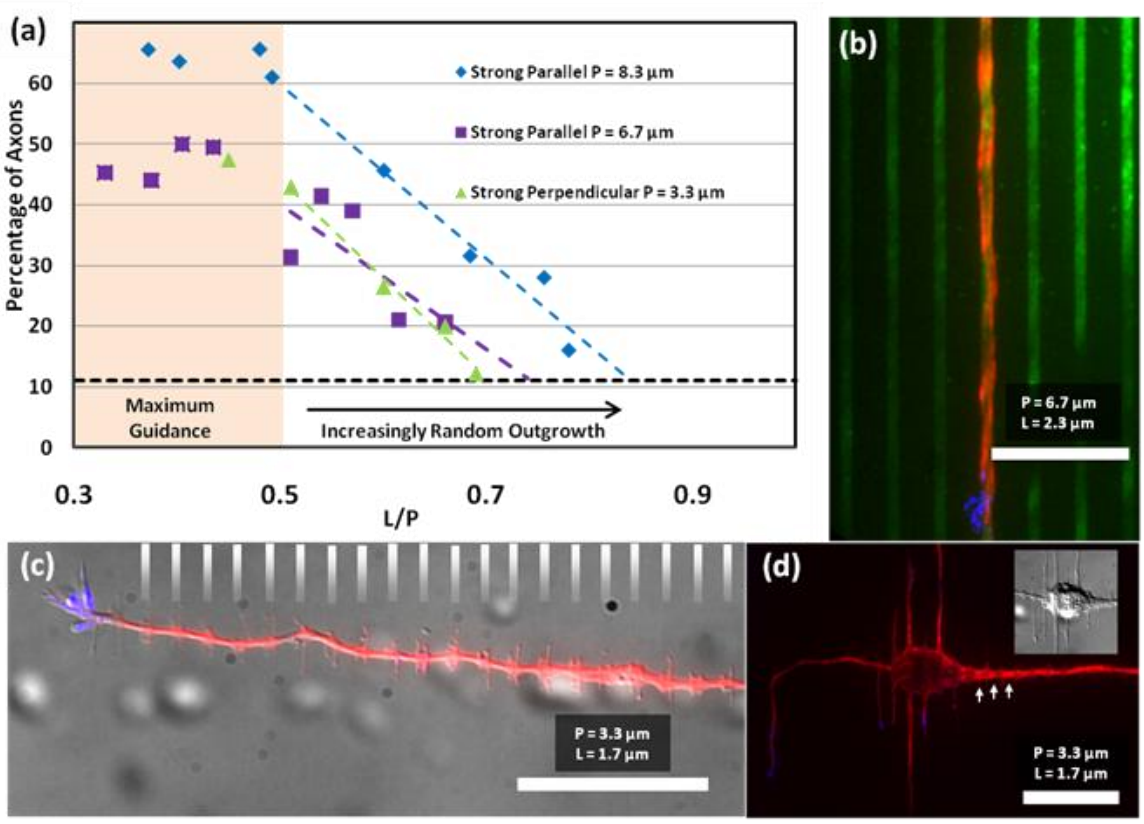

Figure 4. Axonal Guidance Fidelity: Investigating L/P
(a) Strongly guided axonal outgrowth is prevalent when L/P is small, that is, when line widths are small relative to the periodicity, largely independent of the actual value of P. However, as L/P increases above a value of 0.5, dominantly parallel (P = 8.3, 6.7 µm) or perpendicular (P = 3.3 µm) outgrowth decreases. The percentage of axons experiencing strong guidance approaches a level expected by random outgrowth (horizontal dashed line at 11%). Strong parallel guidance is defined as an outgrowth angle from 0° - 10° (strong perpendicular: 80° - 90°) relative to the micro-lines. **(b)** When L/P is small on P = 6.7 µm micro-lines, the likelihood of strongly parallel outgrowth is maximized. **(c - d)** For small L/P on P = 3.3 µm, strong perpendicular outgrowth is maximized. Vinculated growth, predominant dendritic alignment to the micro-lines, intra-somatic microtubule alignment, and increased microtubule density at gaps (arrows) are all evident in these images. The gray hash lines in (c) indicate the location of the micro-lines. All scale bars: 20 µm.

However, the increase in perpendicular guidance with decreasing gap width is anticipated to result from a unique, independent guidance mechanism.

Axonal guidance on micro-lines with constant G, varying L: In the next set of experiments, the result of changing L was examined (Fig 3). Now G was maintained at 1.8 ± 0.2 µm, while values of L = 6.4 µm, 4.8 µm and 1.7 µm were obtained by stamps of P = 8.3 µm, 6.7 µm, and 3.3 µm, respectively. On the widest lines, axonal growth was fairly random, though

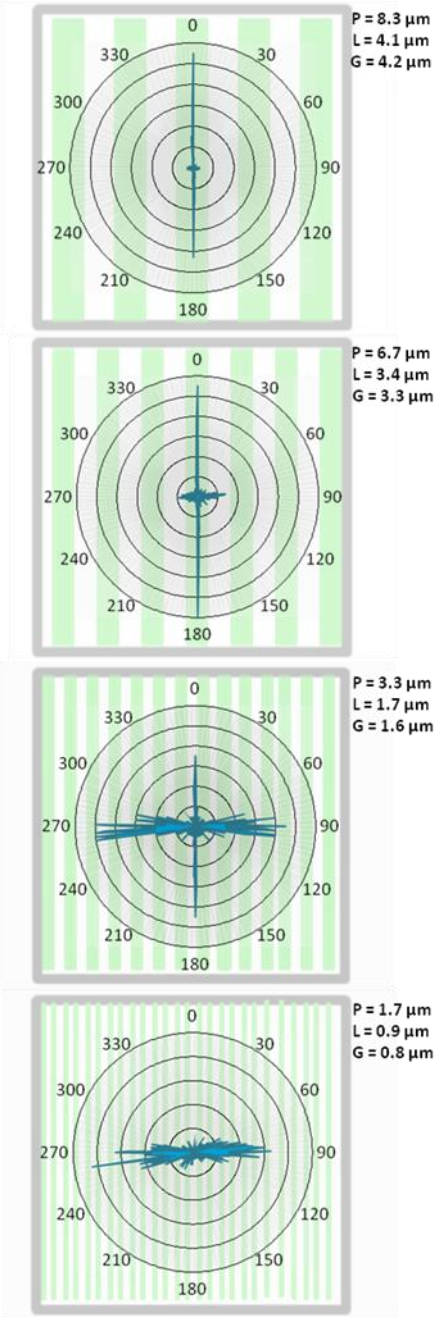

more often parallel than other directions. As the line width decreases, and especially when the line width is comparable to the gap width (L = 1.7 µm, G = 1.6 µm), perpendicular orientation becomes dominant. Moreover, this perpendicular guidance is much stronger than it was for the same P with larger L (or smaller G), as in Figure 2.

Axonal guidance on micro-lines with constant L/P (or L/G): A common element to the various results thus shown is that increasingly narrow micro-lines or gaps alone do not induce random guidance. Rather, it is when L is large relative to P that random guidance is produced. In fact, there exists a threshold L/P value above which growth increasingly becomes more random, and below which growth is strongly guided (±10° of given orientation), seemingly independent of P (Fig. 4). This threshold is seen fairly clearly for P = 8.3 µm and P = 6.7 µm at L/P = 0.5. Neurons on lines of these

Figure 5. Polar Distribution of Axonal Outgrowth: Varying P, Fixed L/P
Axonal outgrowth direction observed when varying P while holding L/P fixed (L/P = 0.5, or equivalently, L/G = 1). In addition to values of P seen previously, P = 1.7 µm is now also included. Angles are indicated around each plot. Data are grouped in 1° bins, where the length of a line indicates the relative number of axons for a given direction, normalized for each value of P. All data are overlaid upon representative micropatterns. For each pattern dimension, n ≥ 509 (number of counted axons) obtained from at least six independent samples. Guidance dramatically varies from predominantly parallel (P = 8.3 µm) to perpendicular (P = 1.7 µm). In fact, obvious parallel guidance entirely vanishes on the smallest periodicity. As can be seen in the data, the distribution of parallel growth tends to be very narrow, while the distribution of perpendicular growth is much wider.

dimensions prefer to grow parallel to the lines. It is also consistent with the results seen for P = 3.3 μm, although in this case the preferred orientation is perpendicular. Strong guidance in the preferred direction asymptotes when $L/P \leq 0.5$, but as L/P grows, the guidance becomes increasingly lessened, until it is entirely random by L/P = 0.7-0.8. For this reason, it is sensible to look at the guidance results when L/P is held constant. This has the additional benefit of keeping the areal density of poly-lysine coverage constant. When L/P is held at 0.5 (L/G = 1), there is a clear transition from dominant parallel guidance at P = 8.3 μm, to dominant perpendicular guidance at P = 1.7 μm (Fig 5, 6). It is interesting that at P = 1.7 μm, parallel guidance seems to entirely vanish. It can also be seen that where it occurs, parallel growth has a very tight distribution. Indeed, growing axons were often observed to have followed a single micro-line for hundreds of microns. In contrast, the perpendicular guidance has a much wider angular distribution.

2.5.3 *Vinculated Growth and Immuno-staining*

So called 'vinculated' growth was exhibited by axons growing perpendicular to the micro-lines. This phenotype is characterized by small, filopodia -like extensions along the axonal shaft. These may occur at every location where the axon crosses a micro-line, extending up to 30 μm (Figs 2b, 3c, 4c, 6c). Vinculated growth is observed for any value of P, regardless of whether perpendicular guidance is preferred.

To begin to discern the underlying mechanism of this type of growth we fixed and labeled neurons with an antibody to tubulin to label microtubules. When the orthogonal filopodia are longer than 20 μm (Figs 2d, 3c), we found that microtubules had invaded the orthogonal growth, which is oftentimes coincident with stabilization of branches.[25] Also, an

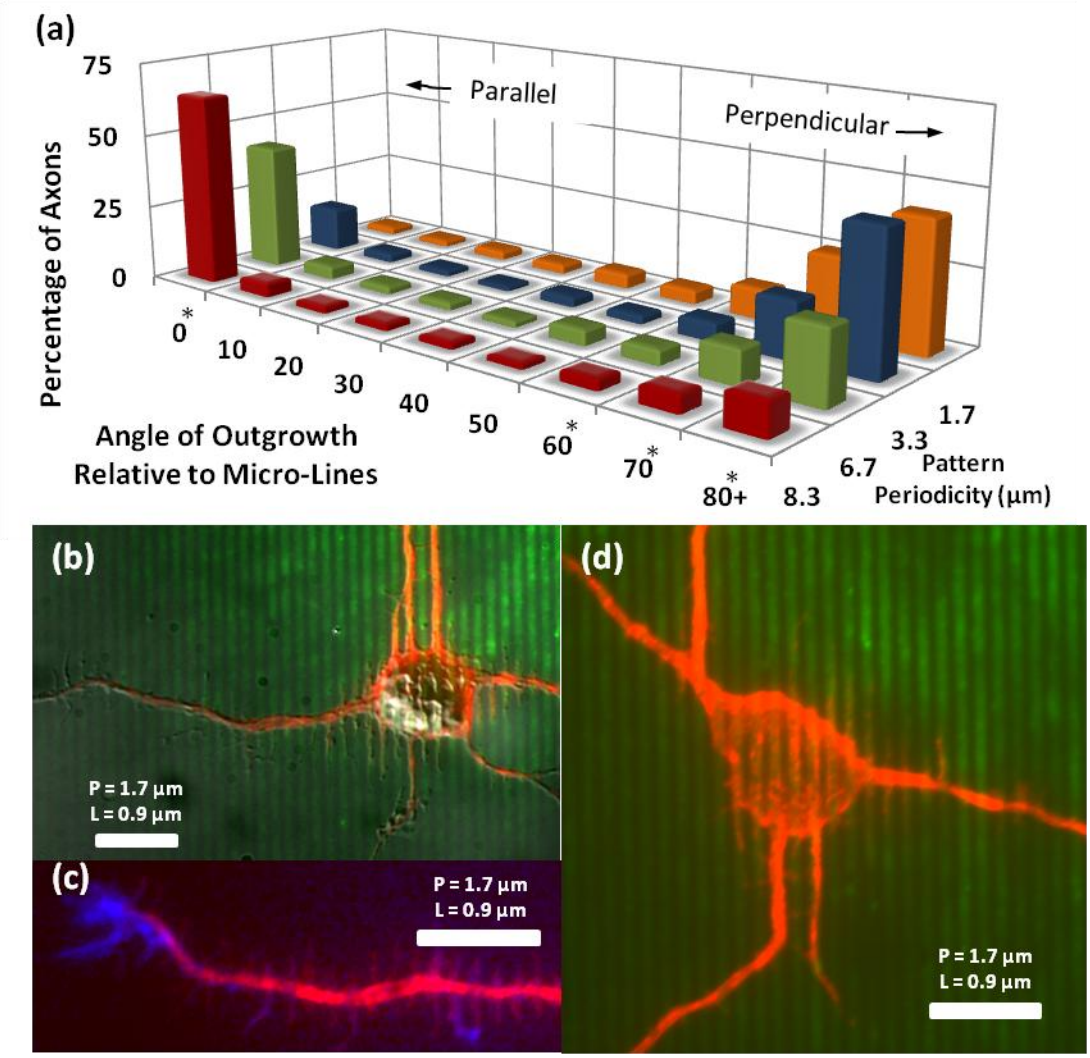

Figure 6. Axonal Outgrowth: Varying P, Fixed L/P
(a) Directional outgrowth of axons is measured and grouped into 10° bins. The transition from parallel to perpendicular guidance is seen as periodicity (P) decreases, while L/P is held at 0.5. * indicates $p<0.01$ for a given orientation by ANOVA. **(b - d)** Outgrowth on P = 1.67 µm micro-lines. At this scale parallel axonal alignment is all but absent, although microtubules are still seen to align within the soma (d). Perpendicular vinculated growth is very dominant (b, c). All scale bars: 10 µm.

increased concentration of microtubules was observed in the main axonal shaft at the gaps between micro-lines (Figs 2b, 4d). Growth of axons or dendrites parallel to micro-lines exhibits none of these effects (Figs 2c, 3b, 4b).

In examining microtubules, the somatic region is also of interest. Microtubules are observed, even within the soma, to align themselves with the micro-lines (Figs. 3b, 4d, 6d). This is seen especially on the P = 3.3 μm, and the P = 1.7 μm substrates. For larger P, the cell body would frequently be found in between two adjacent micro-lines (Fig 2c). Microtubules aligned along the edges of the somatic region would then typically extend into neurites growing parallel to the lines. Short neurites, constituting the presumptive dendrites, were frequently aligned with the micro-lines (Figs. 3b, 4d, 6b, 6d) especially for large P and small L. For example, 90% of neurons growing parallel (within 10°) to P = 8.3 μm micro-lines had mostly parallel dendrites (92% of all dendrites) and also 90% of neurons growing perpendicular to P = 3.3 μm micro-lines had mostly parallel dendrites (74% of all dendrites). Therefore, although the change in periodicity leads to a dramatic shift in axonal guidance, dendritic guidance over the same length scale seems to rely on pattern continuity. Interestingly, dendritic outgrowth becomes more random when P = 1.7 μm, and dendrites are not observed to align with the micro-lines.

Another unusual observation that we made was that the regions of the neurons that were on the lines, either the axonal branches running parallel with the lines (Fig. 2b) or at the cell body (Fig. 3b, 4d, 6b), exhibited inverse shadow-cast circular indentations. These appeared only along the micro-lines and may represent vesicles or vacuoles inside the cells. These structures also appear to exclude microtubules within the neurons, contributing to the discontinuous nature of tubulin labeling within the axons and at the cell bodies.

2.6 Discussion

It would be difficult to over-emphasize the ease with which the methodology here employed could be widely adopted. A biology-based lab of neither engineering expertise, nor

access to any specialized fabrication facilities could quickly produce these micro-line patterns. Not only can line width, gap width, and periodicity of microlines be controlled, but simple developments of the technique yield access to a wide variety of patterns. For example, tunable-line width grids can be formed by stamping twice, with the two stampings orthogonal (See Supplementary Data.) It is trivial to vary line width and the angle of the grid. It would also be very easy to print multiple species in succession in order to create synergistic of competitive guidance cues. Either by printing a repulsive compound or by employing a two-step stamping technique, it is possible to create cell-permissive micro-island arrays. These arrays would be variable in size, spacing and aspect ratio. While this is all possible using traditional micro-stamping techniques, each new pattern would require a new master stamp, requiring time and expense. Moreover, the high resolution demonstrated in this work would require a mask which would be more expensive than low-resolution masks. Other high-resolution patterning techniques could also produce these patterns, but only with tedium and expense.

Systematic control of pattern geometry, particularly at the length scales studied in this work, has hitherto not been satifactorily demonstrated. Only a few studies have focused on repetitive micropatterns approaching this length scale, and most of those focus on other aspects such as gradient generation, [26,27] while ignoring possibly confounding effects of geometric variability.

Axon outgrowth is an excellent study candidate on these patterns for several reasons. Perhaps most importantly, the scale of patterning achieved here is one which reflects the typical scale of axons and growth cones, making neuronal behavior exquisitely sensitive to the scale of patterning here performed. Beyond axon outgrowth, this technique could easily be incorporated in any system where micron scale patterning is intrinsically linked to cell behavior. Possible

biological assays include stem cell differentiation, cancer and other cell migration, or neuron/glia co-culture. Neurobiological assays, such as a turning assay (see Supplemental Data) or a branching assay would benefit from precise spatial control of the studied behavior. Furthermore, this microstamping could be combined with mechanical stimuli, such as surface topography or substrate elasticity, or with diffusive chemical stimuli, by incorporating this system into a micro-fluidic device. All such factors are known to affect cell behavior. The ease of the microstamping enhances the ability to study these factors in combination.

The deviation of the results here from the results published by Clark et al.[12] is highly significant. Their seminal paper concludes that as the period of printed micro-lines of laminin decreases, axon growth direction becomes increasingly random. When 2 μm lines are separated by 2 μm gaps, they observed nearly entirely random outgrowth. Some differences in methodology require attention. Clark and colleagues used chick embryonic 'brain' neurons, grown on a laminin patterned quartz substrate, as compared to mouse embryonic cortical neurons, grown on poly-lysine patterned PDMS used in this study. Perhaps more subtly, Clark and colleagues measured orientation with only two possibilities, aligned or not. If a transition toward perpendicular alignment were beginning, but not completed, it may have been misjudged as random, though this runs contrary to the raw data presented. Whatever the cause, whether in neuron type, substrate, patterned compound, or otherwise, further investigation is warranted.

The unique morphology of the vinculated growth is perhaps one of the most salient details in this work. Whether the orthogonal filopodia-like structures along the axon have a causative or merely associative relationship with perpendicular guidance remains to be determined. When measuring growth cone dynamics, it was found[28] that dynamic microtubules were present in greater quantity on the sides rather than the leading edge of growth cones, likely

due to decoupling from actin retrograde flow. Similar dynamic activity would be intriguing to explore on the micro-line substrates. In any case, it appears that expansive restructuring of the cytoskeleton is occurring. This is observed in both the extending axons and also the soma, where periodic spatial variability in concentrations of microtubules is observed. Somatic cytoskeletal restructuring cannot be assumed to be the only cause which initiates perpendicular axonal outgrowth, however, as quite frequently perpendicularly guided axons were seen originating from what were initially parallel-guided neurites. It is also significant that perpendicular guidance begins at a pattern scale consistent with the size of a growth cone. Future directions of this work include a full characterization and quantification of the sub-cellular components of the vinculated growth.

The remarkable shift in axonal guidance from parallel to perpendicular relative to the micro-lines is reminiscent of results published concerning axonal guidance of hippocampal neurons on micro-topography. Rajnicek and colleagues showed that topographies consisting of a series of grooves in quartz could elicit perpendicular guidance responses.[16] In an accompanying paper which explored guidance mechanisms, perpendicular growth exhibiting orthogonal filopodial extensions was reported,[29] much like the vinculated growth described here. Gomez and colleagues studied hippocampal neurons on micro-topography, instead using PDMS as the substrate, and observed similar perpendicular guidance.[17] In both of these efforts a relatively rigid, topographical surface was created, coated, and then cultured with cells. The current work differs in that the initial surface is smooth, and any topography created is by the coating of poly-lysine alone. Though it remains undetermined, it seems likely that the results seen in this work are not caused primarily by incidental topography. Furthermore, it is possible that elsewhere witnessed perpendicular axonal guidance on topographically modified surfaces is not due to the

actual 3-D topography, but rather to the 2-D geometric surface patterning of available adhesive surfaces, i.e. the surface of successive adhesive ridge tops could function much like the patterned micro-line surface in this work. Regardless, more investigation is warranted to identify the mechanisms of axonal guidance resulting from competitive and cooperative combinations of adhesion and topography.

Inevitably it must be questioned whether this perpendicular guidance is necessary for *in vivo* development, or simply the result of experimental design. In support of the former possibility, it has been reported[30] that pioneering axons in the rat corticospinal tract are found to grow perpendicular to aligned astroglial cells.

2.7 Conclusions

Poly-lysine micro-lines of sub-cellular dimensions were patterned using a non-traditional micro-stamping technique. This technique enables control over patterned line width, and patterns at a scale and over an area which is difficult to achieve using more common methods. Moreover, this method is simple and inexpensive.

Cortical neurons grown on these adhesive micro-lines were shown to be strongly guided in their axonal orientation. Lines of larger periodicity reliably produced parallel axonal outgrowth, while lines of smaller periodicity induced perpendicular outgrowth. It was shown that periodicity, not line width or gap width independently, was the critical dimension that effected a transition from parallel to perpendicular axonal guidance.

Perpendicular axonal outgrowth was especially distinctive in its morphology. Growth exhibiting periodic filopodial extensions and nascent branches, oriented perpendicular to the

growing axon, or parallel to the traversed micro-lines, was frequently observed. This vinculated growth occurred along axons growing perpendicular to micro-lines of all dimensions, even on micro-lines where parallel growth was favored.

Neurite outgrowth on variable line-width micro-grids of poly-lysine demonstrates ease of application of the presented methodology. Growing neurites were less likely to turn at grid intersections when growing on grids formed with narrow lines.

2.8 References

1 C. E. Schmidt and J. B. Leach, Neural tissue engineering strategies for repair and regeneration, *Annual Review of Biomedical Engineering,* 2003, **5**, 293-347.

2 K. Bossers, G. Meerhoff, R. Balesar, J. W. Van Dongen, C. G. Kruse, D. F. Swaab and J. Verhaagen, Analysis of gene expression in Parkinson's disease: possible involvement of neurotrophic support and axon guidance in dopaminergic cell death, *Brain Pathololgy,* 2009, **19**, 91-107.

3 D. A. Heller, V. Garga, K. J. Kelleher, T. C. Lee, S. Mahbubani, L. A. Sigworth, T. R. Lee and M. A. Rea, Patterned networks of mouse hippocampal neurons on peptide-coated gold surfaces, *Biomaterials*, 2005, **26**, 883-889.

4 B. C. Wheeler and G. J. Brewer, Designing neural networks in culture, *Proceedings of the IEEE,* 2010, **98**, 398-406.

5 M. O'Donnell, R. K. Chance and G. J. Bashaw, Axon growth and guidance: receptor regulation and signal transduction, *Annual Review of Neuroscience,* 2009, **32**, 383-412.

6 D. Koch, W. J. Rosoff, J. Jiang, H.M. Geller and J. S. Urbach, Strength in the periphery: growth cone biomechanics and substrate rigidity response in peripheral and central nervous system neurons, *Biophysical Journal,* 2012, **102**, 452-460.

7 D. Falconnet, G. Csucs, H. Michelle Grandin and M. Textor, Surface engineering approaches to micropattern surfaces for cell-based assays, *Biomaterials*, 2006, **27**, 3044-3063.

8 H. C. Tai and H. M. Buettner, Neurite outgrowth and growth cone morphology on micropatterned surfaces, *Biotechnology Progress*, 1998, **14** 364-370.

9 M. Song and K. E. Uhrich, Optimal micropattern dimensions enhance neurite outgrowth rates, lengths, and orientations, *Annals of Biomedical Engineering*, 2006, **35**, 1812-1820.

10 L. Kam, W. Shain, J. N. Turner and R. Bizios, Axonal outgrowth of hippocampal neurons on micro-scale networks of polylysine-conjugated laminin, *Biomaterials*, 2001, **22**, 1049-1054.

11 K. G. Sharp, G. S. Blackman, N. J. Glassmaker, A. Jagota and C. Y. Hui, Effect of stamp deformation on the quality of microcontact printing: theory and experiment, *Langmuir*, 2004, **20**, 6430-6438.

12 P. Clark, S. Britland and P. Connolly, Growth cone guidance and neuron morphology on micropatterned laminin surfaces, *Journal of Cell Science.*, 1993, **50**, 203-212.

13 Y. Xia, J. Tien and G. M. Whitesides, Non-photolithographic methods for fabrication of elastomeric stamps for use in microcontact printing, *Langmuir*, 1996, **12**, 4033-4038.

14 C. Y. Hui, A. Jagota, Y. Y. Lin and E. J. Kramer, Constraints on microcontact printing imposed by stamp deformation, *Langmuir*, 2002, **18**, 1394-1407.

15 Y. Xia and G. Whitesides, Extending microcontact printing as a Microlithographic technique, *Langmuir*, 1997, **13**, 2059-2067.

16 A. M. Rajnicek, S. Britland and C. D. McCaig, Contact guidance of CNS neurites on grooved quartz: influence of groove dimensions, neuronal age and cell type, *Journal of Cell Science*, 1997, **110**, 2905-2913.

17 N. Gomez, Y. Lu, S. Chen and C. E. Schmidt, Immobilized nerve growth factor and microtopography have distinct effects on polarization versus axon elongation in hippocampal cells in culture, *Biomaterials*, 2007, **28**, 271-284.

18 W. K. Cho, K. Kang, G. Kang, M. J. Jang, Y. Nam and I. S. Choi, Pitch-dependent acceleration of neurite outgrowth on nanostructured anodized aluminum oxide substrates, *Angewandte Chemie International Edition*, 2010, **49**, 10114-10118.

19 C. Viesselmann, J. Ballweg, D. Lumbard, and E. W. Dent, Nucleofection and primary culture of embryonic mouse hippocampal neurons, *Journal of Visualized Experiments: JoVE*, 2011, **pii**, 2373.

20 E. W. Dent and K. Kalil, Axon branching requires interactions between dynamic microtubules and actin filaments, *The Journal of Neuroscience*, 2001, **21**, 9757-9769.

21 S. Sarkar, M. Dadhania, P. Rourke, T. A. Desai and J. Y. Wong, Vascular tissue engineering: microtextured scaffold templates to control organization of vascular smooth muscle cells and extracellular matrix, *Acta Biomaterialia*, 2005, **1**, 93-100.

22 A. W. Feinberg, W. R. Wilkerson, C. A. Seegert, A. L. Gibson, L. Hoipkemeier-Wilson and A. B. Brennan, Systematic variation of microtopography, surface chemistry and elastic modulus and the state dependent effect on endothelial cell alignment, *Journal of Biomedical Materials Research Part A*, 2008, **86**, 522-534.

23 D. Fuard, T. Tzvetkova-Chevolleau, S. Decossas, P. Tracqui and P. Schiavone, Optimization of poly-di-methyl-siloxane (PDMS) substrates for studying cellular adhesion and motility, *Microelectronic Engineering*, 2008, **85**, 1289–1293.

24 M. N. De Silva, R. Desai and D. J. Odde, Micro-patterning of animal cells on PDMS substrates in the presence of serum without use of adhesion inhibitors, *Biomedical Microdevices*, 2004, **6**, 219–222.

25 E. W. Dent, J. L. Callaway, G. Szebenyi, P. W. Baas and K. Kalil, Reorganization and movement of microtubules in axonal growth cones and developing interstitial branches, *The Journal of Neuroscience*, 1999, **19**, 8894-8908.

26 A. C. von Philipsborn, S. Lang, J. Loeschinger, A. Bernard, C. David, D. Lehnert, F. Bonhoeffer, and M. Bastmeyer, Growth cone navigation in substrate-bound ephrin gradients, *Development*, 2006, **133**, 2487–2495.

27 R. Fricke, P. Zentis, L. Rajappa, B. Hofmann, M. Banzet, A. Offenhäusser, S. Meffert, Axon guidance of rat cortical neurons by microcontact printed gradients, *Biomaterials*, 2011, **8**, 2070-2076.

28 A. C. Lee and D. M. Suter, Quantitative analysis of microtubule dynamics during adhesion-mediated growth cone guidance, *Developmental Neurobiology*, 2008, **68**, 1363-1377.

29 A. Rajnicek and C. McCaig, Guidance of CNS growth cones by substratum grooves and ridges: effects of inhibitors of the cytoskeleton, calcium channels and signal transduction pathways, *Journal of Cell Science*,1997, **110**, 2915-2924.

30 E. A. J. Joosten and D. P. Bär, Axon guidance of outgrowing corticospinal fibres in the rat, *Journal of Anatomy*, 1999, **194**, 15-32.

3.1 Title:

Modulating Perpendicular Axonal Outgrowth by Combined Topographical and Chemical Cues

3.2 Abstract:

Axonal outgrowth perpendicular to anisotropic substratum topography is exhibited by cortical neurons *in vitro*. The topography consists of poly-dimethylsiloxane (PDMS) microgrooves of variable depth created using a simple, single-step replication molding method. The topographically modified PDMS surface is rendered cell-adhesive by poly-lysine applied in one of three ways: uniformly, exclusively on the ridge-tops, or in patterned micro-lines stamped onto the grooved surface. Dependent on the poly-lysine application, the depth of the grooves may enhance, have no effect upon, or inhibit the preference for axonal outgrowth perpendicular to the grooves. Because of asymmetry inherent in the surface profile of the grooved substrata, it is possible to create a favored direction in perpendicular axonal guidance, i.e. the axons prefer to grow 'downstairs'. Also, when the axons grow perpendicular to the grooves, the outgrowth angular distribution displays a consistent shift of the mean, 6° to the right of the expected value. Time lapse imaging of growth cone morphology reveals the tendency for filopodia to rotate clockwise about an axis normal to the surface, passing through the center of the growth cone.

Insight, Innovation and Integration: Micro-engineered, artificial environments which mimic *in vivo* conditions enhance the study of cellular behavior. Advances in the simplification of soft-

lithographic techniques present an opportunity for studying cellular response to external stimuli. Reaction to a stimulus is commonly modulated by another co-localized stimulus, so the development of platforms that enable integration of multiple cues in the cellular environment has vast potential. For example, neuronal growth cones are exquisitely sensitive to a wide variety of external stimuli. By presenting a combination of spatially-patterned biochemical cues and physical topographical features to a growing axon, it is possible to induce behavior that is absent when one type of cue is presented in isolation.

3.3 Introduction

Biomimetic surfaces, on which a variety of mechanical and chemical features may be presented to a growing cell, are invaluable for the *in vitro* study of cellular function. Mechanical features of interest include substratum elasticity[1], surface roughness (isotropic topography)[2], and ordered (anisotropic) surface topography. The most commonly studied anisotropic topography consists of parallel grooves and ridges. Even topographies featuring a simple topographic step have been found to affect cell orientation and migration[3]. Neuronal response on multiple-grooved substrata has also been frequently examined. Early work examining chick embryonic neurons found greater alignment on deeper grooves[4]. While parallel alignment of neuronal processes to grooves is commonly observed and even expected, a most curious finding is the occasional behavior of perpendicular orientation. For example, CNS neuroblasts were observed migrating perpendicular to neurite bundles radiating outward from microexplants[5]. When cultured on engineered substrates, the neuroblasts were found to extend processes perpendicular

to microgrooved structures of 1 μm width and sub-micron depth[6]. Another group demonstrated that perpendicular axonal outgrowth on similarly scaled grooves could be the dominant growth paradigm, contingent upon neuron type, topographic dimension, and cell age[7]. While axonal guidance perpendicular to topography has been found by others[8], and while some attempts have been made to understand the cellular mechanisms underlying such guidance[9], there still remains a lack of understanding of the full significance and causation of this paradoxical behavior.

Cells *in vivo* must integrate information simultaneously from both mechanical and chemical stimuli. When studying cells in culture, some effort has been made to create environments with integrated topographical and chemical cues. For example, a grooved substratum was overlaid with orthogonal adhesive tracks, and it was found that baby hamster kidney cells would align preferentially with the tracks, independent of groove dimension[10]. In another study, variations on grooved topography, surface chemistry, and substratum elasticity were found to affect the alignment of endothelial cells[11]. Neuronal response to combinations of topography and surface chemistry has received more limited attention. One study of interest[12] examined the effect of topography on axon guidance, with or without a gel permitting 3-D growth overlaid. On bare topography, the extending neurites would grow down into grooves. With added gel, extending neurites would ignore encountered grooves, instead growing directly into the gel. Another interesting study presented differentiating neurites with a choice between two spatially discrete surfaces, either modified chemically or topographically. Most neurons polarized into the topographically modified region[13]. Some work has been done to study the effect of topography on neuron behavior in the presence of variably concentrated, but unpatterned, chemical cues[14, 15]. Absent, however, is a dedicated platform which presents a growing axon with spatially synchronous, patterned topographical and chemical cues. Such a

platform should be capable of modification in a controlled fashion to cause multiple cues to work synergistically or competitively to guide axonal outgrowth, elucidating the hierarchy of cue integration by growth cones of extending axons.

In our work, we present a novel, simple method to create microgrooved structures, relative to which embryonic cortical neurons will extend axons perpendicularly. The microgrooves are made of polydimethylsiloxane (PDMS), a transparent and biocompatible material, cast off of inexpensive, commercially-available diffraction gratings. This platform is ideal for studying axonal perpendicular guidance, as the fabrication process is exceptionally simple and robust. Moreover, as demonstrated in previous work[16], these PDMS molds can also be used to stamp patterned micro-lines of adhesive poly-D-lysine (PDL). We combine both the patterned lines and microtopography in competitive and cooperative schemes, and thus show not only that neuronal guidance perpendicular to the grooves is feature-scale dependant, but also that this dependency is strongly modulated by the PDL application

3.4 Methods

3.4.1 *Preparation of Topographically Modified Surfaces*

Commercially obtained diffraction gratings (Optometrics) were employed as molding masters. Each master used has a groove density of 600 grooves/mm, equivalent to a periodicity of 1.7 μm. We chose this length scale as it is consistent with other research which achieved perpendicular axonal growth. Each master has a different blaze angle, resulting in a variable maximum depth (Figure 1a, 1b). Polydimethylsiloxane (PDMS, 184 Sylgard -Dow Corning)

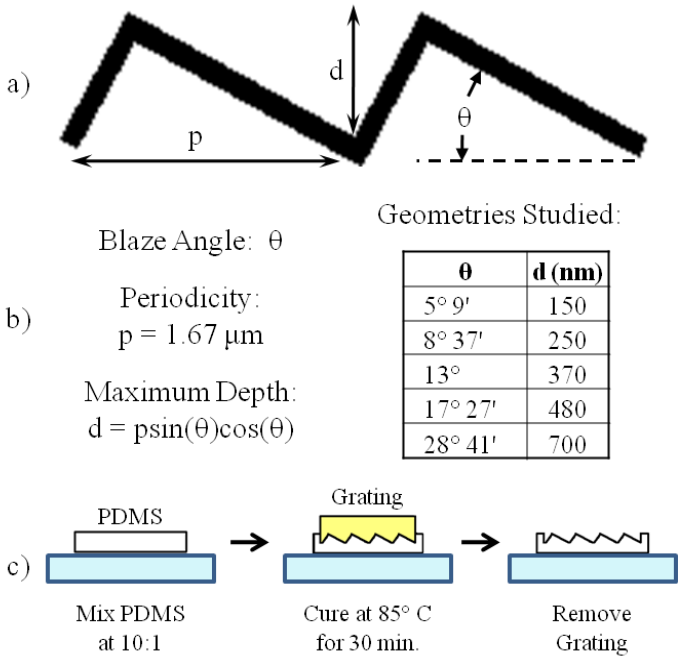

Figure 1 ***Topography Characterization and Fabrication.*** **a)** Microgrooves, having an asymmetric profile, are characterized by a periodicity, p and a blaze angle, θ, which in turn determine the maximum depth, d. **b)** In the present study, d was varied while keeping p constant. **c)** The fabrication process consists of placing uncured PDMS (10:1 ratio) upon a glass coverslip, pressing a grating into the PDMS while curing, and removing the grating after the PDMS has cured.

base was mixed with the curing agent in a 10:1 ratio by weight, placed in a vacuum chamber for 30 minutes to remove air bubbles, and a small amount placed on a 25 mm glass coverslip, which had previously been wiped clean. A master was then placed in the PDMS (Figure 1c), with a weight (100g) placed on top to ensure uniformity of the PDMS layer. The PDMS was cured at 85° C, covered, on a hot plate for 30 min, after which the master and excess PDMS were removed. The PDMS on the glass was then autoclaved for 60 min. at 120° C, after which the coverslip was mounted into a 35 mm Petri dish and sealed with paraffin wax. The entire assembly was soaked in 100% ethanol for 1 hr. and then rinsed with sterilized water. Once dry, the PDMS was plasma treated with a plasma wand (ETP Model BD-20) for 20 sec. This step was only necessary on surfaces to be micro-stamped, but was performed on all surfaces for consistency, and was done immediately prior to coating with PDL.

3.4.2 *Poly-D-Lysine Coating or Stamping*

Uniformly coated substrates were covered with 300 μL of PDL (1 mg/mL) for 45 minutes. The PDL was removed, and the surfaces washed 3x with sterilized water. To create ridge-top coated substrates, a smooth-surface PDMS block (~1.5cm^3) served as a stamp. To create micro-lines, a PDMS stamp was created by molding from a master with a periodicity of 8.3 μm. We chose this length scale for the lines, as it encourages growth parallel to the lines, allowing the lines and grooves to be combined competitively or cooperatively. Whether stamping lines or ridge tops via a smooth stamp, the stamp was coated with PDL for 30 min. and rinsed 2x with water. This process was repeated 3x. Then the stamp was inverted, placed on a topographically modified PDMS substrate with 200g of mass placed on top, and removed after 60 sec.

3.4.3 *Neural Cell Culture*

Cortical neurons (E15.5) from Swiss Webster mice were used in this study. All mouse procedures were approved by the University of Wisconsin Committee on Animal Care and were in accordance with NIH guidelines. Cells were isolated and cultured according to established methods[17]. Briefly, cells were dissociated by treating with trypsin (0.25%, 15 min, 37 C), triturated with a micropipette tip, and diluted in plating medium (neurobasal medium with 5% FBS, Hyclone, B27 supplement, 2mM glutamine, 37.5mMNaCl, and 0.3% glucose). Cells were plated onto the PDMS substrates at a density of 6,000 cells/cm^2. One hour later, the sample was flooded with serum-free medium (plating medium without FBS) and incubated for 48 hours. To

prepare for imaging, neurons were fixed in 4% PKS[18] (PFA/Krebs Solution) for 15 min, before being washed three times with PBS.

3.4.4 *Imaging and Data Analysis*

Fixed neurons were imaged with a 20x phase objective inverted microscope, captured using Metamorph software. 80-100 neurons were imaged per sample, with a redundancy of four for each experimental condition. Axonal outgrowth analysis was performed using ImageJ and a spreadsheet application. Values given are an average of the four independent results, with the standard error of the four samples given as plus/minus. Where indicated, statistical significance was performed by Single Factor ANOVA. Time lapse phase contrast images of growth cones were obtained using the Nikon Biostation with 80x magnification, captured in the range of 24-48 hrs after plating.

3.5 Results

3.5.1 **Uniform Coating of PDL on Topographically Modified PDMS**

All topographically modified surfaces used in this study are characterized by a periodic series of ridges and grooves in a sawtooth-profile (Figure 1). All surfaces have a groove density of 600 grooves/mm, or a periodicity of 1.67 μm. Maximum depth was varied from 150 nm to 700 nm.

Directional axonal outgrowth was measured for neurons cultured on the topographically modified PDMS, with each surface uniformly coated with PDL. The direction of outgrowth,

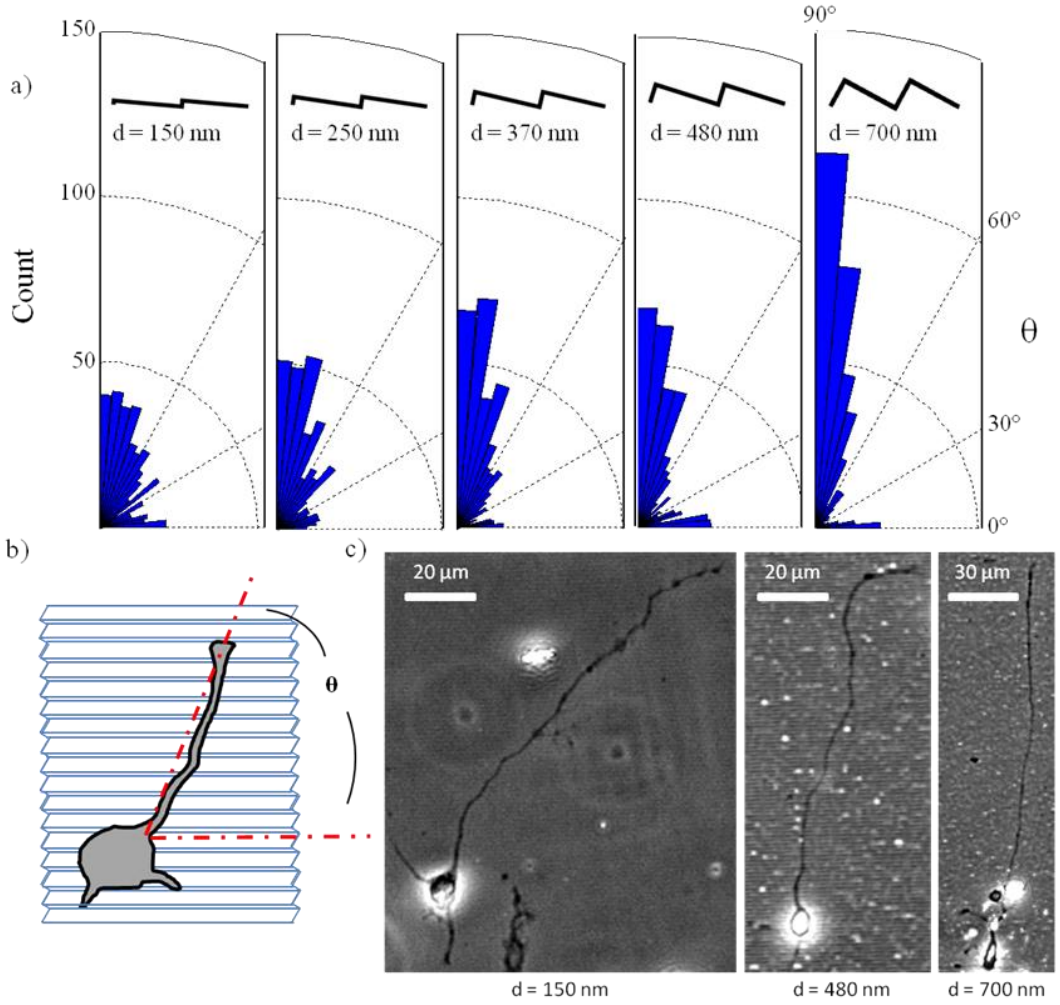

Figure 2 ***Uniform PDL coating: perpendicular guidance is enhanced by topographic scale.*** **a)** Polar histograms of axonal outgrowth on grooves uniformly coated with PDL. As depth increases, perpendicular guidance becomes more pronounced, revealing a significant relationship between depth and perpendicular (±30°) guidance ($p<0.01$). For each depth, 400 total axons counted from four independent samples were used to construct the histograms. The profile at each depth is depicted at the top, each profile's shape drawn to scale. **b)** Method of angle measurement, e.g. 90° = perpendicular alignment. **c)** Representative phase-contrast images of neurons growing on microgrooves of variable depth.

measured relative to the groove direction, was defined by a line drawn from the soma to the tip of the growth cone. The outgrowth direction of 400 axons, gathered from four independent

samples for each depth, was measured after 48 hours of growth. The results (Figure 2) indicate a strong relationship ($p<0.01$) between the depth of the topography and the perpendicular alignment of the axons.

3.5.2 Ridge-Top Coating of PDL on Topographically Modified PDMS

By pressing a PDL-coated flat PDMS sample onto an uncoated, micro-grooved PDMS sample, we achieved the goal of topography with a ridge-top coating of PDL. The same measurements of axonal

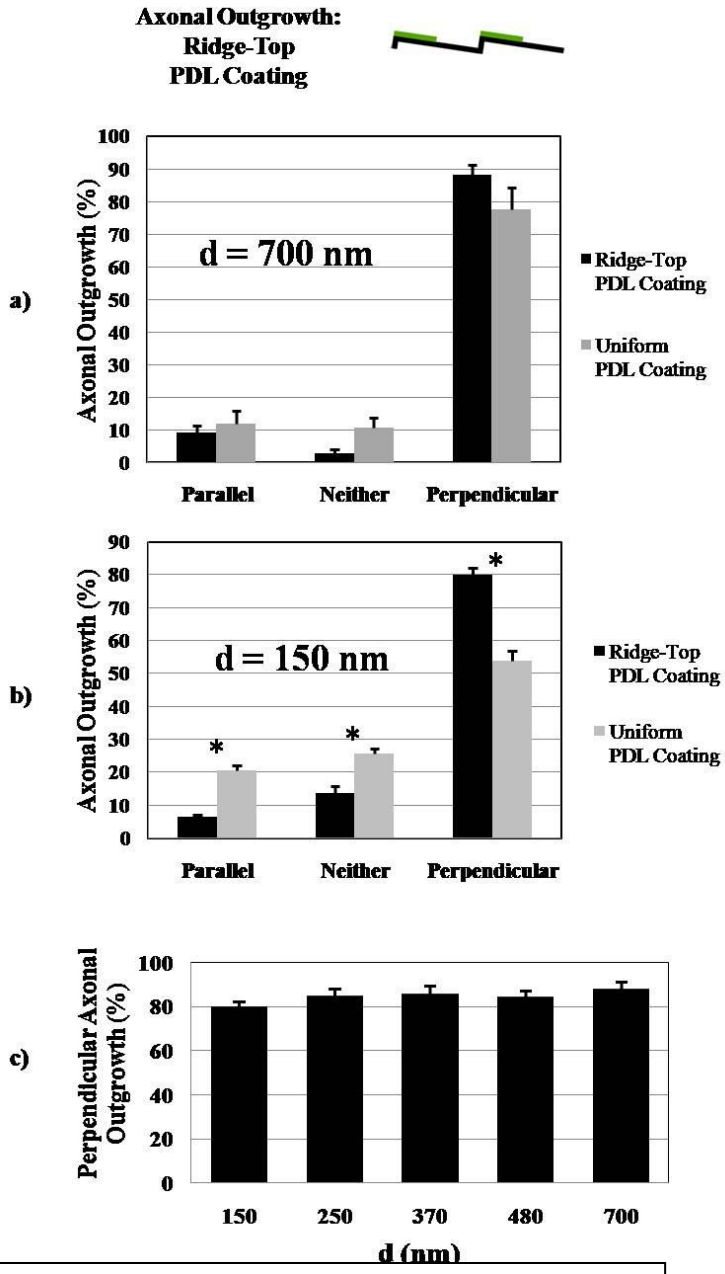

Figure 3 ***Coating Only Ridge-Tops with PDL: guidance is independent of topographic scale.*** By microstamping a grooved surface with a smooth PDMS stamp coated with PDL, it is possible to coat only the ridge-tops, while leaving the valleys uncoated. **a)** There is no significant difference ($p>0.05$) in axonal guidance between uniform coating and ridge top coating on the deepest topography. **b)** Perpendicular guidance is significant enhanced (* indicates $p<0.01$) on the most shallow topography. **c)** In contrast to the result with uniform coating, when ridge-top coating is employed, there is no significant relationship ($p>0.05$) between topographic depth and perpendicular guidance.

outgrowth on various topographic dimensions were made as were performed with the uniformly coated specimens.

We found (Figure 3a, 3b) that perpendicular guidance was statistically unchanged on the deepest topography ($p>0.05$), but greatly enhanced on the most shallow ($p<0.01$). Interestingly, we found no significant correlation (Figure 3c) between the depth of topography and the frequency of perpendicular guidance ($p > 0.05$), suggesting that perhaps the overall depth is relatively unimportant if the deepest portion of the grooves are uncoated.

3.5.3 **Micro-lines of PDL Stamped onto Topographically Modified PDMS**

Micro-lines of PDL were created using a grating-cast PDMS sample as the stamp. Lines were created in an array of 8.3 μm periodicity, each line having a width of 2.8±0.2 μm, as verified by stamping fluorescent poly-lysine (data not shown). Previous work[16] has shown that on a topographically smooth substrate, axons exhibit a preferential outgrowth parallel to line patterns of this dimension.

Cooperative Topographical and Chemical Cues: First, we stamped the micro-lines orthogonally on the grooves (Figure 4a). Like the ridge-top coating method explored earlier, this method results in the valleys remaining uncoated. Because the stamped lines are orthogonal to the grooves, both topographical and chemical cues are working cooperatively. Axons in this instance are predictably guided to grow perpendicular to the grooves (parallel to the lines). Two details are of particular interest. First, the fidelity of guidance is very pronounced, an effect which increases with increasing topographical depth. On the deepest topography, 99±1% of axons grew perpendicular to the grooves. Even if the definition of perpendicular guidance is

narrowed from a ±30° to a ±10° window, there are still 97±2% of axons in this category. Axons would typically be found to follow a single PDL line for the entirety of their growth.

Figure 4 ***Combined micropatterns and topography: topographic scale may enhance or inhibit perpendicular guidance.***

PDL microlines with a periodicity of 8.3μm are stamped onto the microgrooves in both an orthogonal (a) and parallel (b) orientation on microgrooves with depths from 150 nm to 700 nm. (* indicates microlines stamped onto a smooth PDMS surface, with the data representing growth parallel or perpendicular to the lines for a) and b) respectively.) As the depth of the microgrooves increased, axonal perpendicular guidance relative to the grooves was enhanced when the adhesive lines and grooves are orthogonal. However, a similar increase in groove depth causes a decrease in axonal perpendicular guidance relative to the grooves when the adhesive lines and grooves are parallel.

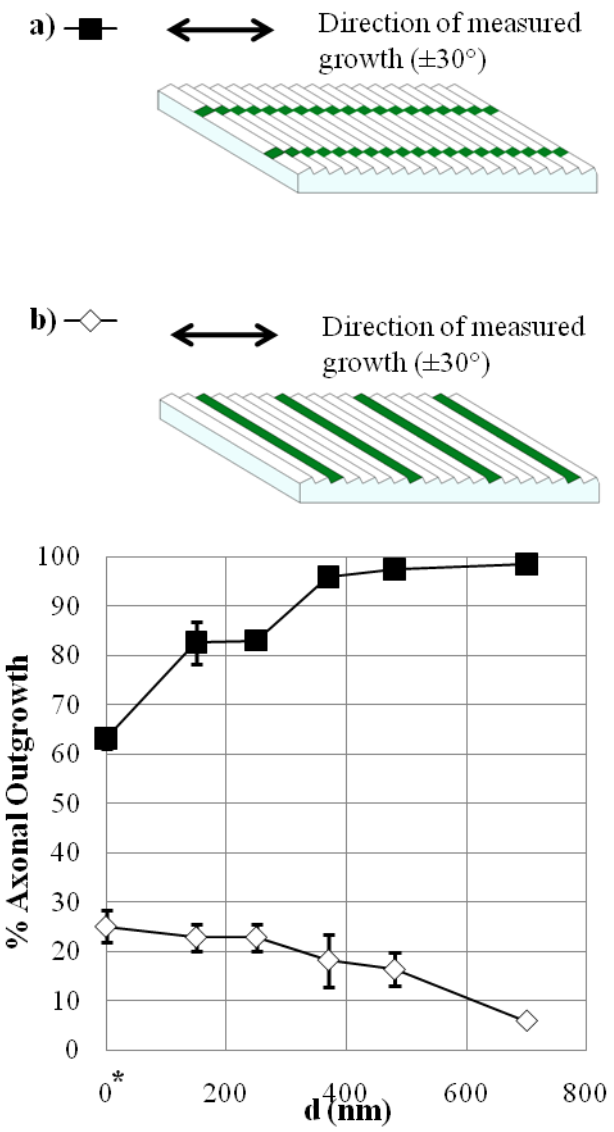

The second detail of note is the jump (62%-82%) in perpendicular guidance from d = 0 nm (topographically smooth) to d = 150 nm. Whether this is caused by the topography itself, or

merely by the discontinuity in the line pattern caused by the topography, remains to be investigated.

Competitive Topographical and Chemical Cues: Next, we printed the micro-lines parallel to the grooved topography. As the majority of axons prefer to grow perpendicular to the topography alone, and parallel to the lines alone, this arrangement is competitive. Broadly, the axons chose to follow the printed PDL, rather than be guided perpendicularly by the topography.

We examined more closely the minority of axons that grew perpendicular to the lines and the topography. As the depth of the topography increased, this subset of axons diminished in number (Figure 4b). On topographically smooth surfaces, 25±3% of axons grew perpendicular to the lines. However, when the lines were stamped on the topography of 700 nm depth, only 5.0±0.5% of axons grew perpendicular to the grooves (and printed lines). Rather than enhancing perpendicular guidance, increased topographic depth in this case actually inhibits said guidance, instead encouraging fidelity to the patterned PDL lines.

3.5.4 **Downstairs and to the Right**

Downstairs Directional Bias: Inherent to the gratings from which the PDMS is molded is an asymmetry in the surface profile (Figure 1a). As an axon growing perpendicular to the grooves approaches a ridge, the contact surface may be nearly parallel with the direction of growth, or it may be closer to perpendicular if the axon is growing the opposite direction. Considering the aspect ratios of the length of the fore and aft surfaces of a ridge, it may be said that the former case of axon growth is ‘downstairs’, and the latter is ‘upstairs’ (Figure 5a). The degree of asymmetry is greatest when the groove depth is most shallow.

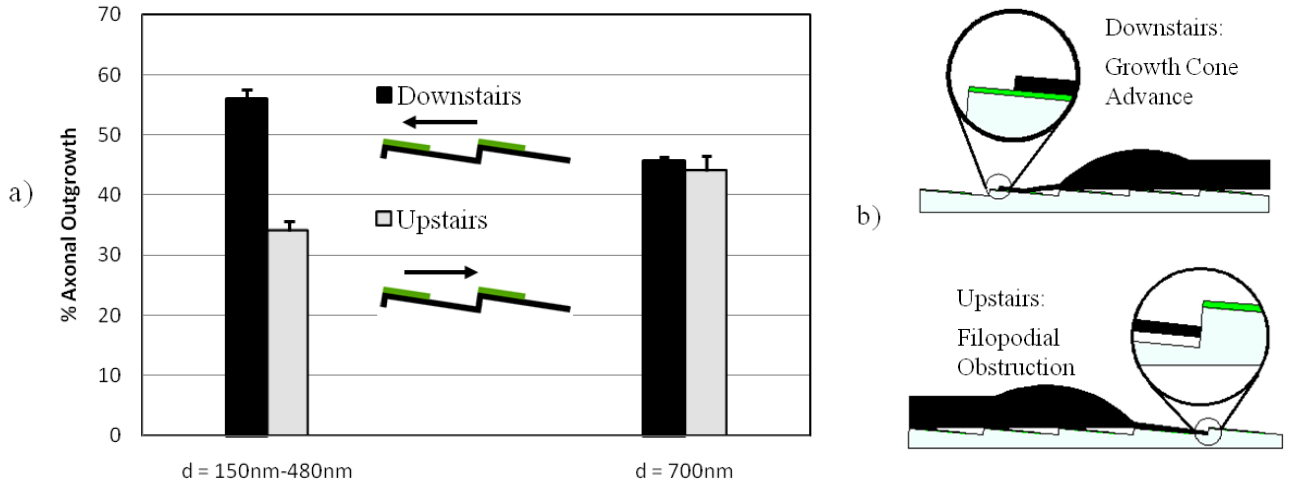

Figure 5 ***Downstairs directional bias.*** **a)** When only the ridge tops are coated, or when micro-lines are stamped orthogonal to grooves, an interesting directional bias in the perpendicular axonal guidance became evident. Axons demonstrated a distinct preference to grow 'downstairs' – so named given the profile shape. This was evident only on the more shallow grooves, which not incidentally have a greater degree of asymmetry in their topographic profile (See Figure 2a). On depths from 150nm to 480 nm, the bias showed no dependence on depth ($p>0.05$). However, at d = 700nm, the bias vanished entirely. **b)** A proposed mechanism that could give rise to the guidance bias: When axons grow downstairs, filopodia extending off of the growth cone will be uninhibited. Following the adhesiveness up to a ridge vertex, they are able to then extend to the next ridge. Axons growing upstairs, however, will occasionally experience filopodial in inhibition in the form of an uncoated surface, oriented approximately normal to the growth direction. When the microgrooves are coated uniformly, this directional bias is absent.

When the grooves were uniformly coated with PDL, we found no bias in either the upstairs or downstairs direction. However, when only ridge-tops were coated, a downstairs directional bias was revealed. 56±2% of axons grew downstairs, as compared to 34±2% that grew upstairs. Each was determined by counting axons that grew within 45° of the specified direction. This bias was not evident for d = 700 nm, which is not entirely unexpected, as the degree of asymmetry is minimized. Between d = 150 nm to d = 450 nm, the directional bias was consistent and failed to show any significant relationship to depth. Although the bias in growth

direction is pronounced, we found no significant difference in average axonal length, only in orientation.

In figure 5b, we introduce a possible explanation for the downstairs bias. The growth cone of an axon growing perpendicular to the grooves is considered. Filopodia at the leading edge of a growth cone oriented downstairs will consistently be enabled to reach each ridge top by following the adhesive PDL. Because each successive ridge is oriented almost parallel to the direction of growth, growth cone advance is allowed. However, when the growth cone is oriented upstairs, occasionally a filopodium will contact the uncoated surface of the next ridge. In combination with the lack of adhesiveness, this surface is oriented almost orthogonal to the direction of growth, and could obstruct filopodial extension. Occasionally this could lead to growth cone collapse.

Right-Shift Bias: The axonal guidance on uniformly-coated substrates can be characterized as perpendicular to the grooves. However, closer scrutiny of the distribution of growth unveils an unexpected behavior. Rather than displaying a growth distribution centered at 90° relative to the grooves, the distribution is shifted to the right. For example, when d = 700nm on uniformly coated topography, the distribution is obviously shifted (Figure 6a), with an average angle of outgrowth of 85.5±0.9°. The right-shift in the mean outgrowth angle is independent of direction (i.e. upstairs vs. downstairs), and does not have a significant relation to depth ($p>0.05$). Across all dimensions, the mean outgrowth angle was found to be 84.1±0.6°. On ridge-top coated substrates a similar, but not as dramatic, shift was observed, with a mean outgrowth angle of 87.4±0.5°.

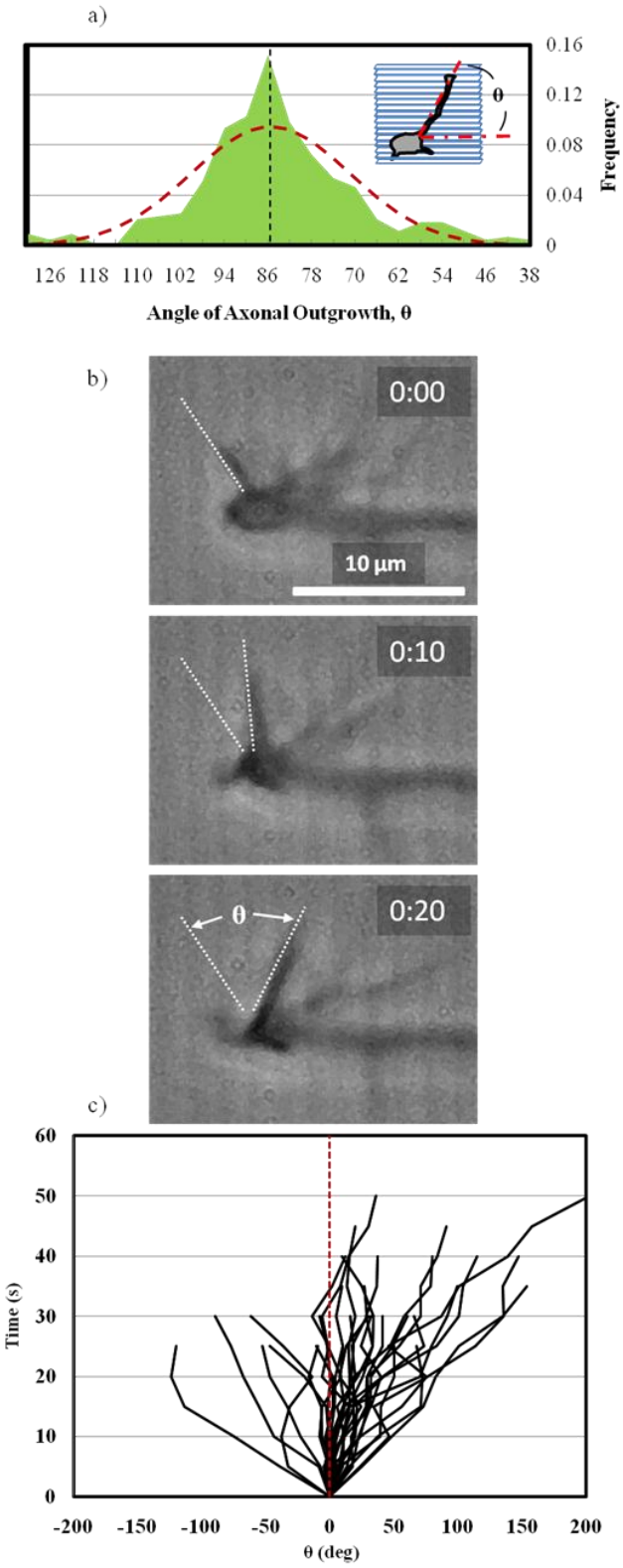

Figure 6 ***Right-shift of outgrowth distribution and clockwise rotation of filopodia.*** **a)** Axonal outgrowth angle histogram from d = 700 nm, with mean angle of 85.5°. On uniformly coated substrates, the mean outgrowth angle was consistently shifted to the right of the expected value by 4-6°. **b)** Time lapse images of a growth cone growing perpendicular on the grooved substrate. A filopodia is seen rotating clock-wise about the center of the growth cone. **c)** Angular displacement of filopodia vs. time. Persistent filopodia (distinguishable for t>20s) were identified (n = 68), and their orientation tracked relative to their initial orientation. The majority (77%) experienced clockwise angular displacement. This filopodial rotation bias was absent in topographically smooth controls. Approximately half of the total, randomly selected, are plotted in the figure.

To further understand what may underlie this unexpected result, we analyzed growth cone morphology on the topography using time-lapse microscopy. Once a filopodium became distinguishable (Figure 6b), its subsequent orientation was tracked relative to its initial position (n = 68). Many filopodia were unable to be tracked due to prohibitively short time persistence, but the persistent filopodia showed a pronounced tendency to rotate clockwise (Figure 6c). Overall, 77% of tracked filopodia experienced a clockwise displacement, experiencing an average rotational velocity (ω) of 1.8±0.3°/sec, up to a maximum of 4.3°/sec. Those filopodia rotating counterclockwise had an identical magnitude of rotational velocity (ω = -1.8±0.6°/sec), but persisted on average for only 27 seconds, as compared to an average of 36 seconds persistence for clockwise-rotating filopodia. Occasionally, the entire growth cone, or branches thereof, can be observed to be rotating clockwise in a dramatic fashion. Controls on smooth PDMS revealed growth cones that were much less dynamic, including an absence of distinguishable clockwise rotation.

3.6 Discussion

When cellular behavior on patterned surfaces is examined, often the focus is primarily on either topographic modifications, or on patterned chemistry. Because chemical patterns will often exhibit topography at the nano-scale, a scale at which cellular behavior is sensitive[19], it is important to consider possible effects of topography when patterning chemically. Similarly, topographically modified surfaces can affect the chemical landscape on which cells grow by affecting protein adsorption[20]. Because topographical and chemical cues are simultaneously

presented to cells *in vivo*, and also because to some degree both cues are present even when attempts are made to study one type in isolation, it is very important to construct experiments where both types of cues are controlled and varied. For example, in our work we showed that neurons predominantly followed adhesive lines of PDL when overlaid on grooved topography, irrespective of relative orientation. Interestingly, increased depth of topography inhibited perpendicular growth that did not conform to the lines, even though this same topographic depth encouraged perpendicular growth when PDL was uniformly applied to the surface.

In many studies involving topography and neurons[21, 22], growth is not so much guided by the topography as restricted by it. In our work this is not the case, as growth cones and axons could freely grow over and across topographic features. And yet some uncertainty remains as to how much of the behavior is caused by the 3-D topography, and how much is caused by chemical patterning, inadvertently created by the topography. For example, we found perpendicular guidance on grooved substrates to have some topographic depth dependence, which agrees with work that others have performed[7, 8]. However, when we only coated the ridges, the depth of the topography became irrelevant. In previous work[16], we showed that periodic adhesive lines of poly-lysine were sufficient to cause perpendicular guidance, where line periodicity was the determining factor. While these lines, like all chemical patterns, have some inherent topography, it seems that perpendicular guidance is much more a result of adhesive 2-D surface geometry, than it is of contact guidance on 3-D topography. Furthermore, a very compelling recent study showed that actin and other cytoskeletal elements occur with regular spatial periodicity along an axonal shaft[23]. Although the reported periodicity of ~185 nm is significantly smaller than the topographic periodicity explored in our work, it is interesting that upon division of the latter by the former we obtain: 1.6667/0.185 = 9.01, hinting that an

integer number of cytoskeletal structural units could fit within the periodicity of our substrate. While this remains largely speculative, it provides some possibilities for future exploration.

A particularly useful and novel result we found is the ability to bias axons to grow in a unidirectional fashion. Although some excellent recent work has demonstrated the ability to bias axon growth with an asymmetric topography[24], our work adds two improvements: First, the substrate fabrication we employ is exceptionally robust and inexpensive, making our system universally accessible to biology-based laboratories. Second, by incorporating patterned PDL lines, we demonstrate the ability to bias axons to grow uni-directionally. Should it prove possible to enhance this so called 'downstairs' bias to the point of true one-way growth, it would prove very useful for a variety of neuron assays and experiments.

The clock-wise rotation of filopodia about the growth cone is an observation that raises many questions. A right-hand screw rotation of filopodia about their axis has previously been reported[25]. While the rotation we observed is about a different axis, this discrepancy alone does not eliminate the possibility that we are observing the same phenomenon. The most immediate question is: Why is this not observed more frequently? Although the above cited work on filopodia rotation was observed in the absence of external cues, we consider it likely that it is our grooved substrate, itself, which enabled the observation of this behavior. The advantage of an isotropic background possibly lies in the subtlety of the rotational phenomenon. It is difficult to establish that axons are being guided a few degrees to the right of expected, when there is no absolute reference point. By examining outgrowth direction on grooved topography, we can establish with respect to *what* the axons are experiencing a right-shift. And this, in turn, led us to examine the growth cones with greater scrutiny. Additionally, we consider it possible that the grooved substrate enabled this observation by providing a periodically adhesive growth surface.

Growth cones on the grooved substrata were much more dynamic, with many of the filopodia detached from the surface, than were growth cones on controls of smooth PDMS. It is possible that continuously adhesive surfaces, such as those typically found in neuronal cultures, will act to inhibit the rotational behavior.

3.7 Conclusions

Axonal perpendicular guidance on grooved substrata is depth dependent when the grooves are uniformly adhesive. When only ridge-tops are adhesive, perpendicular guidance is enhanced, and is no longer depth-dependant. Axons grew perpendicular to grooves when following adhesive lines. When adhesive lines and grooves are parallel, axons followed the lines, and did so with greater fidelity with increasing topographic depth. Thus uncoated topographical modification can inhibit axon growth.

The asymmetry of the groove profile allowed a directional bias in the axon growth in the 'downstairs' direction, on ridge-top coated grooves. Also, the axonal angular growth distribution on uniformly coated grooves was consistently shifted to the right. Time lapse images of growth cones showed an inclination of filopodia to rotate clockwise about the growth cone.

3.8 References

1 A. J. Engler, S. Sen, H. L. Sweeney and D. E. Discher, Matrix elasticity directs stem cell lineage specification, *Cell*, 2006, **126**, 677–689.

2 R. A. Gittens, T. McLachlan, R. Olivares-Navarrete, Y. Cai, S. Berner, R. Tannenbaum, Z. Schwartz, K. H. Sandhage, and B. D. Boyan, The effects of combined micron-/submicron-scale surface roughness and nanoscale features on cell proliferation and differentiation, *Biomaterials*, 2011, **13**, 3395-3403.

3 P. Clark, P. Connoly, A. S. Curtis, J. A. Dow and C. D. Wilkonson, Topographical control of cell behavior. I. Simple step cues, *Development*, 1987, **99**, 439-448.

4 P. Clark, P. Connoly, A. S. Curtis, J. A. Dow and C. D. Wilkonson, Topographical control of cell behavior: II. Multiple grooved substrata, *Development*, 1990, **108**, 635-644.

5 N. Nakatsuji and I. Nagata, Paradoxical perpendicular contact guidance displayed by mouse cerebellar granule cell neurons in vitro, *Development*, 1989, **106**, 441-447.

6 I. Nagata, A. Kawana, and N. Nakatsuji, Perpendicular contact guidance of CNS neuroblasts on artificial microstructures, *Development*, 1993, **117**, 401-408.

7 A. Rajnicek, S. Britland and C. McCaig, Contact guidance of CNS neurites on grooved quartz: influence of groove dimensions, neuronal age and cell type, *J Cell Sci*, 1997, **110**, 2905-2913.

8 N. Gomez, Y. Lu, S. Chen and C. E. Schmidt, Immobilized nerve growth factor and microtopography have distinct effects on polarization versus axon elongation in hippocampal cells in culture, *Biomaterials*, 2007, **28**, 271-284.

9 A. Rajnicek and C. McCaig, Guidance of CNS growth cones by substratum grooves and ridges: effects of inhibitors of the cytoskeleton, calcium channels and signal transduction pathways, *J Cell Sci*, 1997, **110**, 2915-2924.

10 S. Britland, H. Morgan, B Wojiak-Stodart, M. Riehle, A. Curtis and C. Wilkinson, Synergistic and hierarchical adhesive and topographic guidance of BHK cells, *Exp Cell Res*, 1996, **228**, 313-325.

11 A. W. Feinberg, W. R. Wilkerson, C. A. Seegert, A. L. Gibson, L. Hoipkemeier-Wilson and A. B. Brennan, Systematic variation of microtopography, surface chemistry and elastic modulus and the state dependent effect on endothelial cell alignment, *J Biomed Mater Res A*, 2008, **86**, 522-534.

12 N. Li and A. Folch, Integration of topographical and biochemical cues by axons during growth on microfabricated 3-D substrates, *Exp Cell Res*, 2005, **311**, 522-534.

13 N. Gomez, S. Chen and C. E. Schmidt, Polarization of hippocampal neurons with competitive surface stimuli: contact guidance cues are preferred over chemical ligands, *J Roy Soc Interface*, 2007, **4**, 223-233.

14 J. D. Foley, E. W. Grunwald, P. F. Nealey, C. J. Murphy, Cooperative modulation of neuritogenesis by PC12 cells by topography and nerve growth factor, *Biomaterials*, 2005, **26**, 3639-3644.

15 C. Miller, S. Jeftinija and S. Mallapragada, Synergistic effects of physical and chemical guidance cues on neurite alignment and outgrowth on biodegradable polymer substrates, *Tissue Eng*, 2002, **8**, 367-378.

16 S. R. Hart, Y. Huang, T. Fothergill, D. C. Lumbard, E. W. Dent and J. C. Williams, Adhesive micro-line periodicity determines guidance of axonal outgrowth, *Lab Chip*, 2013, **13**, 562-569.

17 C. Viesselmann, J. Ballweg, D. Lumbard and E. W. Dent, Nucleofection and primary culture of embryonic mouse hippocampal and cortical neurons, *J. Vis. Exp.*, 2011, 2373.

18 E. W. Dent and K. Kalil, Dynamic imaging of neuronal cytoskeleton, *Methods Enzymol.*, 2003, **361**, 390-407.

19 K. Baranes, N. Chejanovsky, N. Geva, A. Sharoni and O. Shefi, Topographic cues of nano-scale height direct neuronal growth pattern, *Biotechnol Bioeng*, 2012, **109**, 1791-1797.

20 M. S. Lord, M. Foss, and F. Besenbacher, Influence of nanoscale surface topography on protein adsorption and cellular response, 2010, *Nano Today*, **5**, 66-78.

21 J. Zhang, S. Venkataramani, H. Xu, Y. K. Song, H. K. Song, G. T. R. Palmore, J. Fallon and A. V. Nurmikko, Combined topographical and chemical micropatterns for templating neuronal networks, *Biomaterials*, 2006, **27**, 5734-5739.

22 M. Merz and P. Fromherz, Polyester microstructures for topographical control of outgrowth and synapse formation of snail neurons, *Adv Mater*, 2002, **14**, 141-144.

23 K. Xu, G. Zhong and X. Zhuang, Actin, spectrin, and associated proteins form a periodic cytoskeletal structure in axons, *Science*, 2013, **339**, 452-456.

24 R. Beighley, E. Spedden, K. Sekeroglu, T. Atherton, M. C. Demirel and C. Staii, Neuronal alignment on asymmetric textured surfaces, 2012, *Appl Phys Lett*, **101**, 143701-143705.

25 A. Tamada, S. Kawase, F. Murakami and H. Kamiguchi, Autonomous right-screw rotation of growth cone filopodia drives neurite turning, 2010, *J Cell Biol*, **188**, 429-441.

4.1 Title:

From neuritogenesis to axonal guidance, radius of curvature of topographical features directs neurite outgrowth

4.2 Abstract

Anisotropic surface topography is known to guide neurite outgrowth. Finer details, such as the radius of curvature of feature corners, have not been investigated. We present a method of replica molding, based on variable time curing, which results in topographical features with varied radius of curvature. Varying the radius of curvature of patterned ridges has a strong effect due to the unique sawtooth profile of the topography. Elements of neuritogenesis, such as neurite sprouting sites and neurite orientation, are strongly affected when the ridges are sharper. Time-lapse imaging reveals that outgrowth rates are unaffected up to the time of axonal specification, but then faster for axons on sharp ridges. Axonal orientation is determined by feature curvature, with axons preferentially growing perpendicular to the more rounded ridges, and parallel to the sharper ridges.

4.3 Introduction:

The extra-cellular environment *in vivo* is of fundamental importance with regard to many aspects of cellular behavior. Behaviors such as differentiation[1], migration[2], outgrowth[3], and proliferation[4] have been identified as being influenced by external conditions. Modifying the

extra-cellular environment in a controlled manner *in vitro* allows for detailed study while mimicking the native extracellular conditions. Among cell types, neurons exhibit particularly interesting behaviors on surface topography, due to the inherently complex morphological characteristics of neurite outgrowth. Perhaps the simplest and most commonly studied surface is that of parallel grooves. Neuronal outgrowth can be guided along relatively large grooves[5, 6], or along micro-[7, 8] and nano-scale grooves[9], although the response is varied. Outgrowth is sometimes found to be perpendicular to grooves[10, 11] of certain dimension. Thus overall scale and basic geometry (e.g. width, depth) of the groove profile are important in determining the neuronal response.

While it is understood that the scale and basic geometry of topographic features are important, more subtle feature details may also have an important role. An interesting possibility is that of groove profile. While a rectangular groove profile is the most commonly studied, additional profiles types have also been examined, such as sinusoidal[12] and periodic concave-down as may be created by aligning nanofibers[13] or carbon nanotubes[14], for example. An additional aspect to consider is the effective radius of curvature of topographical edges. This aspect of the surface topography has been given very limited consideration. When varying the radius of curvature of an otherwise rectangular-grooved profile, embryonic fibroblasts were found to have aligned stress fibers somewhat independent of curvature, but were more polarized and less spread on surfaces with smaller radii of curvature[15]. Neuronal response on topographies exhibiting varying curvature has hitherto remained unreported.

Neuritogenesis and neurite extension on topographical surfaces are topics which have received some attention. In one study, neuritogenesis was found to occur more readily on ridges of 75-200 nm width than on wider ridges[16]. In another study, neuritogenesis and neuronal

maturation were accelerated on fibers of 600-800 nm diameter[17]. Generally, neuritogenesis is required not only for neural outgrowth, but also for neuronal migration, both critical activities in the developing nervous system[18]. Topographical surfaces may enhance or at least influence neuritogenesis by modulating filopodial formation, where filopodia have been found to be required for neurite extension[19].

In the current work, we demonstrate a simple method for the creation of a saw-tooth profile grooved topography. By altering the effective radius of curvature of the edges, we find that neuritogenesis, neurite outgrowth rate, and axonal guidance are all influenced.

4.4 Methods and Materials

4.4.1 *Substrate Preparation*

Substrates are fabricated from polydimethylsiloxane (PDMS) in a manner described previously[20]. Briefly, commercially obtained diffraction gratings (Optometrics) were employed as molding masters. The masters used have a groove density of 600 grooves/mm, equivalent to a periodicity of 1.7 μm. PDMS (184 Sylgard -Dow Corning) base was mixed with the curing agent in a 10:1 ratio by weight, placed in a vacuum chamber for 30 minutes to remove air bubbles, and a small amount placed on a 25 mm glass coverslip, which had previously been wiped to remove visible debris. The master was then placed in the PDMS, with a weight (100g) placed on top of the master to ensure uniformity of the PDMS layer. The PDMS was cured at 85° C, covered, on a hot plate for either 60 or 100 minutes, after which the master and excess PDMS were removed. The PDMS on the glass was then autoclaved for 60 min. at 120° C, after

which the coverslip was mounted into a 35 mm Petri dish and sealed with paraffin wax. The entire assembly was soaked in 100% ethanol for 1 hr. and then rinsed with sterilized water. PDMS surfaces were then covered with 300 μL of poly-D-lysine (PDL - P7886 Sigma-Aldrich) at 1 mg/ml concentration. After 45 minutes, the PDL was removed and the surface washed 3x with sterile water. At this stage, substrates either were characterized or cultured with neurons.

4.4.2 *Scanning Electron Microscopy (SEM)*

Substrates to be characterized by SEM were coated with 10 nm of Platinum using a CHA-600 metal e-beam evaporator. Substrates were oriented in such a manner so as to ensure adequate coverage on the corner of the sample. Profile images of the substrates were acquired using a Hitachi S-570 scanning electron microscope with a beam energy of 10 keV. Substrates cured for 60 min. and 100 min. were imaged, with at least 12 independent locations for each substrate type. Analysis was performed using ImageJ, Matlab and Microsoft Excel.

4.4.3 *Neuron Culture, Imaging*

Cortical neurons (E15.5) were obtained from Swiss Webster mice. All mouse procedures were approved by the University of Wisconsin Committee on Animal Care and were in accordance with NIH guidelines. Cells were isolated and cultured according to established methods[21]. Briefly, cells were dissociated by treating with trypsin (0.25%, 15 min, 37 C), triturated with a micropipette tip, and diluted in plating medium (neurobasal medium with 5% FBS, Hyclone, B27 supplement, 2mM glutamine, 37.5mMNaCl, and 0.3% glucose). Cells were plated onto the PDMS substrates at a density of 12,000 cells/cm^2. One hour later, the sample was flooded with serum-free medium (plating medium without FBS) and incubated. Time lapse

images were captured as soon as possible, obtained with the Nikon Biostation at 20x and 40x magnifications (phase). Alternatively, after 48 hours of incubation neurons were fixed in 4% PKS[22] (PFA/Krebs Solution) for 15 min, before being washed three times with PBS. Fixed neurons were imaged with a 20x phase objective inverted microscope, captured using Metamorph software. Analysis was performed using Image J, including the NeuronJ plugin, and Microsoft Excel.

4.5 Results

4.5.1 *Varying radius of curvature of topographical features*

Grooved substrates were fabricated using poly-dimethlysiloxane (PDMS). PDMS is biocompatible, transparent, well-suited for replicate molding and therefore an attractive choice for a biomaterial substrate with topographical modification. Commercially available ruled reflective diffraction gratings are used as a replica master, thus simplifying the process of creating grooved substrata.

Uncured PDMS is placed in contact with the master and then cured at 85°C for a controlled time. We found that if we allowed the PDMS to cure longer while in contact with the master, we would obtain widely varying results when culturing cells on these surfaces. Longer curing times can cause many changes, including increasing the elastic modulus and decreasing uncrosslinked monomers[23]. However, as all surfaces were autoclaved at a higher temperature (120°C) upon removal from the master, these changes should be somewhat neutralized. We therefore hypothesized that more compliant PDMS would deform more upon removal from the

master, giving the topography a larger effective radius of curvature on the ridge edges. To test our hypothesize we imaged slices of PDMS with a scanning electron microscope (SEM). We collected data from samples that had been cured for 60 minutes and 100 minutes (Figure 1a, 1b).

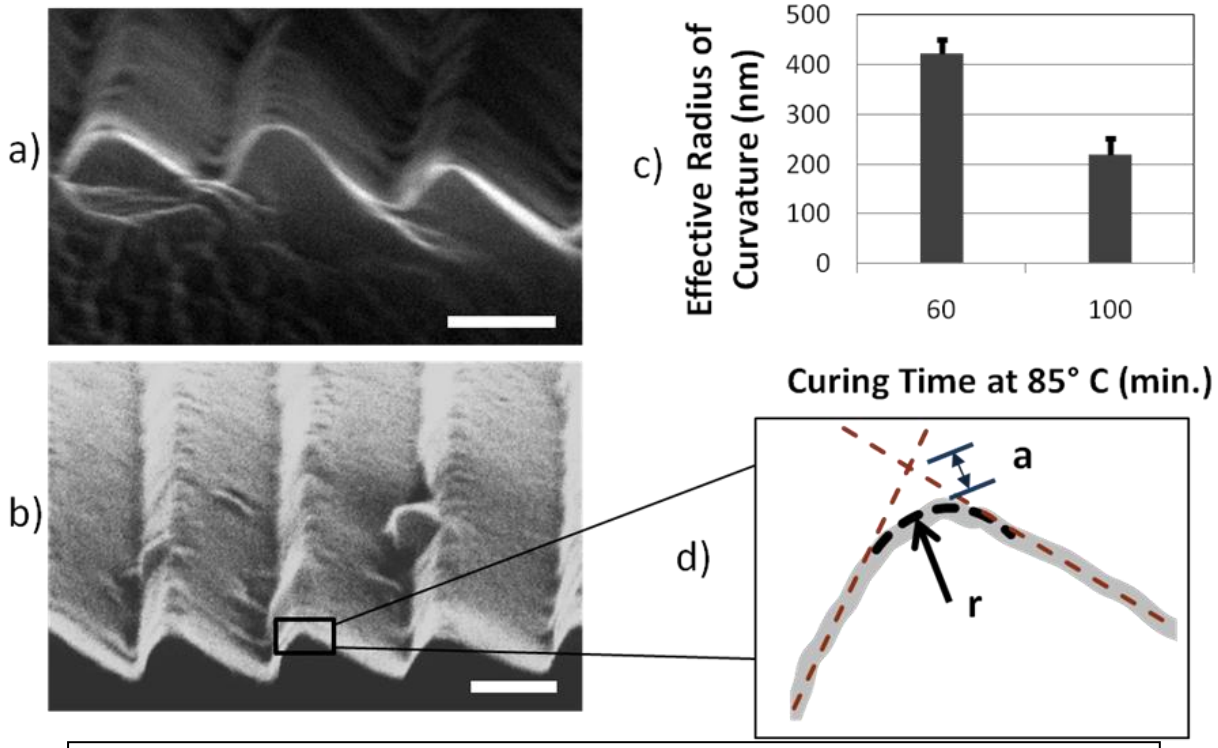

Figure 1. SEM characterization of variable cured PDMS grooves

a,b) Profile SEM image of surface topography of PDMS cured for 60 minutes and 100 minutes, respectively. Image taken at 10 keV, scale bars: 1μm. c) The effective radius of curvature was significantly greater for PDMS cured for shorter times. d) Determining the radius of curvature **r**, based on the measurement **a**.

An ideal replication would have a very sharp edge on the ridge, with an effective radius of curvature approaching zero. As can be seen in Figure 1c, there was a distinct difference in the radius of curvature for the two different curing conditions. The radius of curvature was found by fitting each side of the vertex in question with a line, and extrapolating to the intersection (Figure

1d). The distance, **a**, from the intersection to the surface was measured. The effective radius of curvature is then related to **a** by the following:

$$(r + a)^2 = 2r^2,\ r = a/(\sqrt{2-1}) \quad (1)$$

This measurement was performed on three redundant samples, in multiple locations on each sample, for a total of 36 for each condition. When cured for 60 minutes, the ridge edge had an effective radius of curvature of 423±28 nm. When cured for 100 minutes, the ridge edge had a radius of 219±33nm. Curing for shorter times (~30 min.) or curing for longer times (~8 hours) preliminarily gave results not significantly different (data not shown) than that seen for curing times of 60 or 100 minutes, respectively, and therefore we focused on the given time values.

4.5.2 *Neuritogenesis: sprouting sites and neurite orientation*

Phase-contrast time-lapse images were captured shortly after seeding neurons on the grooved surfaces to examine the dynamics of neuritogenesis and neurite outgrowth. In summary, the neurons are at first very round, with no notable protrusions. Within the first few hours, the first neurites, or neurite progenitors, begin to sprout. These are initially highly dynamic and sporadic, typically no longer than 15 μm. Typically from 4-6 hours after seeding, the initial neurites begin to stabilize and lengthen somewhat. The next stage of growth typically sees one neurite very rapidly become much longer than the others, which neurite will become the axon.

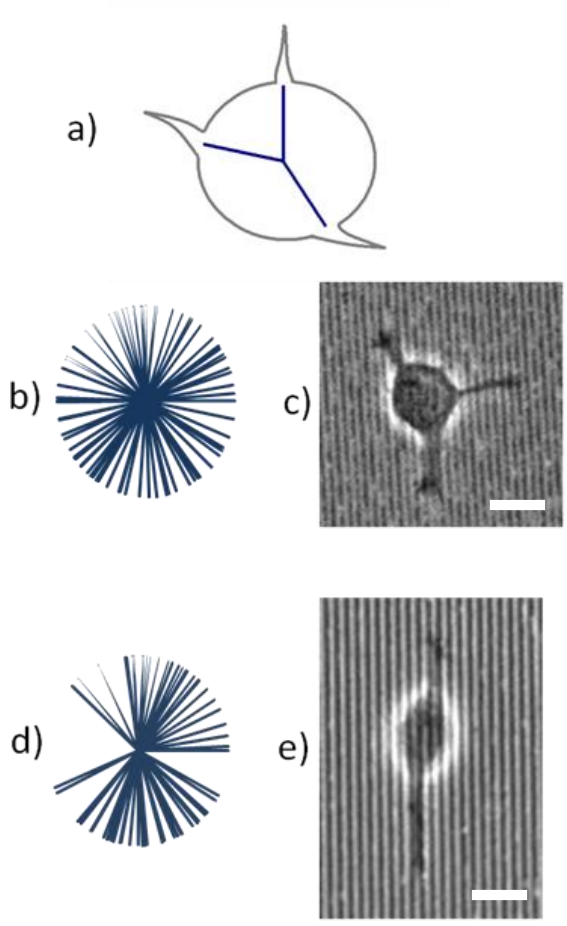

Figure 2. Site of neurite sprouting affected by feature curvature

a) Illustration of how figures b,d) are generated, by drawing a line from the center of the cell to the point of neurite sprouting on the perimeter (n = 75 for each). b,c) Neurite sprouting on the rounded ridges happens at random locations around the perimeter. d,e) Neurite sprouting on sharp ridges is biased to occur at the ends of the cell parallel to the grooves. Both scale bars: 10 μm.

In the early stages of neuritogenesis, 4 hours after seeding, we found notable variation in cell behavior, dependant on the curing time, or equivalently, the ridge curvature. We first characterized the behavior of neurite sprouting sites around the neuronal perimeter (Figure 2). We found that on the more rounded ridges, the neurites would spout from nearly random sites around the cell (Figure 2b, 2c), consistent with a control on a topographically smooth surface. However, on the sharper ridges, the distribution was noticeably skewed, so that neurites tended to sprout from opposing ends of the cell, aligning with the grooves (Figure 2d, 2e). Indeed, the cells on this surface were more likely than the others to display a bipolar morphology. On the

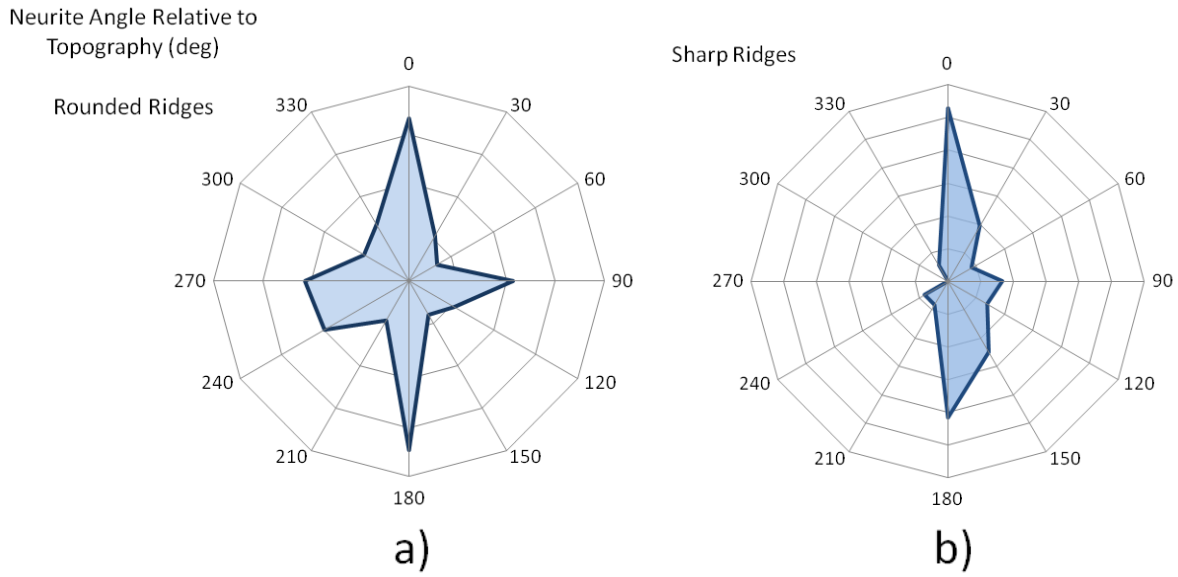

Figure 3. Initial neurite orientation on rounded and sharp ridges

a) On the rounded ridges, neurite orientation is characterized as quadrilinear, either parallel or perpendicular to the topography (n = 150). b) On the sharp ridges, neurite orientation is strongly biased in the direction of the topography (n = 72).

rounded ridges 59% of neurites sprout in a direction within 45° of parallel to the topography, while 76% do on the sharp ridges. For the rounded and sharp ridges, respectively, neurons had an average of 2.4±0.2 and 2.3±0.1 neurites. In contrast, on a topographically smooth substrate there were 3.6±0.4 neurites per cell.

Beyond examination of the neurite sprouting sites, we measured the orientation of the neurites themselves, as defined by a line drawn from the distal tip of the neurite to the sprouting site. Unlike a control surface upon which neurites grow in random directions, we saw that on the rounded ridges, the orientation was somewhat quadrilinear, that is, the neurites tended to orient

themselves parallel or perpendicular to the grooves (Figure 3a). On the sharper ridges, however, the growth was very distinctly bilinear (Figure 3b).

4.5.3 *Dynamics of neurite extension*

As the neurites continue to extend, a critical time period, T_0, is reached when one neurite is specified as the axon. This can be observed as a marked increase in growth rate. Dozens of cells were analyzed by tracking the length of each neurite as time progressed (Figure 4). Most notable is the high axonal growth rate on the sharp ridges. Otherwise, the results are fairly independent of substrate condition. By temporally aligning the results of several individual cells, it is possible to construct a model of neurite extension. Figure 4a shows such a construction for cells on the rounded topography. At the point in time of axonal specification, other neurites gradually cease to extend, while the axon rapidly accelerates. To further explore the dynamics of outgrowth on the rounded vs. sharp ridges, we examined the growth rate as a function of direction. We found that on the rounded ridges, growth was significantly increased when in a direction perpendicular to the grooves (Figure 5). On the sharp ridges, the growth rate was much more sporadic. However, generally it was unaffected by direction, and was faster than that seen on the rounded ridges.

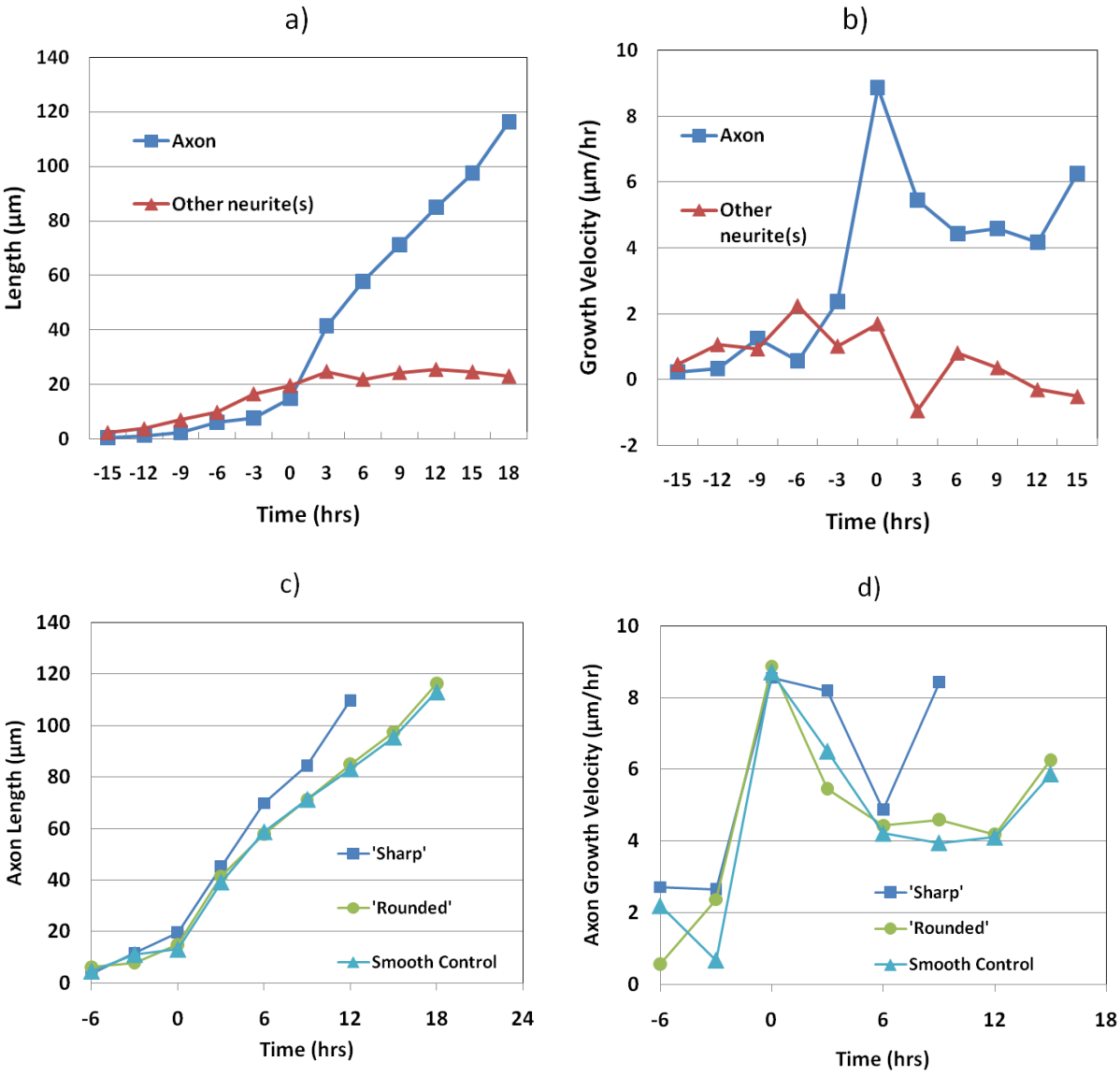

Figure 4. Axon outgrowth length and velocity on rounded and sharp ridges

a,b) Axon and all other neurites on rounded ridges. c, d) Axon length and velocity on rounded ridges, sharp ridges, and smooth PDMS control. All figures were made by normalizing several plots (n=12-24) to the time of axonal specification – seen as spike in axon growth velocity.

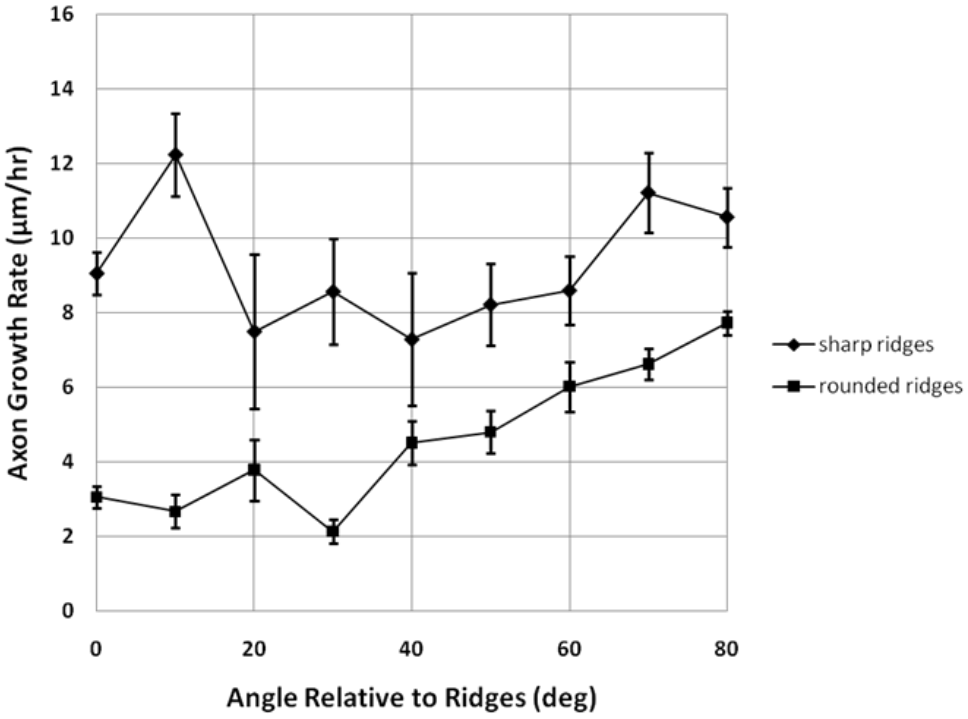

Figure 5. Axon Segment Growth rate vs Direction

Rather than considering the overall orientation of the axon, here is plotted the growth rate of axonal segments (segments were defined as 3 hrs of growth, n = 660). While growth rate increased with orthogonal orientation on the rounded ridges, on the sharp ridges growth rate was faster, and largely independent of orientation.

4.5.4 *Axonal guidance*

After 48 hours, neurons were fixed and imaged, allowing further examination into directional guidance. Individual neurons were traced from soma to distal axonal tip. Each

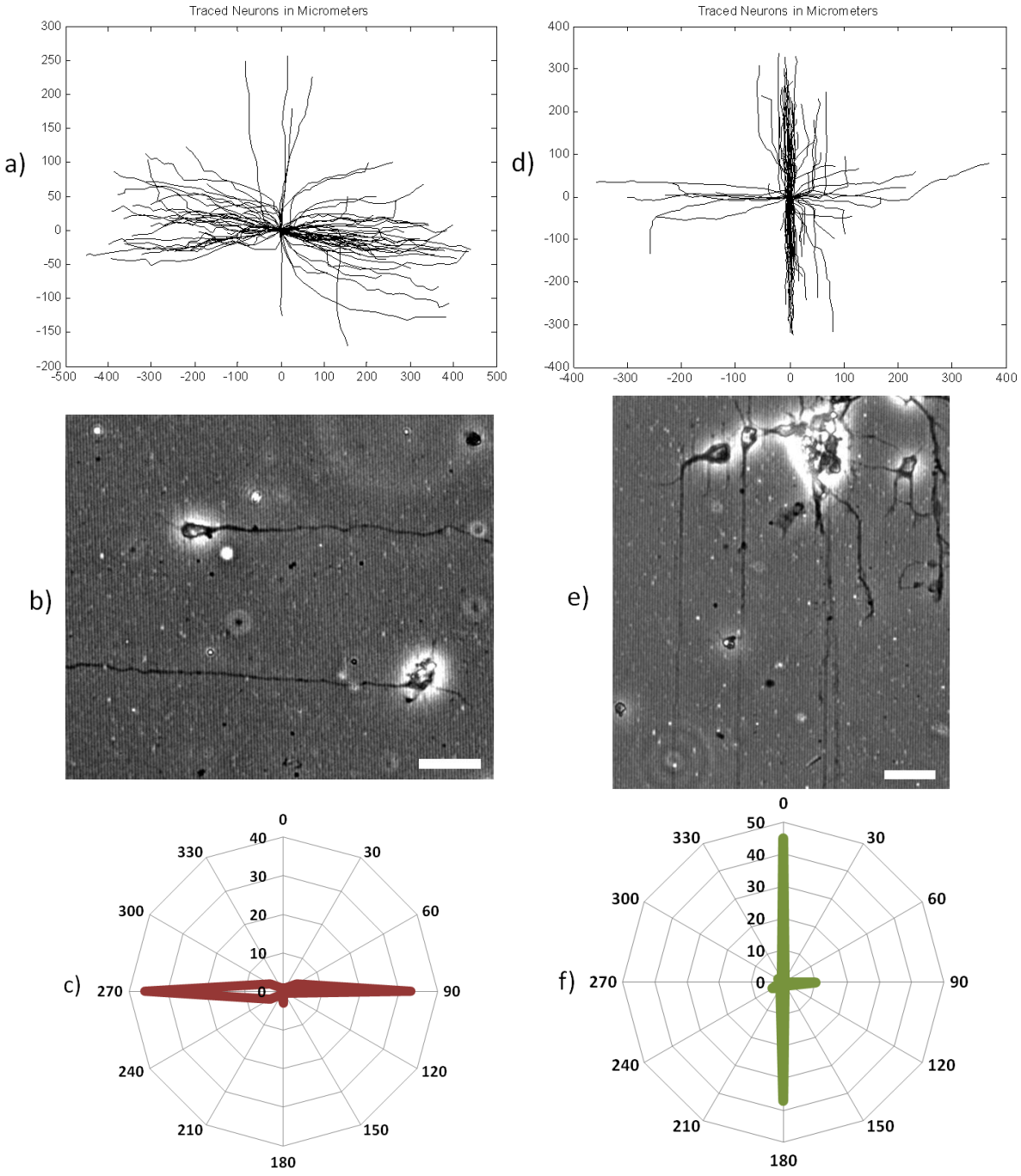

Figure 6. Axon Orientation on Rounded and Sharp Ridges

a,d) Axonal traces on round and sharp ridges, respectively. 80 axons were randomly chosen to create a representative illustration. b,e) Phase images of neurons on round and sharp ridges, respectively. In both cases, the ridges are running from top to bottom in the image. Scale bars: 20 µm. c, f) Polar histograms of the axonal outgrowth direction.

individual trace was given a common origin in order to construct a visualization of outgrowth direction (Figure 6). As shown by the figure, there seems to be a bimodal guidance effect. On the rounded ridges, 91% of the axons grow perpendicular (±30°) to the ridges. On the sharp ridges 80% grow parallel (±30°) to the ridges. Axonal length is somewhat longer on the rounded ridges: 285±13μm vs. 218±16μm on the sharper ridges. This is interesting, given the generally faster growth rates on the sharper ridges. A likely explanation is that axons growing perpendicular on the rounded ridges are able to maintain their growth for longer time periods.

4.6 Discussion

The ability to form nano-scale features through PDMS methodologies has been a matter of investigation. Our finding that the radius of curvature varied from ~200-400 nm is consistent with reports that it is impossible to replicate features in standard PDMS smaller than hundreds of nanometers[24]. Moreover, it has been theoretically calculated[25] that the smallest possible radius of curvature r, is going to be $r = \gamma/E$, where γ is the surface energy, and E is the elastic modulus. Given that E will increase with curing time, our results are very consistent with this formulation, as we saw the expected inverse relationship.

The sawtooth profile of the topography in the present study is unique in that a feature edge is presented to the cell, oriented normal to the surface on which the cell adheres. This allows a unique interaction between the cell and the feature, which is impossible to duplicate with a rectangular or large-scale concave down profile. It would possible to create concave-up anisotropic topography by taking a negative mold of aligned fibers. Recent work by Cho and

colleagues[26] demonstrated that neurite growth was accelerated on concave-up *isotropic* topography, although the increase in acceleration was attributed to pitch, and the feature curvature remained unconsidered. It has been found that nano-rough surfaces increase neuronal viability and outgrowth[27]. However, if surface roughness is too great, cell viability begins to decrease. This was verified in a recent study by Brunetti and colleagues[28], who showed that increasing nanoscale-roughness led to greater necrosis of cultured neurons. Representative profiles of nanorough surfaces indicate the scale of topographical modification was similar to the work we present, albeit in an isotropic fashion. It may be that we observed neurons growing parallel to the sharper ridges in order to avoid surface interactions that would otherwise lead to cell death. That the neurons prefer to grow perpendicular to the more rounded grooves is consistent with work demonstrated previously[10, 11]. Further investigation concerning this bimodal mechanism of guidance is needed.

The dynamics of neurite outgrowth on patterned surfaces was investigated in detail by Wissner-Gross and colleagues[29]. A key finding was that neurites will grow competitively, an aspect which we observed as one neurite would undergo axonal specification, leading to a deceleration of growth by the other neurites. It is particularly interesting that the dynamics of neurite outgrowth on a smooth surface and the rounded ridges was very similar. Neurite and axonal growth rates were largely unaffected by the surface with rounded ridges, but growth rate was increased on the sharp ridges. This suggests that the guidance of axons may often be independent of the rate of growth.

Initial neurite guidance on the sharp ridges was strongly influenced by the underlying surface. Although the rate of initial neurite extension was unchanged, both the site of neurite sprouting and the orientation of immature neurites were directed along the ridges. Later, both

axonal growth rate and directional guidance were also affected by the sharp ridges. Although there is some suggestion from previous work that an increase in substrate curvature will inhibit axonal outgrowth[30], our work represents the first study of its kind at this scale. The ability to alter the guidance of axons based only on the curvature of substrate features represents a new tool for the design of neuronal networks in culture. An important, and yet unanswered, question is whether the bimodal guidance induced by a change of feature curvature has an *in vivo* basis.

4.7 References

1 J. Y. Lim and H. J. Donahue, Cell sensing and response to micro-and nanostructured surfaces produced by chemical and topographical patterning, *Tissue Engineering*, 2007, **13**, 1879-1891.

2 R. J. Petrie, A. D. Doyle and K. M. Yamada, Random versus directionally persistent cell migration, *Nature Reviews Molecular Cell Biology*, 2009, **10**, 538-549.

3 P. Clark, P. Connolly, A. S. Curtis, J. A. Dow and C. D. Wilkinson, Cell guidance by ultrafine topography in vitro, *Journal of Cell Science*, 1991, **99**, 73-77.

4 Y. Ito, Surface Micropatterning to regulate cell functions, *Biomaterials*, 1999, **20**, 2333-2342.

5 N. Li and A. Folch, Integration of topographical and biochemical cues by axons during growth on microfabricated 3-D susbstrates, *Experimental Cell Research*, 2005, **311**, 307-316.

6 T. Houchin-Ray, L.A. Swift, J. H. Jang and L. D. Shea, Patterned PLG substrates for localized DNA delivery and directed neurite extension, *Biomaterials*, 2007, **28**, 2603-2611.

7 T. Hirono, K. Torimitsu, A. Kawana and J. Fukuda, Recognition of artificial microstructures by sensory nerve fibers in culture, *Brain Research*, 1988, **446**, 189-194.

8 C. Miller, J. Srdija and S. Mallapragada, Synergistic effects of physical and chemical guidance cues on neurite alignment and outgrowth on biodegradable polymer substrates, *Tissue Engineering*, 2002, **8**, 367-378.

9 F. Johansson, P. Carlberg, N. Danielsen, L. Montelius and M. Kanje, Axonal outgrowth on nano-imprinted patterns, *Biomaterials*, 2006, **26**, 1251-1258.

10 A. Rajnicek, S. Britland and C. McCaig, Contact guidance of CNS neurites on grooved quartz: influence of groove dimensions, neuronal age and cell type, *Journal of Cell Science*, 1997, **110**, 2905-2913.

11 N. Gomez, Y. Lu, S. Chen and C. E. Schmidt, Immobilized nerve growth factor and microtopography have distinct effects on polarization versus axon elongation in hippocampal cells in culture, *Biomaterials*, 2007, **28**, 271-284.

12 J. K. Lee, H. Baac, S. H. Song, S. D. Lee, D. Park and S. J. Kim, The topographical guidance of neurons cultured on holographic photo-responsive polymer, *Engineering in Medicine and Biology Society, 2004, IEMBS'04, 26th Annual International Conference of the IEEE*, 2004, **2**, 4970-4973.

13 D. R. Nisbet, J. S. Forsythe, W. Shen, D. I. Finkelstein and M. K. Horne, Review paper: a review of the cellular response on electrospun nanofibers for tissue engineering, *Journal of Biomaterials Applications*, 2009, **24**, 7-29.

14 M. P. Mattson, R. C. Haddon and A. M. Rao, Molecular functionalization of carbon nanotubes and use as substrates for neuronal growth, *Journal of Molecular Neuroscience*, 2000, **14**, 2000.

15 A. Mathur, S. W. Moore, M. P. Sheetz and J. Hone, The role of feature curvature in contact guidance, *Acta Biomaterialia*, 2012, **8**, 2595-2601.

16 J. D. Foley, E. W. Grunwald, P. F. Nealey and C. J. Murphy, Cooperative modulation of neuritogenesis by PC12 cells by topography and nerve growth factor, *Biomaterials*, 2005, **26**, 3639-3644.

17 C. C. Gertz, M. K. Leach, L. K. Birrell, D. C. Martin, E. L. Feldman and J. M. Corey, Accelerated neuritogenesis and maturation of primary spinal motor neurons in response to nanofibers, *Developmental Neurobiology*, 2010, **70**, 589-603.

18 J. S. Da Silva and C. G. Dotti, Breaking the neuronal sphere: regulation of the actin cytoskeleton in neuritogenesis, *Nature Reviews Neuroscience*, 2002, **3**, 694-704.

19 E. W. Dent, A. V. Kwiatkowski, L. M. Mebane, U. Philippar, M. Barzik, D. A. Rubinson, S. Gupton and F. B. Gertler, Filopodia are required for cortical neurite initiation, *Nature Cell Biology*, 2007, **9**, 1347-1359.

20 S. R. Hart, A. Pierce, E. W. Dent and J. C. Williams, Modulating perpendicular axonal outgrowth by combined topographical and chemical cues, *In Review*, submitted April 2013.

21 C. Viesselmann, J. Ballweg, D. Lumbard and E. W. Dent, Nucleofection and primary culture of embryonic mouse hippocampal and cortical neurons, *J. Vis. Exp.*, 2011, 2373.

22 E. W. Dent and K. Kalil, Dynamic imaging of neuronal cytoskeleton, *Methods Enzymol.*, 2003, **361**, 390-407.

23 D. T. Eddington, J. P. Puccinelli and D. J. Beebe, Thermal aging and reduced hydrophobic recovery of polydimethylsiloxane, *Sensors and Actuators B: Chemical*, 2006, **114**, 170-172.

24 C. Pina-Hernandez, J.S. Kim, L. J. Guo and P. F. Fu, High-throughput and etch-selective nanoimprinting and stamping based on fast-thermal-curing poly (dimethylsiloxane) s, *Advanced Materials*, 2007, **19**, 1222-1227.

25 C. Y. Hui, A. Jagota, Y. Y. Lin and E. J. Kramer, Constraints on microcontact printing imposed by stamp deformation, *Langmuir*, 2002, **18**, 1394-1407.

26 W. K. Cho, K. Kang, G. Kang, M. J. Jang, Y. Nam and I. S. Choi, Pitch-dependent acceleration of neurite outgrowth on nanostructured anodized aluminum oxide substrates, *Anewandte Chemie International Edition*, 2010, **49**, 10114-10118.

27 Y. W. Fan, F. Z. Cui, S. P. Hou, Q. Y. Xu, L. N. Chen, and I. S. Lee, Culture of neural cells on silicon wafers with nano-scale surface topograph, *Journal of Neuroscience Methods*, 2002, **120**, 17-23.

28 V. Brunetti, G. Maiorano, L. Rizzelo, B. Sorce, S. Sabella, R. Cingolani and P. P. Pompa, Neurons sense nanoscale roughness with nanometer sensitivity, *Proceedings of the National Academy of Science*, 2010, **107**, 6264-6269.

29 Z. D. Wissner-Gross, M. A. Scott, D. Ku, P. Ramaswamy and M. F. Yanik, Large-scale analysis of neurite growth dynamics on micropatterned substrates, *Integrative Biology*, 2011, **3**, 65-74.

30 R. M. Smeal, R. Rabbitt, R. Biran and P. A. Tresco, Substrate curvature influences the direction of nerve outgrowth, *Annals of Biomedial Engineering*, 2005, **33**, 376-382.

Note to Readers: This project is very near completion and will soon be submitted to a journal for publication. A hearty acknowledgement must be made to the tremendous contribution of Josh Kolz, who has spearheaded the effort of data collection and analysis.

5.1 Title:

Parallel and Cross-alignment of Neurons and Glia in Co-culture By Topographical and Chemical Patterning

5.2 Abstract:

Numerous recent efforts have focused on aligning neurons and glial cells in co-culture. We present a model substrate, patterned chemically and modified topographically, which not only is capable of creating parallel alignment of neurons and glia, but also perpendicular or cross-alignment. Neuron-glia interactions are very diverse, and often very pronounced. In particular, neuronal soma migration is dramatically increased in cross-alignment conditions. Our system opens new possibilities in understanding the complex nature of neuron-glia interaction.

5.3 Introduction:

Non-neuronal cells in the brain, so-called glial cells, interact with neurons in order to accomplish brain functionality. Microglia serve as the primary immuneffector cells by using phagocytosis, antigen presentation and cytokine secretion[1, 2]. Astrocytes on the other hand make up most of the brain parenchyma and aid in the maintenance of healthy brain activity. This is done by generating precursors for glutathione, γ-aminobutyric acid (GABA), and glutamate

production[3, 4] and covering pre and post synaptic neural elements to assist in uptake of excess glutamate and potassium therein preventing hyperexcitability in the neuronal population[5, 6, 7]. In addition, astrocytes have been shown to modulate neuronal synapses with GABA, glutamate, and ATP release leading to neuronal plasticity, heterosynaptic depression, and long term potentiation (LTP)[8-11], regulate neurite growth throughout development[12], and control neurovascular microstructure[13]. Although these cell types aid in normal brain protection and function, when injury occurs, they lead to a glial scar preventing regeneration. Astrocytes undergo cell division and randomly pack tightly together in the injury site to become the main component of the glial scar[14]. They also begin to secrete molecules such as chondroitin and keratin sulphate proteoglycans, which serve to inhibit axon regrowth and repair[15]. Microglia are activated and migrate to the injury site where they can release free radicals, nitric oxide, and arachidonic acid derivatives therein increasing oxidative stress and preventing axon regrowth[14]. However, the presence of microglia have also been shown to be neuroprotective and permissive of axon growth[16]. For these reasons, glial cells are important in the central nervous system (CNS) for both development and injury repair. Therefore, developing culture conditions which enable controllable glial-neuron interaction will allow for increased understanding of the functionalities of glial cells in the nervous system.

There have been many substrates and techniques used to create a reproducible environment and alignment of glia-neuron co-cultures. Similar to behavior sometimes seen in the CNS[17], *in vitro* efforts have focused on demonstrating parallel alignment, which has been accomplished using a variety of techniques. For example, poly-lactide foam matrices were shown to induce glial alignment, which encouraged parallel directed neurite growth[18]. Astrocytes have been aligned using mechanical stress in which the cells elongate perpendicular to the force

vector or on nonuniform nanometer-scale topography using machined nickel surface standards and heat-molding techniques with a laminin coating and the subsequent neuronal growth was parallel to the aligned astrocytes[19]. Astrocytes also induced parallel growth of neurons on micrometer scale polystyrene grooves created with photolithography and coated with laminin[20, 21]. Another group showed astrocytes align perpendicular to a physiologically relevant electric field and neurons again align with the astrocytes[22]. Additionally, etching and laser holography have been used to create micrometer and nanometer topographical contours and when coated with poly-D-lysine (PDL) induce oligodendrocyte and astrocyte alignment but no alignment preference is seen by neurons[23]. Micro-contact printing of laminin lines on glass slides showed a high level of alignment of astrocytes and neurons in a parallel orientation[24]. Nano-imprining lithography has been used to create micron scale topography on poly (methyl methacrylate) (PMMA), which led to parallel alignment of glia and neurons[25]. Polycaprolactone (PCL) substrates with microgroves created with hot embossing and coated with poly-L-lysing (PLL) also cause a parallel alignment of astrocytes and neurons[26]. Finally, neurons were aligned parallel to a bioinspired glial topography by aligning glial cells using a PLL micropattern on glass then replicating their topography using impression replication and 3D printing[27]. Although parallel alignment is predominantly observed in neuron-glia interactions, perpendicular alignment is also seen in the hippocampus[28, 29] and the cortex[30], although this has not been demonstrated in culture.

Here we describe a simple and robust technique utilizing diffraction gratings as soft lithography masters to create micro/nanoscale topography along with chemical patterning to achieve both parallel and perpendicular alignment of neurons and glia in co-culture. On our substrate, glial cells preferentially align themselves with microgrooves, while neurons strongly

align themselves with patterned poly-D-lysine (PDL) lines. The lines may be oriented as desired relative to the topography, making parallel or cross alignment possible. Three distinct glia-neuron interactions are seen in the co-culture condition (1) neuronal soma migration inducement, (2) weak interactions, and (3) transient interactions.

5.4 Methods:

5.4.1 *Construction of Topographically Modified PDMS Stamps and Substrates*

Polydimethylsiloxane (PDMS) stamps and substrates were created according to previously established methods[31, 32]. Briefly, PDMS (184, Slygard – Dow Corning) base was mixed with the curing agent in a 10:1 ratio by weight and placed in a vacuum chamber for 20 minutes to remove air bubbles. A drop of PDMS was then placed on a clean 25mm glass coverslip and an optical diffraction grating with a periodicity of 1.7µm and a maximum depth of 700nm (Optometrics 3-4616) was placed in the PDMS drop. A 100g weight was placed on top of the grating to ensure uniformity of the PDMS layer and the PDMS covered and cured at 85^{o}C for 30 minutes on a hot plate. After curing, the weight, diffraction grating, and excess PDMS were removed. Similarly, PDMS was spin coated onto clean 25mm glass coverslips, covered, and cured at 85^{o}C for 30 minutes on a hot plate to construct uniformly coated PDMS substrates. Likewise, a diffraction grating with a periodicity of 32µm was placed in a custom PDMS mold and the mold then filled with PDMS mixed in a 10:1 (base to curing agent) ratio by weight to create the stamps. The mold was covered and placed on a hot plate and cured for 30 minutes at 85^{o}C. The diffraction grating was removed and the stamps cut from the mold. Both stamps and PDMS substrates were autoclaved for 60 minutes at 120^{o}C for 1 hour. PDMS substrates were then mounted in a 35mm Petri dish and sealed with paraffin wax. These devices were then

soaked in 100% ethanol for 30 minutes and rinsed 3x with sterilized water. PDMS stamp surfaces were washed with 100% ethanol and rinsed 3x with sterilized water.

5.4.2 *PDL Coating and Stamping*

Uniformly coated PDMS substrates were covered with 300 µL of poly-D-lysine (PDL, 1 mg/mL) for 1 hour, PDL removed, and rinsed 3x with sterilized water to generate a constant PDL coating. PDMS stamps were covered with 200uL of PDL for 30 minutes and rinsed 2x with sterilized water. This process was repeated 3x per stamp. The stamp was then inverted and positioned on a topographically modified PDMS substrate with 100g of mass placed on top. The stamp was removed after 1 minute if the modified substrate was plasma treated for 20 seconds with a plasma wand (ETP Model BD-20) or 2 minutes if the substrate was not plasma treated.

5.4.3 *Cell Culture*

Cortical neurons (E15.5) and glia (P1-P3) from Swiss Webster mice were utilized in this study. Cells were removed, isolated, and cultured according to previous methods [DentPaper]. Briefly, neurons were dissociated with 2.5% trypsin for 20 minutes at 37^{o}C, titurated with a micropipette, and diluted in plating medium (neurobasal medium with B27 supplement, 2mM glutamine, 0.3% glucose, 37.5mM NaCl and 5% fetal bovine serum). Neurons were then plated onto the PDMS substrates at a density of 10,000 cells/cm^2 for 1 hour then flooded with 2mL of serum free medium (plating medium without fetal bovine serum) and incubated for 2 days. Glia were dissociated with 0.25% trypsin for 10 minutes at 37^{o}C, agitated with a micropipette, and 5x10^6 cells diluted in 15mL of glial medium (minimum essential media with 0.3% glucose, penicillin/streptomycin, and 10% horse serum) in 75cm^2 flasks. Media was changed every 3 days

and glia was harvested after 2 weeks of growth in the flasks. Glia were plated onto PDMS substrates at a density of 10,000 cells/cm^2 for 1 hour then flooded with 2mL of glial media for 2 days. For co-culture studies, neurons were plated onto the PDMS substrates at a density of 10,000 cells/cm^2 for 1 hour then flooded with 2mL of serum free medium and incubated for 2 days. Medium was removed and glia plated at a density of 10,000 cells/cm^2 for 1 hour then flooded with 2mL of serum free media and incubated for an additional 2 days. All cells were fixed for imaging in 4% PKS (PFA/Krebs Solution) for 15 minutes followed by washing 3x with PBS and 0.25% azide. All mouse procedures were approved by the University of Wisconsin Committee on Animal Care and were in accordance with NIH guidelines.

5.4.4 *Imaging and Data Analysis*

Fixed cultures were imaged with a Nikon Biostation IM-Q with a 20x contrast objective or an inverted fluorescence microscope with a 20x phase objective. For alignment studies, 4 samples were imaged for each experimental condition and 50-100 cells per sample were analyzed. Alignment analysis was performed using FIJI software. Graphs were created using KaleidaGraph and polar plots generated in Matlab. Values given are an average of the four independent samples, with standard error given as a plus/minus. Migration studies were captured using a Nikon Biostation IM-Q with a 20x phase contrast objective between 0-48 hours after plating. Migration analysis was performed using manual tracking on FIGI software.

5.5 Results and Discussion

5.5.1 Neuronal Alignment

Topographically features, consisting of parallel grooves of 1.7 μm periodicity, were overlaid with patterned lines of poly-D-lysine (PDL) with a periodicity of 32 μm. The lines were stamped using a PDMS master so as to result in the lines and grooves either being parallel or perpendicular. Before applying this arrangement to co-culture conditions, we tested the efficacy of our substrate in aligning neuronal outgrowth. Whether the lines were printed perpendicular to the grooves (Figure 1c) or parallel (Figure 1d), neuronal alignment was excellent, with virtually all axons growing along a single line for the entirety of their growth.

5.5.2 Glial Alignment

Likewise, we tested glial alignment to the grooved substrates without the presence of neurons. Glial cell orientation was measured by a line drawn from distal ends of the cell, and comparing it relative to the direction of the grooved topography. Whether PDL was stamped perpendicular to the grooves or parallel to the grooves, the glia preferred to elongate parallel to the grooves (Figure 2). Typically 80% of the glia were aligned within 10° of the groove direction. On topographically smooth substrates, it was not unusual for the glia cells to elongate (Figure 2b), but their orientation was random. It is crucial for the co-culture that the glia respond strongly to the grooves, but not to the patterned PDL lines.

5.5.3 Co-Culture Alignment and Neuronal Soma Migration

Even in co-culture, neurons and glia largely retained their alignment preferences. Glia still predominantly aligned with the grooves, and neurons to the lines. Interaction between the

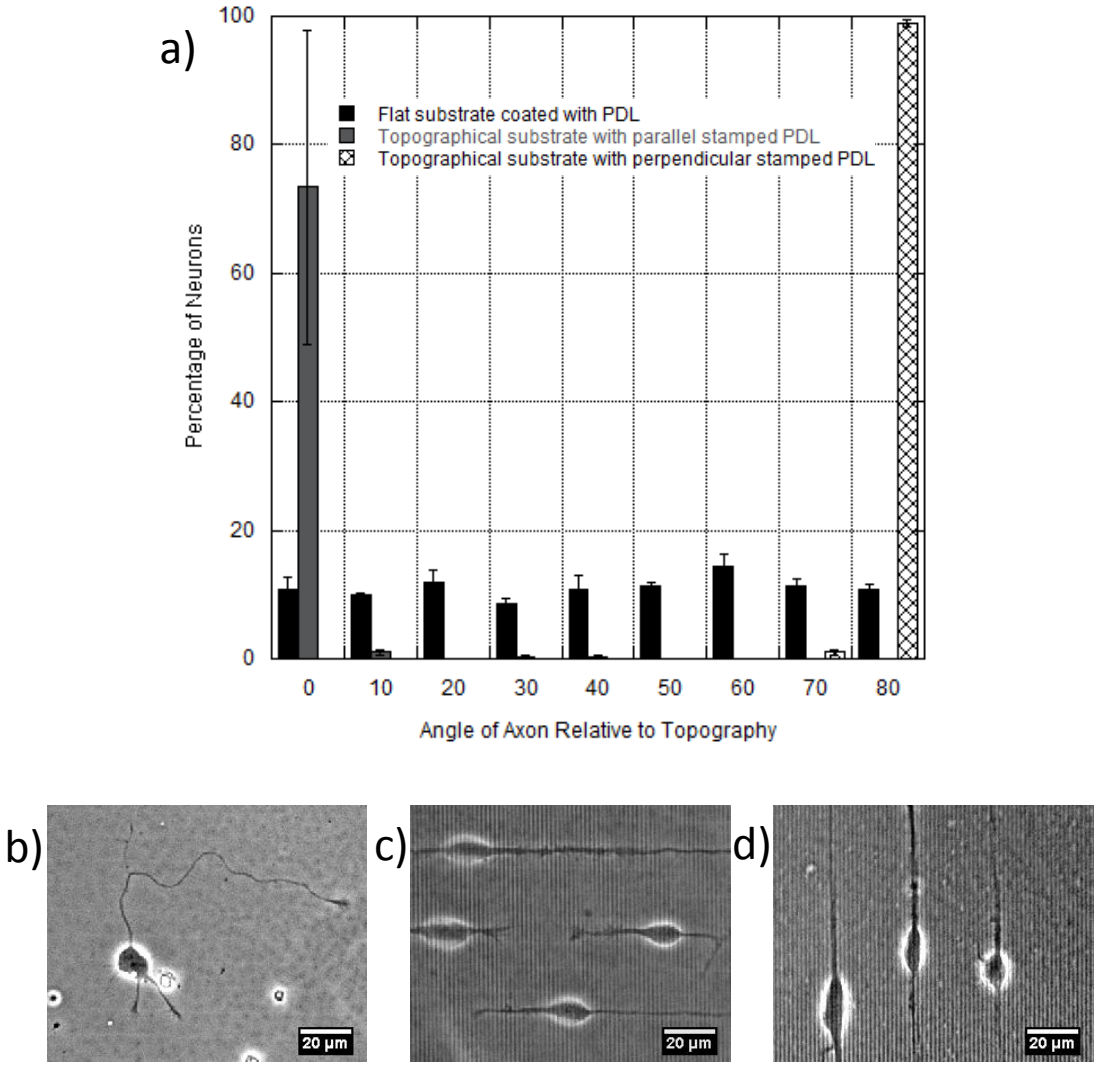

Figure 1. Neurons seeded on PDL stamped topographical substrates align with the PDL lines, mostly independent from the underlying topography. (a) Data shows axonal outgrowth direction relative to the topography on the PDMS substrates. The outgrowth angle is defined as the angle between the topographical lines in the PDMS and a straight line drawn from the neuron soma to axon tip. Over 95% of axons grow within 10 degrees of the topography for parallel stamped PDL lines (grey) and over 98% of axons grow between 80-90 degrees of the topography when PDL lines are stamped perpendicular to the topography. When neurons are seeded on flat substrates with a uniform PDL coating, they show no alignment preference (black). (b) Representative phase image of neurons grown on a flat PDMS substrate uniformly coated with PDL. (c) Representative phase image of neurons grown on topographical PDMS substrates with PDL stamped parallel to the topography. (d) Representative phase image of neurons grown on topographical PDMS substrates with PDL stamped perpendicular to the topography. All scale bars are 20µm.

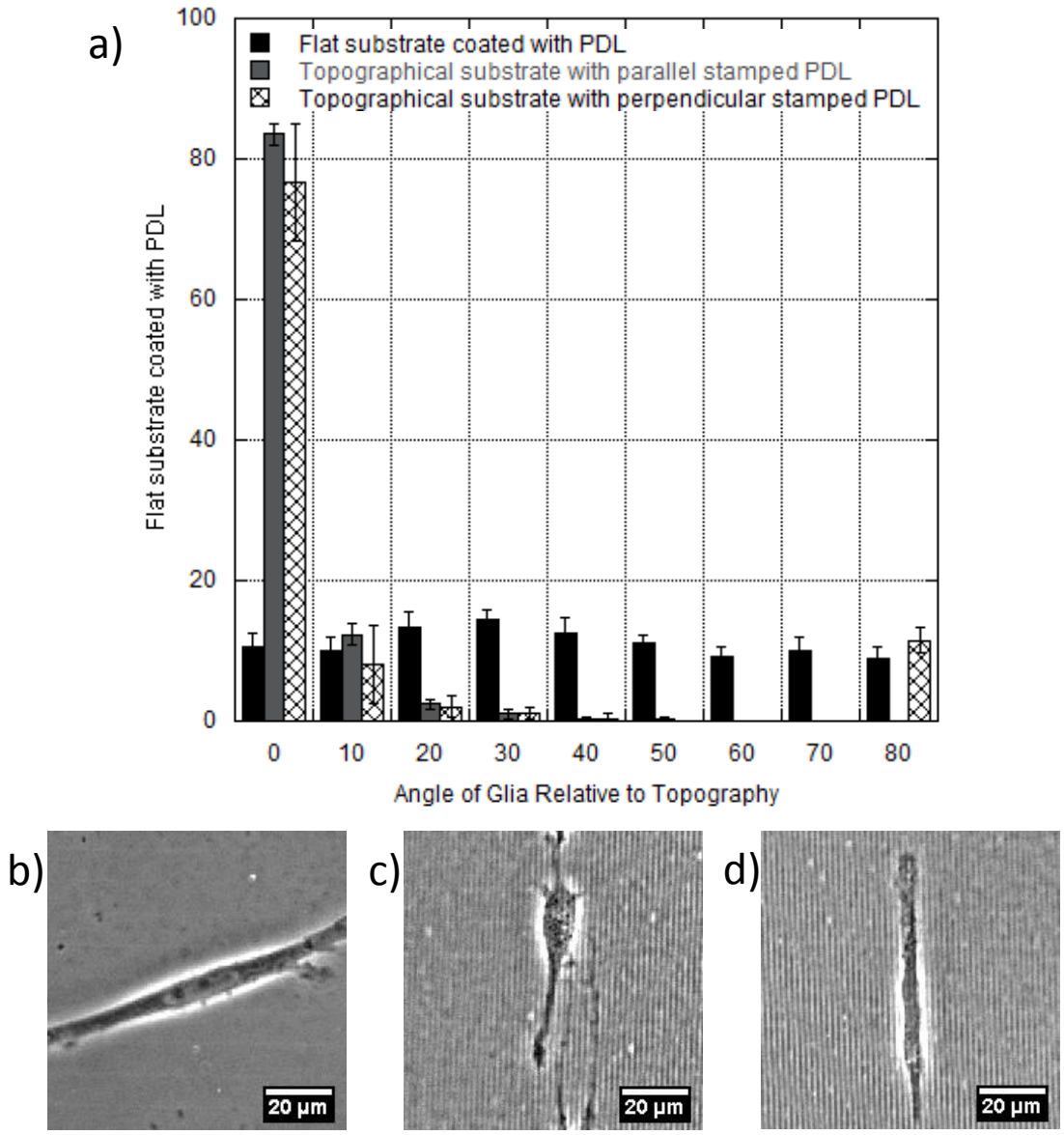

Figure 2. Glia seeded on PDL stamped topographical substrates align with the topography rather than the PDL lines. (a) Data shows glia outgrowth direction relative to the topography on the PDMS substrates. The outgrowth angle is defined as the angle between the topographical lines in the PDMS and a straight line drawn from the two tips of the glial cell. Over 83% of glia grow within 10 degrees of the topography for parallel stamped PDL lines (red) and over 76% of glia grow within 10 degrees of the topography for perpendicular stamped PDL lines. When glia are seeded on flat substrates with a uniform PDL coating, they show no alignment preference (black). (b) Representative phase image of glia grown on a flat PDMS substrate uniformly coated with PDL. (c) Representative phase image of glia grown on topographical PDMS substrates with PDL stamped parallel to the topography. (d) Representative phase image of glia grown on topographical PDMS substrates with PDL stamped perpendicular to the topography. All scale bars are 20µm.

glial cells and neurons was often very strong. Overall alignment, however, remained about as before. In order to create the co-culture, we would culture neurons on the substrates first. 2 days later, glia were added. When done in reverse, it was not uncommon for the neurons to experience decreased outgrowth, instead congregating with one another and the glia. By culturing the neurons first, we allowed the establishment of lengthy neurites.

Migration of neuronal soma proved to be very interesting in co-culture conditions. Whereas the somata of the neurons would migrate but little when cultured in isolation (Figure 3a), when in the presence of the glia, translocation rates increased significantly, from a maximum of about 12 μm/hr up to 51 μm/hr. On topographically modified, but uniformly PDL-coated surfaces, neuronal migration is even more reduced (data not shown). Migration rates were largest (51 μm/hr) when the neurons and glia were parallel, achieved with PDL lines parallel to the topography (Figure 3d). When neurons and glia are perpendicular, although the maximum migration rates are not as high (28 μm/hr), the effect is significant in that soma are very frequently drawn off of the previously occupied PDL line. When this occurs, it is very common for the distal end of the neurite to remain on the patterned line (Figure 3e). Tension generated by this interaction results in the proximal portion of the neurite also getting pulled off of the PDL line. We think it possible that this arrangement could also cause stretch-induced elongation of the neurite, a possibility which should be explored in future work.

5.5.4 Weak Interactions and Transient Interactions

Occasionally, neurons and glia would interact at a very low level. These glia would commonly be less motile, slowly advancing the lamellopodial edge. A growing neurite could extend across the glial cell, with little to no interaction occurring. Whether weak interaction is a

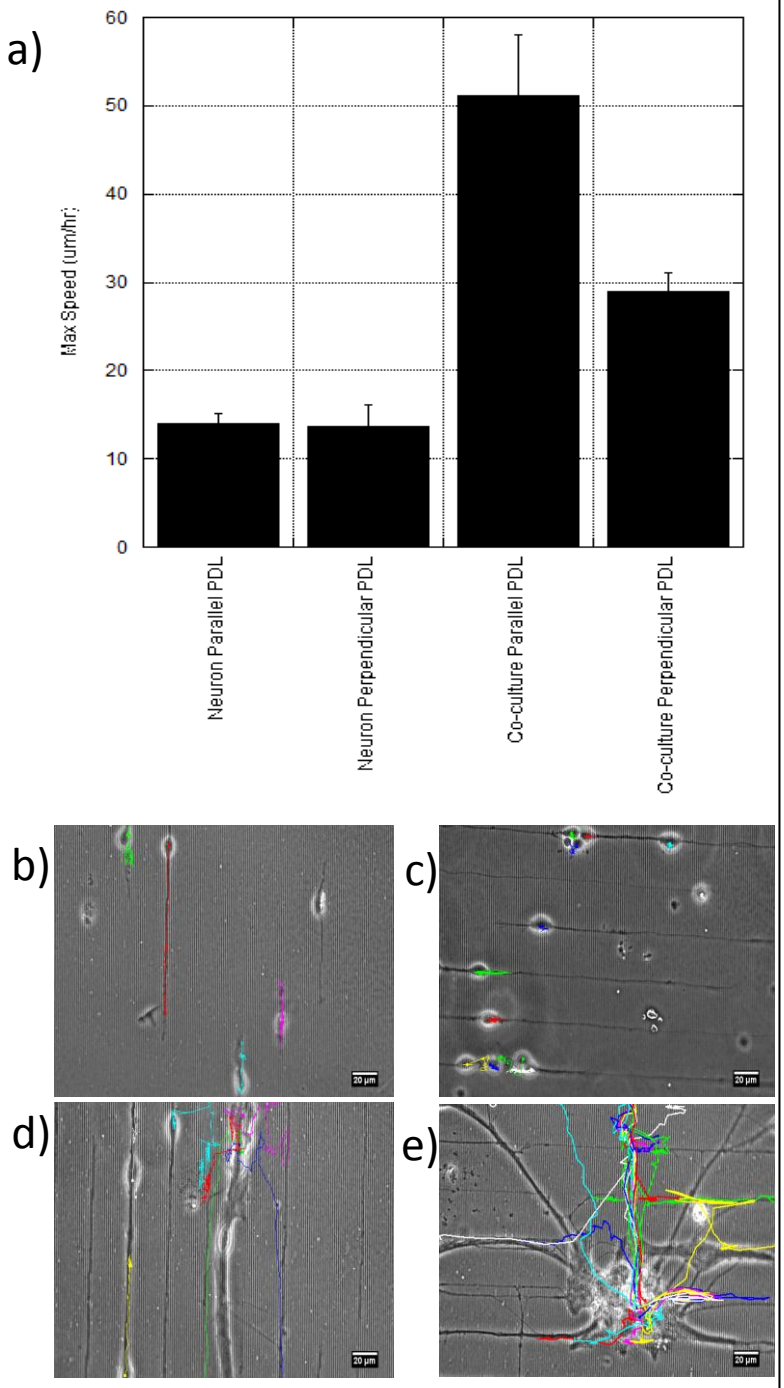

Figure 3. When neurons and glia are cocultured on topographic PDMS with stamped PDL lines, the glia induce migration and line crossing. (a) Data shows the maximum migration speed of neurons in microns per hour over a period of approximately 48 hours. When neurons were cultured alone on topographic PDMS with stamped PDL lines parallel or perpendicular to the topography they migrate around 12µm/hr. But, when glia are added, the maximum migration speeds significantly increased to 28µm/hr when the PDL was stamped perpendicular to topography and 51µm/hr when the PDL was stamped parallel to the topography. Along with increasing the maximum migration speeds, the glia often caused the neurons to change lines as can be seen in the cell tracking images (d) coculture on topographic PDMS with parallel stamped PDL lines and (e) coculture on topographic PDMS with perpendicular stamped PDL lines when compared to neurons alone (b) neurons on topographic PDMS with parallel stamped PDL lines and (c) neurons on topographic PDMS with perpendicular stamped PDL lines. All scale bars are 20µm.

result of glial activity, cell sub-type or some other factor remains to be determined.

Other interactions we classify as transient. Often very motile glia would begin interacting with a nearby neuron. This interaction could last anywhere from minutes to hours. This interaction was distinct from the interaction which induced soma migration in two ways: first, the interaction had a finite lifetime, and second, the glial cells involved did not stay localized on one area of the substrate. Figure 4 details the result of an observed transient interaction. A neuron is growing along a PDL line when a motile glia approaches and initiates interaction (10:30). Within a few hours, the glial cell has enabled a growth cone to be guided off of the original line and onto a new one (14:30), a feat rarely accomplished by a growth cone without external interaction. Several hours later, the glial cell has entirely left the vicinity, but now the neuron has a neurite growing across the gap between two parallel PDL lines. This phenomenon was observed in additional cases, including when the neurons and glia grow parallel to one another.

The cross-alignment of glia and neurons achieved in this work is significant in many ways. Besides the uniqueness of the achievement, it presents many possibilities for various studies and applications. An interesting feature of cross-alignment is the maximization of communication. A single neuron will may potentially interact with several glial cells at once, while a single glial cell may directly communicate with several neurons. Further optimization and characterization of this culture system will continue, with the benefit of increased understanding of neuron-glia behavior in the brain.

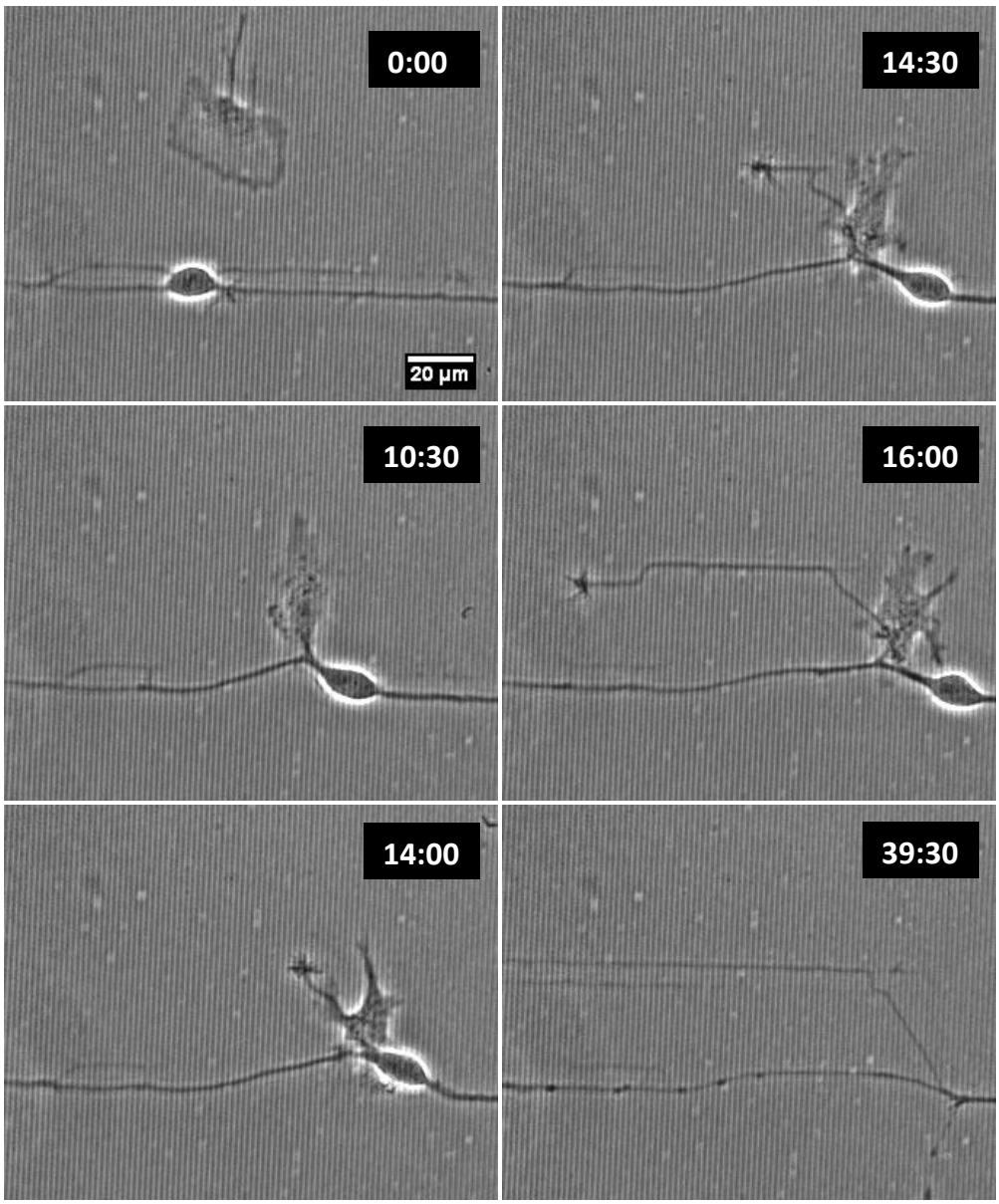

Figure 4. When neurons and glia are cultured together, transient interactions occur. This group of six time lapse photos shows the transient interaction of a neuron and glia. The glial cell interacts with the neuron for approximately 40 hours and guides the neural axon off of its original PDL line and onto a higher PDL line. This process of guiding neural axons to a different PDL lines also happens in the parallel stamped cultures, but on a less frequent basis likely because of the glial cells preference for migration and growth parallel to the PDMS topography. All frames are scaled to the same size and use the 20µm scale bar from the first frame.

5.6 Conclusions

We have created a co-culture system of neurons and glia. By exploiting neuronal tendencies to elongate along PDL lines, and glial tendencies to align with underlying topography, we have made a system with either co- or cross-alignment of glia and neurons. This system creates new opportunities for examining the effects of glial cells on nervous system functionality.

5.7 References

1 K. Nakajima and S. Kohsaka, Functional roles of microglia in the brain, *Neuroscience Research,* 1993, **17**, 187-203.

2 J. Gehrmann, Y. Matsumoto and G. W. Kreutzberg, Microglia: intrinsic immuneffector cell of the brain, *Brain Research Reviews,* 1995, **20**, 269-89.

3 R. Dringen, B. Pfeiffer, B. Hamprecht, Synthesis of the antioxidant glutathione in neurons: supply by astrocytes of CysGly as precursor for neuronal glutathione, *The Journal of Neuroscience*, 1999, **19**, 562-569.

4 M. Sidoryk-Wegrzynowcz, M. Wegrzynowicz, E. Lee, A. B. Bowman and M. Aschner, Role of astrocytes in brain function and disease, *Toxicologic Pathology*, 2011, **39**, 115-123.

5 R. Ventura and K. M. Harris, Three-dimensional relationships between hippocampal synapses and astrocytes, *The Journal of Neuroscience*, 1999, **19**, 6897-6906.

6 D. E. Bergles, J. S. Diamond and C. E. Jahr, Clearance of glutamate inside the synapse and beyond, *Current Opinion in Neurobiology,* 1999, **9**, 293-298.

7 T. A. Fiacco, C. Agulhon and K. D. McCarthy, Sorting out astrocyte physiology from pharmacology, *Annual Review of Pharmacology and Toxicolology*, 2009, **49**, 151-174.

8 A. S. Kozlov, M. C. Anulo, E. Audinat and S. Carpak, Target cell-specific modulation of neuronal activity by astrocytes, *Proceedings of the National Academy of Sciences*, 2006, **103**, 10058-10063.

9 G. Perea and A. Araque, Astrocytes potentiate transmitter release at single hippocampal synapses, *Science*, 2007, **317**, 1083-1086.

10 J. Chen, Z. Tan, L. Zeng, X. Zhang, Y. He, W. Gao, X. Wu, Y. Li, B. Bu, W. Wang and S. Duan, Heterosynaptic long-term depression mediated by ATP released from astrocytes, *Glia*, 2013, **61**, 178-191.

11 O. Pascual, K. B. Casper, C. Kubera, J. Zhang, R. Revilla-Sanchez, J. Y. Sul, H. Takano, S. J. Moss, K. McCarthy and P. G. Haydon, Astrocytic purinergic signaling coordinates synaptic networks, *Science*, 2005, **310**, 113-116.

12 K. Kanemaru, Y. Okubo, K. Hirose and M. Lino, Regulation of neurite growth by spontaneous Ca2+ oscillations in astrocytes, *The Journal of Neuroscience*, 2007, **27**, 8957-8966.

13 C. Ladecola and M. Nedergaard, Glial regulation of the cerebral microvasculature, *Nature Neuroscience*, 2007, **10**, 1369-1376.

14 J. W. Fawcett and R. A. Asher, The glial scar and central nervous system repair, *Brain Research Bulletin*, 1999, **49**, 377-391.

15 J. Silver and J. H. Miller, Regeneration beyond the glial scar, *Nature Reviews Neuroscience*, 2004, **5**, 146-156.

16 A. G. Rabchevsky and W. J. Streit, Grafting of cultured microglial cells into the lesioned spinal cord of adult rats enhances neurite outgrowth, *Journal of Neuroscience Research*, 1998, **47**, 34-48.

17 J. P. Mission, C. P. Austin, T. Takahashi, C. L. Cepko and V. S. Caviness, The alignment of migrating neural cells in relation to the murine neopallial radial glia fiber system, *Cerebral Cortex*, 1991, **1**, 221-229.

18 R. Deumens, G. C. Koopmans, C. G. Den Bakker, V. Maquet, S. Blacher, W. M. Honig, R. Jerome, J. P. Pirard, H. W. Steinbusch and E. A. Joosten, Alignment of glial cells stimulates directional neurite growth of CNS neurons in vitro, *Neuroscience*, 2004, **125**, 591-604.

19 R. Biran, M. C. Noble and P. A. Tresco, Directed nerve outgrowth is enhanced by engineered glial substrates, *Experimental Neurology*, 2003, **184**, 141-152.

20 J. B. Recknor, J. C. Recknor, D. S. Sakaguchi and S. K. Mallapragada, Oriented astroglial cell growth on micropatterned polystyrene substrates, *Biomaterials*, 2004, **25**, 2753-2767.

21 J. B. Recknor, D. S. Sakaguchi and S. K. Mallapragada, Directed growth and selective differentiation of neural progenitor cells on micropaterned polymer substrates, *Biomaterials*, 2006, **27**, 4098-4108.

22 J. K. Alexander, B. Fuss and R. J. Colello, Electric field-induced astrocyte alignment directs neurite outgrowth, *Neuron Glia Biology*, 2006, **2**, 93-103.

23 A. Webb, P. Clark, J. Skepper, A. Compston and A. Wood, Guidance of oligodendrocytes and their progenitors by substratum topography, *Journal of Cell Science*, 1995, **108**, 2747-2760.

24 F. Meng, V. Hlady, P. A. Tresco, Inducing alignment in astrocyte tissue constructs by surface ligands patterned on biomaterials, *Biomaterials*, 2012, **33**, 1323-1335.

25 M. Mattotti, A. Alvarez, J. A. Ortega, J. A. Planell, E. Engel and S. Alcantara, Inducing functional radial glia-like progenitors from cortical astrocyte cultures using micropatterned PMMA, *Biomaterials*, 2012, **33**, 1759-1770.

26 A. Sorensen, T. Alekseeva, K. Katechia, M. Robertson, M. O. Riehle and S. C. Barnett, Long-term neurite orientation on astrocyte monolayers aligned by microtopography, *Biomaterials*, 2007, **28**, 5498-5508.

27 C. M. Kofron, Y. T. Liu, C. Y. Lopez-Faqundo, J. A. Mitchel and D. Hoffman-Kim, Neurite outgrowth at the biomimetic interface, *Annals of Biomedical Engineering*, 2010, **38**, 2210-2225.

28 B. E. Nixdorf-Bergweiler, D. Albrecht and U. Heinemann, Developmental changes in the number, size, and orientation of GFAP-positive cells in the CA1 region of rat hippocampus, *Glia* 1994, **12**, 180-195.

29 A. Wallraff, R. Kohling, U. Heinemann, M. Theis, K. Willecke and C. Steinhauser, The impact of astrocytic gap junctional coupling on potassium buffering in the hippocampus, *The Journal of Neuroscience*, 2006, **26**, 5438-5447.

30 E. A. J. Joosten and A. A. M. Gribnau, Astrocytes and guidance of outgrowing corticospinal tract axons in the rat. An immunocytochemical study using anti-vimentin and anti-glial fribrillary acidic protein, *Neuroscience*, 1989, **31**, 439-452.

31 S. R. Hart, Y. Huang, T. Fothergill, D. C. Lumbard, E. W. Dent and J. C. Williams, Adhesive micro-line periodicity determines guidance of axonal outgrowth, *Lab on a Chip*, 2013, **13**, 562-569.

32 S. R. Hart, A. Pierce, E. W. Dent and J. C. Williams, Modulating perpendicular axonal outgrowth by combined topographical and chemical cues, *In Review*, submitted April 2013.

Chapter 6

Current and Future Work

Note to readers: This chapter is organized in three distinct sections. Although the projects described in each section are related to the techniques and findings presented in earlier chapters, each project is here presented independently in order to outline current and future possibilities. Each of these projects represents work that is not published, but could be profitably advanced in the near future. (Note: Figure 6.2.1was published as supplementary material for the paper published in Chapter 2. It is included here for thematic consistency.)

6.1.1 **Project Title:**

Compressive Microtubule Forces Cause Axon Coiling on Micropatterned Surfaces

6.1.2 **Abstract:**

Microtubule assays often experience a looping or spooling effect, especially when the microtubules are of sufficiently high density. By examining axons that grow perpendicular to repetitive micropatterned lines and globally inhibiting actin polymerization, we found that the midpoints of the axons would continue to experience growth. This growth first bulges outward, and then spontaneously coils into a loop. The microtubule coils are very dynamic, frequently changing in size and shape. The coils have a diameter from 3.3 μm to 5 μm, typically conforming to the underlying micropattern.

6.1.3 **Introduction**

The cellular cytoskeleton is a highly dynamic system. Polymerization of cytoskeletal elements drives many important cellular processes such as outgrowth, migration, maintenance of morphology and mitosis. The role of cytoskeletal processes in axon elongation is an area of intensive study. The interplay of microtubule bundles and actin filaments is highly complex. It has long been established that the two elements work in concert in determining axonal outgrowth, with actin pulling the growth cone forward, and microtubule polymerization pushing[1]. This represents a fascinating system from a biophysical perspective, and much attention has been given in recent years to the role of various cytoskeletal forces in axonal elongation[2]. Much work is done in protein assays. However, it is often beneficial to examine living cells, which can be pharmacologically treated to create desired growth schemes. For example it has been shown that stabilizing microtubules will decrease axon elongation[3].

In this work, we show an entire axon can be induced to form coils, upon treatment with an actin polymerization inhibitor. As the microtubules continue to polymerize, compressive forces along the length of the axon cause the entire axon to buckle outward, and then form coils.

6.1.4 **Materials and Methods**

Substrate fabrication and neuronal culture The process of creating repetitive micro-line patterns of poly-lysine (PDL) on a polydimethylsiloxane (PDMS) substrate is described in detail in Chapter 2. The creation of microgrooved PDMS substrates is described in detail in Chapter 3. In this study, data is gathered from neurons on micro-lines with a 3.3 μm

periodicity and from neurons on grooves with a 1.7 μm periodicity. This project examined cortical neurons, the culture of which is fully described in Chapter 2.

Pharmacological treatment Cytochalasin-D (Sigma-Aldrich, C8273) in powder form is diluted in DMSO to a molarity of 5 or 10 μM. Nocodazole (Sigma-Aldrich, M1404) and Blebbistatin (Sigma-Aldrich, B0560) were likewise diluted to 500 nM and 50 μM, respectively. Neurons were allowed to grow from 12-24 hours before treatment.

Data Collection and Analysis Time lapse data were collected in the Nikon Biostation incubator/phase microscope, using either a 40x or 80x objective. Measure of coil radius was performed by manually fitting a circle to the coil in Image J, and determining the radius from the area.

6.1.5 **Results**

Control on uniform PDMS

Control experiments were conducted on smooth PDMS uniformly coated with 1 mg/ml PDL. 24 hours after seeding neuronal cells onto the surface, Cytochalasin D (cytoD) was added at a molarity of 10 μM. As expected, the cytoD caused growth cone collapse (Figure 6.1.1) through actin polymerization inhibition.

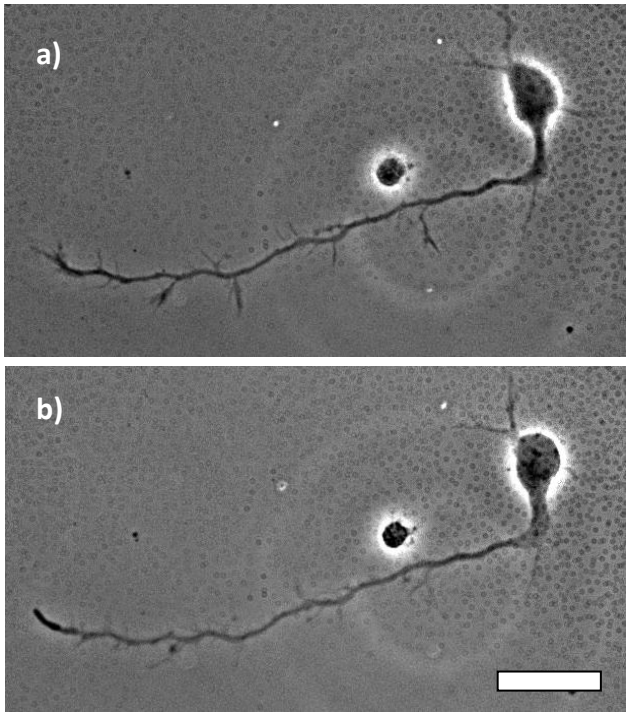

Figure 6.1.1 A neuron a) before and b) after treatment with 10 μM cytochalasin D (cytoD). Actin polymerization inhibition leads to growth cone collapse. Scale bar: 20 μm.

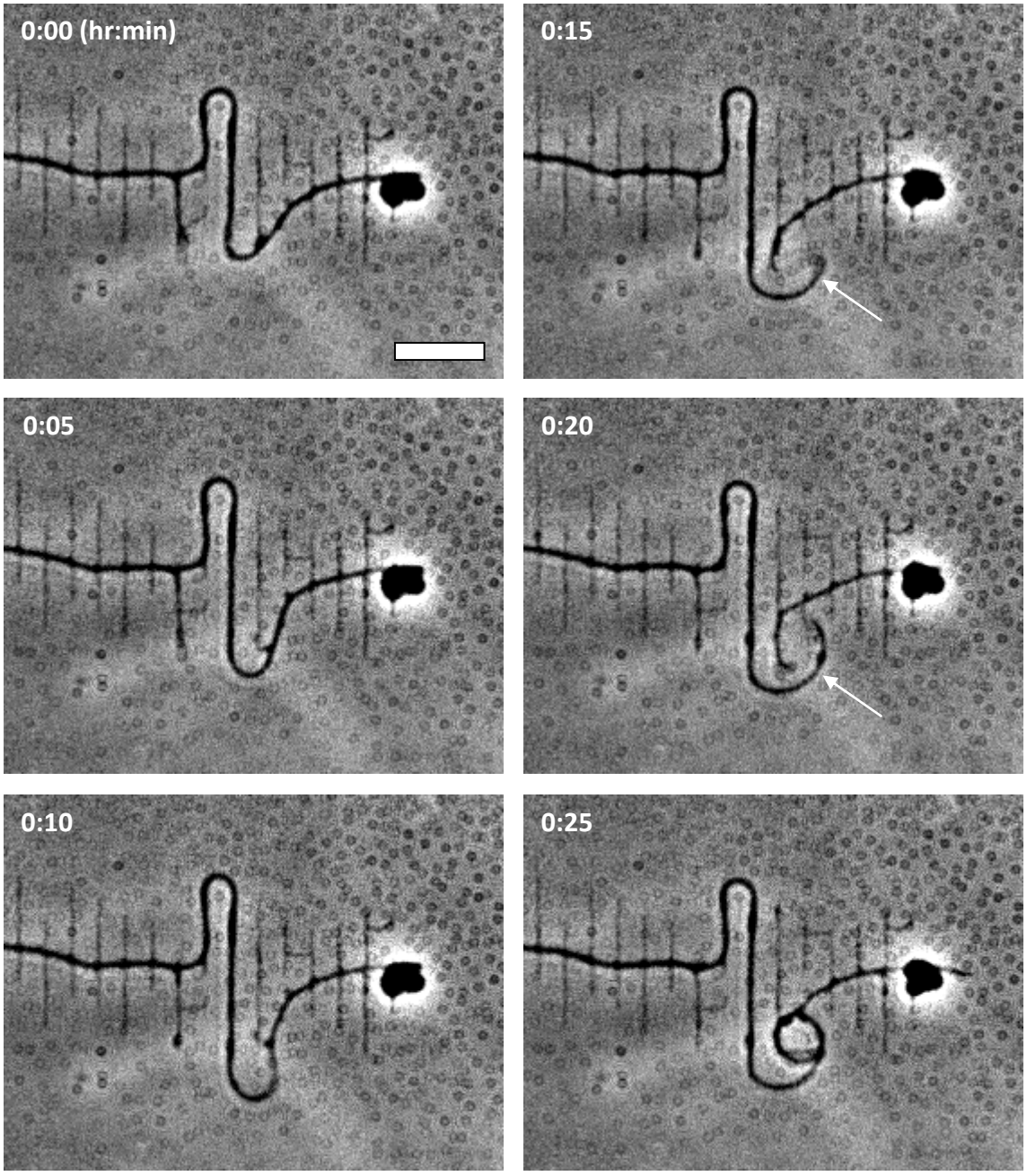

Figure 6.1.2 Time lapse images of an axon grown on micropatterned lines (running vertical) of poly-lysine. The images begin one hour after treatment with CytoD. At 15 and 20 minutes, the axon is not broken (arrows); rather, the axon is lifted off of the surface and out of the imaging plane before completing the coil by 25 min. The object to the right is the collapsed growth cone. Scale bar: 10 μm.

This was the only significant morphological change.

CytoD treatment on micropatterns

Once again, smooth PDMS is used as a substrate. In this case, however, a periodic line pattern is printed onto the surface, with a periodicity of 3.3 μm. As reported in Chapter 2, axons preferentially orient themselves orthogonal to lines of this geometry. Upon treatment with cytoD, the growth cone immediately collapsed as expected. But soon after, several axons began to display very unique growth characteristics (Figure 6.1.2). First, the axons would buckle outward, typically in a region in between two lines. This outward growth would continue some time, but commonly would result in the leading edge of the bulge lifting off of the surface, twisting, and creating a coil out of the axon. The coils were highly dynamic, changing in size, shape, and thickness. Coils could persist anywhere from 20 minutes to several hours, with an average of 2.1 hours. Some coils were large and abnormally shaped. Those that were circular (~90%) had an average diameter of 5.1 μm. This experiment was repeated on microgrooved substrates of 1.7 μm periodicity. This was chosen as axons preferentially grow perpendicular to such a substrate, mimicking the intermittent adhesion available to axons growing perpendicular to patterned lines. Once again, the axon exhibited coiling behavior (Figure 6.1.3).

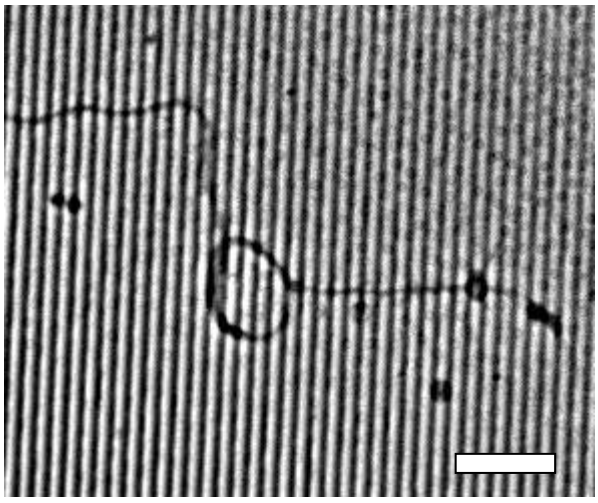

Figure 6.1.3 Coil in cytoD-treated axon on grooved topography of 1.7 μm periodicity. Scale bar: 10 μm.

Treatment with nocodazole and blebbistatin To further ascertain by what mechanism the axons were coiling, we next treated the axons simultaneously with nocodazole,

which inhibits microtubule dynamics, and cytoD. Also, we attempted treatment with blebbistatin, which is myosin IIA inhibitor, leading to a decrease in myosin/actin interaction. Results of pharmacological testing are tabulated in Table 6.1:

Table 6.1

	CytoD – 10 μM	Blebb – 50 μM	Nocod – 500 nM
Result Alone	Growth cone collapse, axon buckling and looping	N/A	Growth cone pause, some axons retract
Result Combined with 10 uM CytoD	N/A	Growth cone collapse, axon buckling and looping	Growth cone pause, some axons retract

It is reasonable to conclude that dynamic microtubule activity is necessary for the looping behavior, as indicated by the test with nocodazole. The neurons in such a case would most commonly experience arrested growth, but no coiling of axons occurred. Inclusion of blebbistatin seemed to have no effect on the coiling of the axons.

6.1.6 **Discussion and Outlook**

These results segue nicely with recent experiments done investigating the biophysics of isolated microtubules. For example it has been found in a microtubule gliding assay, if the microtubule concentration is high enough, that oftentimes the microtubules form looped structures[4]. In another study, surface adhered biomolecular motors were responsible for the self assembly of microtubule based nano-ring structures[5].

Another very compelling idea that stems from these results is the idea of compressive forces along the length of the axon. Much attention has been given to the tensile forces generated by the growth cone. These results, however, seem to suggest that compressive forces generated by microtubule polymerization could be equally important for axonal outgrowth. Moreover, these forces may originate not only near the growth cone, but perhaps along the entire axonal shaft.

In order to better elucidate the mechanisms behind the axon coiling, more experiments should be conducted. At least two seem very good choices: First, additional pharmacological studies should be carried out, using something that modulates the microtubule kinesin motors. Specifically, it has been shown Kinesin-5 regulates microtubule bundle sliding, and inhibition will accelerate axon growth[6]. This will help test the hypothesis that microtubule bundle sliding is the mechanism behind the continued axonal growth under actin inhibition. A second experiment to be conducted would be to transfect dynamic microtubules with a fluorescent tag, and carry out the same experiment but with fluorescent microscopy with high spatial (100x) and temporal resolution. Whether microtubule polymerization, and presumed to be associated compressive buckling, is localized or distributed evenly along the length of the axon could thus be investigated.

6.2.1 **Project Title:**

Dynamics and Modeling of Growth Cone Turning on Patterned Micro-Grids

6.2.2 **Abstract**

Growth cone turning is a complex event, but of immeasurable importance in axonal pathfinding. We present a method of creating micro-grids which can guide neurite outgrowth. Growth cone turning only occurs at grid intersections, thus simplifying and standardizing a measure of a turn as compared with typical turn assays. The grids are of variable spacing, can have tunable line thickness, and are simple to produce or customize. We find that neurites growing on grids with narrow lines are far more likely to grow without turning for long distances, as compared with neurites on grids with wider lines.

6.2.3 **Introduction**

The pathfinding ability of axons is intrinsically linked to the ability of the growth cone to monitor and respond to a myriad of guidance cues[7]. The process is complex, involving sensation by filopodia[8], actin bundle dynamics[9], and microtubule stabilization[10]. Many traditional turning assays utilize a micropipette to disperse a chemoattractant or chemorepellant. Growth cone directional changes, as a rule quite modest, are then measured.

In the process of elongating, axons commonly create many branching points, sites of dynamics cytoskeletal interaction[11]. Many targets *in vivo* are not innervated by the leading

growth cone, but by a growth cone originating from a previous branching point[12]. Although this ability is likely critical for successful pathfinding, it is difficult to predict a branching site in traditional neuronal cell culture.

Using a lithography-free micro stamping technique (See Chapter 2), we created micro-grids of adhesive poly-lysine. We can control several aspects of grid geometry, including independent control of the pitch in multiple directions, grid skew, and the thickness of lines that compose the grid. We present results of neurite outgrowth on micro-grids with a pitch of 8.3 μm with variable line thickness. This represents an opportunity for a highly controllable growth cone turning and branching assay.

6.2.4 **Methods and Materials**

Grid Creation: As described earlier (Chapter 2), substrates of PDMS were stamped upon by diffraction-grating replicated PDMS stamps. Poly-D-lysine (PDL) or fluorescently (FITC) labeled poly-L-lysine (fPLL) were used as ink. The substrate preparation, stamp inking, and stamping procedures were all unchanged from that described previously. In order to create grids, two separate stamps were used in succession. By changing the stamping force, the width of the grid lines could be altered. For the results presented here, orthogonal alignment was achieved by hand.

Neuron Culture, Image capture, Data Analysis: Primary cortical neurons were seeded at a density of 6k/ cm^2, the culture of which was described previously. Images were captured by an inverted phase microscope, with a fluorescent lamp and filter to image the fPLL grids. Data were analyzed using Image J and Microsoft Excel.

6.2.5 **Results**

Characterization of grids, outgrowth direction The width of the grid was measured using Image J; an edge is defined where the fluorescent signal was 30% greater than the background. Although some variation in line widths occurred from the two stamps, only those whose measured values were within 15% of one another were used. Orthogonal lines had an average angular deviation of 2.9°. Directional neurite outgrowth was measured on the micro-grids. Outgrowth direction is defined as a straight line direction from soma to the tip of the longest neurite. As the width of the fPLL lines increased, outgrowth direction became more random (Fig. 6.2.1 b and c). On the narrowest lines, growth was directed in a rectilinear fashion, along either of the orthogonal directions. Where turning occurred, adjacent growth segments were entirely perpendicular.

Additional distinctive morphological characteristics also warrant mention. For example, the soma typically adopted one of two positions: either centered on the gap in the grid, so as to have all outside edges touching a fPLL line (Fig. 6.2.1 b-center), or centered on a line, occupying the gap between two orthogonal lines (Fig. 6.2.1 b-left). These represented 54±4% and 46±4% of the total, respectively, on the thinnest grids (line width $\leq$3.5 μm), and 74±3% and 26±3%, respectively, on the wider grids (line width $\geq$ 3.5 μm). Also, neurites on thick lines would commonly appear to be thicker, suggesting that the narrow lines may influence the size of neurite that would grow upon them.

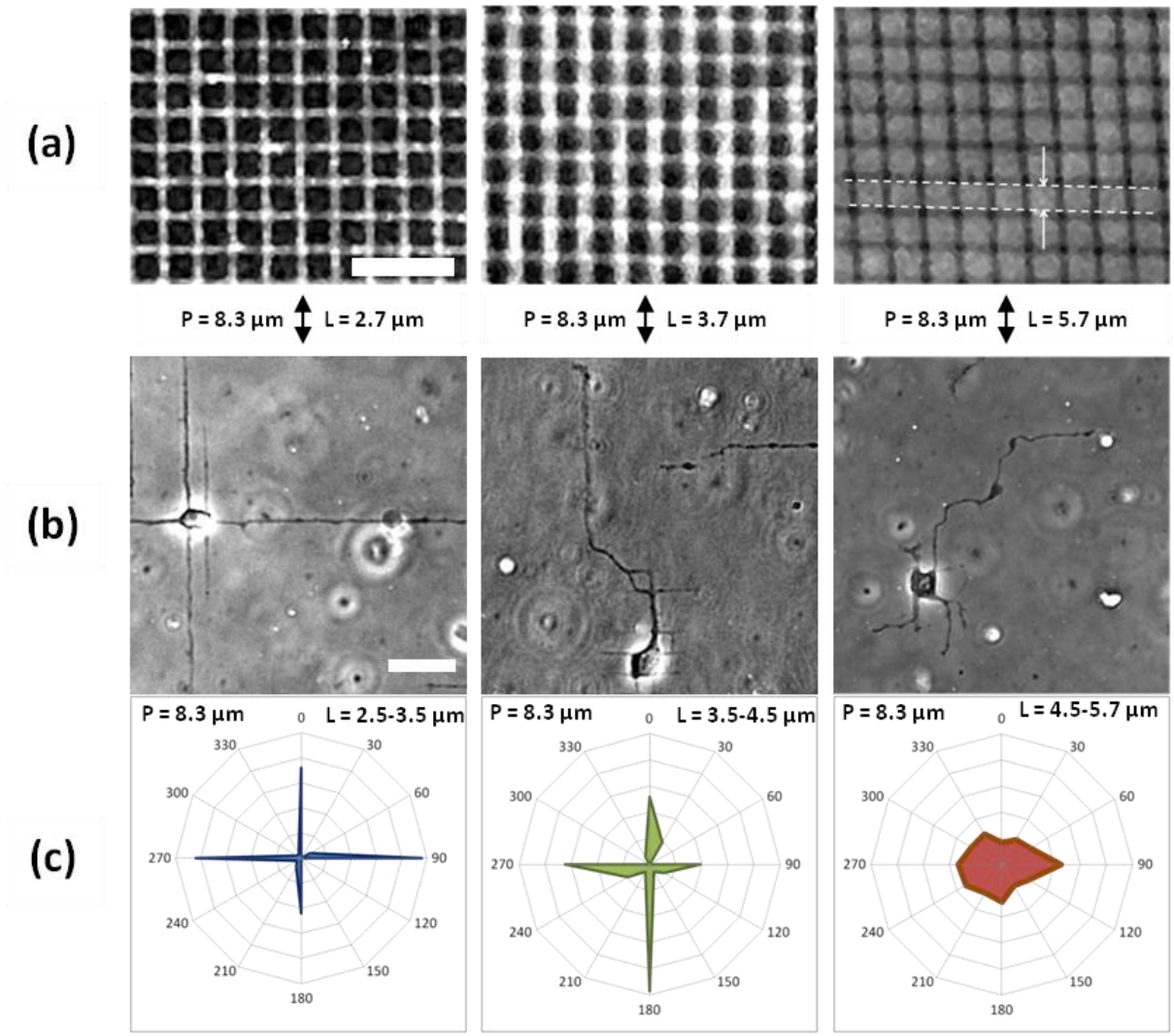

Figure 6.2.1 a) Fluorescent images of fPLL on PDMS. For all patterns, the periodicity (P) = 8.3 µm, while line width (L) is varied from 2.7 µm to 5.7 µm. For clarity, a horizontally printed line is outlined in the right image. Where the vertical lines intersect the horizontal lines, fPLL is deposited twice, causing all intersections to appear brighter. Scale bars in a) and b): 25 µm. b) Phase images of cortical neurons on PLL grid patterns after 48 hours. c) Polar distribution of neurite outgrowth. Although growing neurites interact with the poly-lysine grid in all cases, on more narrow line widths the growth is straighter, and the outgrowth direction more rectilinear.

In order to quantify the likelihood of a growing neurite to turn, we measured the total length of the longest neurite in grid units (each unit being 8.3 μm). We also counted the number of segments. (Number of segments – 1 = number of turns). We found there to be a linear relationship between the average length of the growth segments in the longest neurite, and the inverse of the line width (Figure 6.2.2). Or, simply, the neurites were far less likely to turn on the narrow-lined grids. Performing these measurements on the thinnest grids this was very precise, on the thicker ones, some estimation was performed.

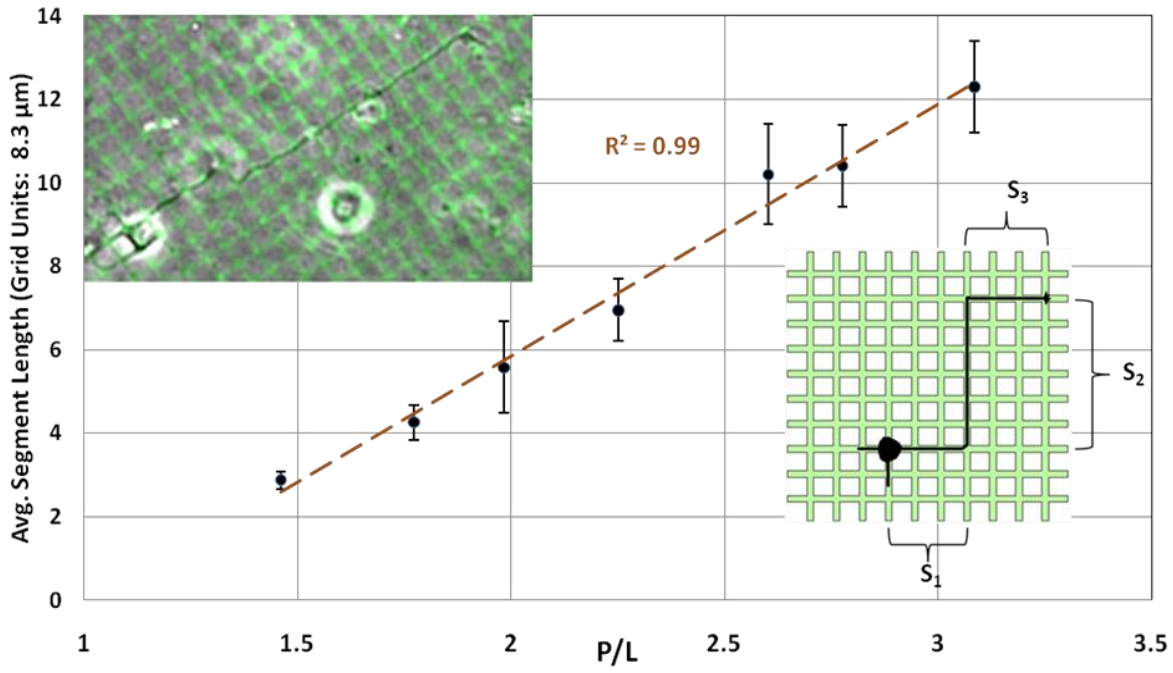

Figure 6.2.2 A neurite growing on the poly-lysine grid (upper left) follows the pattern with high fidelity, making two turns, resulting in three segments. A schematic (lower right) shows multiple segments of a representative neurite. Here the average segment length $((S_1 + S_2 + S_3)/3)$ is 4 grid units (~33 μm). There is a strong relationship between the average segment length of each neuron's longest neurite and the ratio of the periodicity to the line width (P/L). On grids with narrow lines (large P/L) the growing neurite is less likely to turn at any given intersection, resulting in longer neurite segment lengths.

6.2.6 **Discussion and Outlook**

Considering neurite outgrowth on a 2-D lattice, it would be very interesting to model the process as planar self-avoiding walk[13]. It would not be a true random walk; some bias that favored growing straight and scaling inversely with the size of the intersection would need to be introduced. Recent work by Staii and colleagues demonstrated that biased neuron outgrowth on an asymmetric textured surface could be descriptively modeled by a biased self-avoiding walk[14].

Some relatively recent work has been done on examining growth cone behavior and neurite branching at patterned intersections[15]. While valuable, additional insight is still needed to understand the mechanisms of neurite turning. Our setup is unique in that we can easily control line width and skew, or angle of intersection. Moreover, we can create grids that are with differential thickness along the two directions, or of a different aspect ratio (i.e. rectangular grids). Also, because of the accessibility of the method of stamp formation, this could serve as a widely adoptable platform for growth cone turning assays.

6.3.1 **Project Title:**

Patterning Neurons in Multiple Dimensions by Multi-Photon Excited Fabriction

6.3.2 **Introduction**

The creation of micropatterns for cell-based assays involves a variety of surface engineering techniques[16]. Typically, some lithographic procedure is used, followed by

biochemical functionalization of the pattern and/or background, which is of critical importance to successfully pattern cells[17].

Common techniques for micropatterning neurons typically suffer from one of two drawbacks: Many methods lack sufficient flexibility to allow for design modification without significant cost of time and resources; other methods are very flexible, commonly with excellent patterning resolution, but suffer from low throughput and lack scalability. We are preparing a project to employ multi-photon excited (MPE) fabrication, parallelized to achieve greater throughput. Not only will it be possible to pattern with flexibility, but it will also be possible to fabricate free-form 3-D structures. This work is in collaboration with members of the Campagnola lab, who have built the MPE instrumentation[18] and developed photo-activators for efficient photo-crosslinking of proteins and polymers[19]. We have achieved preliminary success, described below, in patterning in two dimensions and guiding neuron outgrowth.

6.3.3 **Materials and Methods**

MPE fabrication Bovine serum albumin (BSA) was crosslinked using rose bengal, onto a poly-L-lysine (PLL) coated glass substrate. Neurons adhere well to PLL and avoid BSA. Due to the difficulty of creating PLL patterns directly, a negative patterning approach was used. Thus BSA was patterned as a background, leaving PLL areas exposed for cell adhesion.

Neuronal culture and imaging We used embryonic mouse neurons, as described in chapter 2. After dissection, disassociation and resuspension, we seeded the neurons at a density of 10k/cm^2. In order to contain the neurons, a PDMS (Dow-Sylgard 184 – 10:1) ring was constructed and autoclaved before adhesion to the device. Imaging took place in the Nikon

Biostation – incubator plus imaging system. Time lapse images were initiated immediately, lasting up to 72 hours.

6.3.4 **Preliminary Results**

Negative BSA patterns on PLL yielded excellent results, as seen in Figure 6.3.1. Not only did neurons follow the intended pattern, they also grew very nearly in the center of the

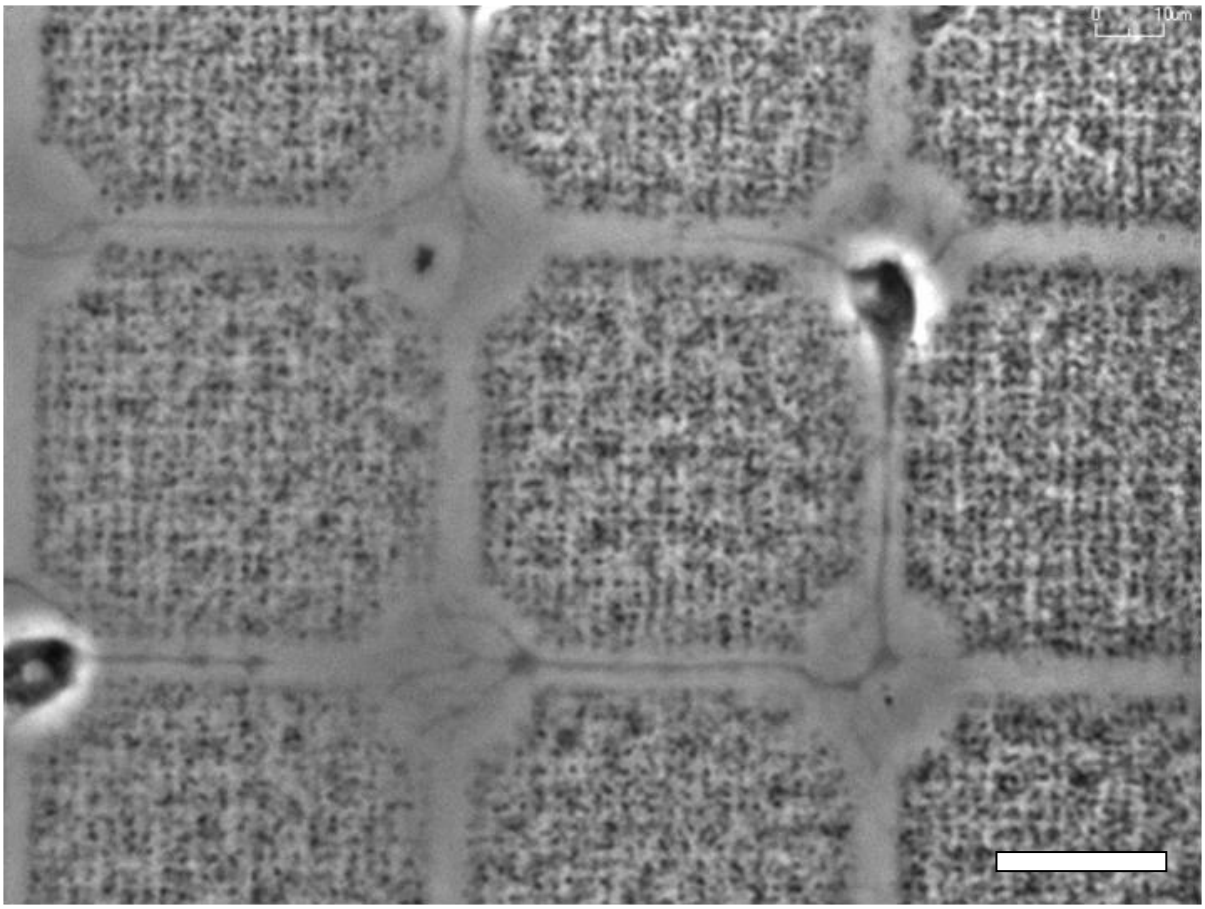

Figure 6.3.1 Neurons 12 hours after seeding onto MPE fabricated patterns. The growing neurite follows the poly-lysine pattern, entirely avoiding the BSA background. Scale bar: 25 μm.

patterned lines. Neurons were viable for several days, indicative of acceptable surface biocompatibility. Creation of positive patterns is yet under development. Directly patterning PLL is impractical, due to its ease of adsorption onto the substrate during the photocrosslinking process. Preliminary tests with fibronectin show some promise, but need further development.

Upon assessing the success of neuron growth on a basic pattern, we attempted some more complex patterns. One attempt was to assess the willingness of a neurite to 'jump' across the background. In Figure 6.3.2, we see a growing neurite which, after fully exploring the contiguous patterned area, proceeds to extend across the background, making contact with another pattern. Upon exploration of the adjacent pattern, the neurite adjusts the position of the branching segment (arrows). We observed this dynamic process on dozens of similar patterns.

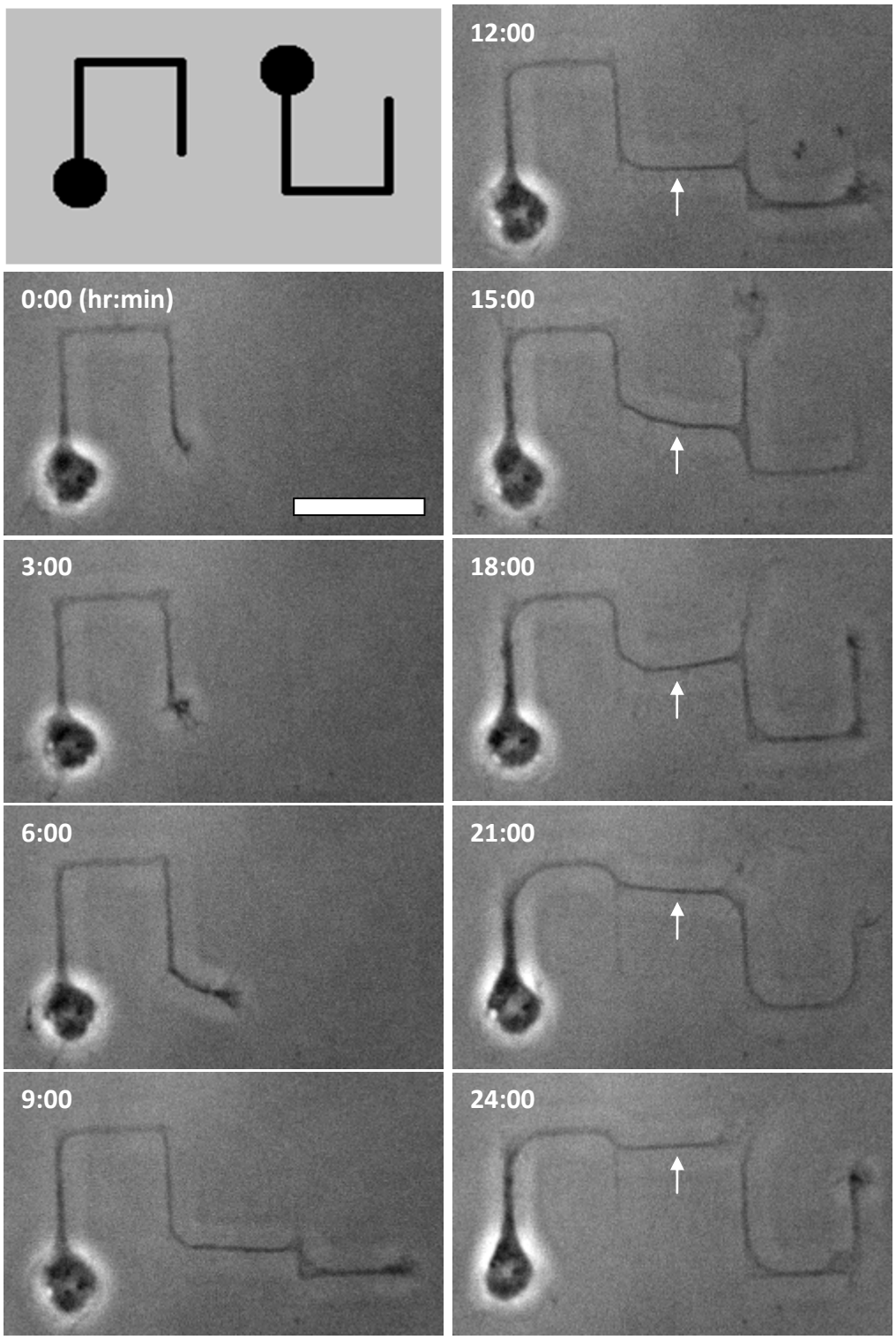

Figure 6.3.2 Time-lapse images of a neuron exploring a pattern, and then jumping to a new pattern. The first frame depicts the underlying pattern. After exploring the second pattern, the branching segment slides to a new location (arrows). Scale bar: 25 μm.

6.3.5 **Future Outlook**

As evidenced by the preliminary data, time-lapse data on a customized pattern may serve as a rich source of information in the study of neurite outgrowth and neuronal network formation. As an initial application of this process, we plan to make patterns (Figure 6.3.3) to

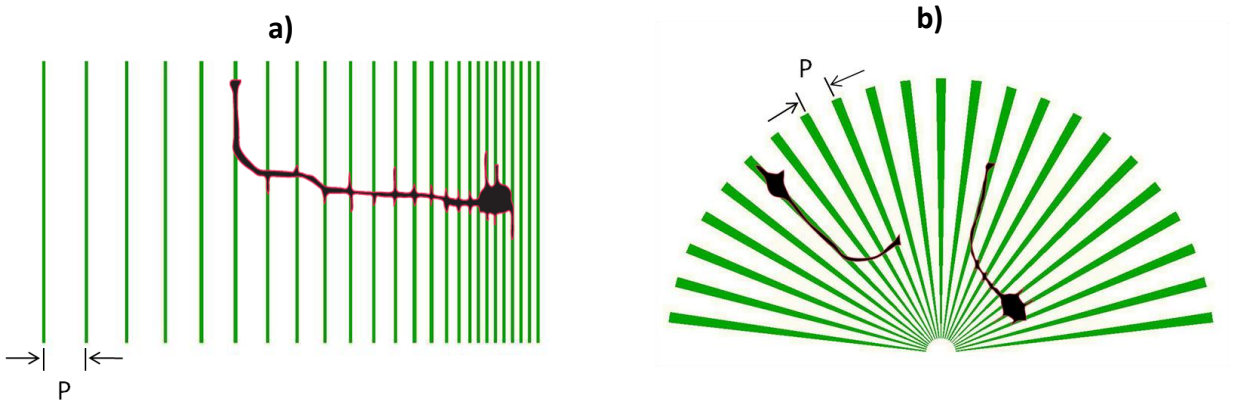

Figure 6.3.3 Proposed experiments to explore periodic cue guidance. **a)** Periodicity, P, is altered semi-continuously. This type of pattern should yield a perpendicular to parallel guidance transition measure. **b)** In this pattern P is varied continuously. Both the transition from parallel to perpendicular guidance and vice versa could be measured.

better study the periodic cue effect, as described in Chapter 2. We there demonstrated that neurite outgrowth predominantly grows parallel to lines with a periodicity of 8 μm, but perpendicular to lines with a 3.3 or 1.7 μm periodicity. We hypothesize that a growing neurite will transition from type of guidance to another, given the appropriate pattern geometry. Characterizing the transition and studying the dynamics of the decision making would form the backbone of a future project.

Additional efforts are underway to fabricate 3-D structures to guide neuron outgrowth. A goal with widespread ramifications is the interaction-free axonal intersection. When axons in

culture cross paths they often fasciculate and simply follow the same path. Even when they do successfully intersect, there is going to be intercellular communication through the contacting membranes. Successful achievement of an interaction-free intersection would dramatically further the goal of creating complex, specifically designed neuronal networks. We are attempting to grow neurons across an overpass-like structure, with an additional axon passing underneath. Once combined with additional 2-D patterning and perhaps an underlying micro-electrode array, this would enable the study of designed neural networks with an unprecedented level of control.

6.4 References

1 P. C. Letourneau, T. A. Shattuck and A. H. Ressler, "Pull" and "push" in neurite elongation: observations on the effects of different concentrations of cytochalasin B and taxol, *Cell Motility and the Cytoskeleton*, 1987, **8**, 193-209.

2 D. M. Suter and K. E. Miller, The emerging role of forces in axonal elongation, *Progress in Neurobiology*, 2011, **94**, 91-101.

3 M. W. Rochlin, K. M. Wickline and P. C. Bridgman, Microtubule stability decreases axon elongation but not axoplasm production, *The Journal of Neuroscience*, 1996, **16**, 3236-3246.

4 L. Liu, E. Tuzel and J. Ross, Loop formation of microtubules during gliding at high density, *Journal of Physics: Condensed Matter*, 2011, **23**, 374104.

5 H. Liu, E. D. Spoerke, M. Bachand, S. J. Koch, B. C. Bunker and G. D. Bachand, Biomolecular motor-powered self assembly of dissipative nanocomposite rings, *Advanced Materials*, 2008, **20**, 4476-4481.

6 S. Lin, M. Liu, Y. J. Son, B. T. Himes, D. M. Snow, W. Yu and P. W. Baas, Inhibition of Kinesin-5, As a Strategy for Enhancing Regeneration of Adult Axons, *Traffic*, 2011, **12**, 269-286.

7 M. Tessier-Lavigne and C. S. Goodman, The molecular biology of axon guidance, *Science*, 1996, **274**, 1123-1133.

8 J. Q. Zheng, J. J. Wan and M. M. Poo, Essential role of filopodia in chemotropic turning of nerve growth cone induced by a glutamate gradient, *The Journal of Neuroscience*, 1996, **16**, 1140-1149.

9 F. Q. Zhou, C. M. Waterman-Storer and C. S. Cohan, Focal losss of actin bundles causes microtubule redistribution and growth cone turning, *The Journal of Cell Biology*, 2002, **157**, 839-849.

10 K. B. Buck and J. Q. Zheng, Growth cone turning is induced by direct local modification of microtubule dynamics, *The Journal of Neuroscience*, 2002, **22**, 9358-9367.

11 E. W. Dent and K. Kalil, Axon branching requires interactions between dynamic microtubules and actin filaments, *The Journal of Neuroscience*, 2001, **21**, 9757-9769.

12 M. Bastmeyer and D. D. O'Leary, Dynamics of target recognition by interstitial axon branching along developing cortical axons, *The Journal of Neuroscience*, 1996, **16**, 1450-1459.

13 D. Falconnet, G. Csucs, H. Michelle Grandin and M. Textor, Surface engineering approaches to micropattern surfaces for cell-base assays, *Biomaterials*, 2006, **27**, 3044-3063.

14 R. Beighley, E. Spedden, K. Sekeroglu, T. Atherton, M. C. Demirel and C. Staii, Neuronal alignment on asymmetric textured surfaces, *Applied Physics Letters*, 2012, **101**, 143701-143701.

15 G. S. Withers, C. D. James, C. E. Kingman, H. G. Craighead and G. A. Banker, Effects of substrate geometry on growth cone behavior and axon branching, *Journal of Neurobiology*, 2006, **66**, 1183-1194.

16 P. Colpo, A. Ruiz, L. Ceriotti and F. Rossi, Surface functionalization for protein and cell patterning, *Whole Cell sensing Systems I*, 2010, 109-130.

17 M. Sridhar, S. Basu, V. L. Scranton and P. J. Campagnola, Construction of a laser scanning microscope for multiphoton excited optical fabrication, *Review of Scientific Instruments*, 2003, **74**, 3474-3477.

18 L. P. Cunningham, M. P. Veilleux and P. J. Campagnola, Freeform multiphoton excited microfabrication for biological applications using a rapid prototyping CAD-based approach, *Optics Express*, 2006, **14**, 8613-8621.

19 J. D. Pitts, A. R. Howell, R. Taboada, I. Banerjee, J. Wang, S. L. Goodman and P. J. Campagnola, New photactivators for multiphoton excited three-dimensional submicron

cross-linking of proteins: bovine serum albumin and type 1 collagen, *Photochemistry and Photobiology*, 2002, **76**, 135-144.